ARTIFICIAL RECHARGE OF GROUNDWATER
IN THE KÜÇÜK MENDERES RIVER BASIN, TURKEY

A THESIS SUBMITTED TO
THE GRADUATE SCHOOL OF NATURAL AND APPLIED SCIENCES
OF
MIDDLE EAST TECHNICAL UNIVERSITY

BY

AYŞE PEKSEZER

IN PARTIAL FULFILLMENT OF THE REQUIREMENTS
FOR
THE DEGREE OF MASTER OF SCIENCE
IN
GEOLOGICAL ENGINEERING

MARCH 2010

Approval of the thesis:

**ARTIFICIAL RECHARGE OF GROUNDWATER
IN THE KÜÇÜK MENDERES RIVER BASIN, TURKEY**

submitted by **AYŞE PEKSEZER** in partial fulfillment of the requirements for the degree of **Master of Science in Geological Engineering Department, Middle East Technical University** by,

Prof. Dr. Canan Özgen
Dean, Graduate School of **Natural and Applied Sciences** _____

Prof. Dr. M. Zeki Çamur
Head of Department, **Geological Engineering** _____

Prof. Dr. Hasan Yazıcıgil
Supervisor, **Geological Engineering Dept., METU** _____

Examining Committee Members:

Prof. Dr. Mehmet Ekmekçi
Hydrogeological Engineering Dept., HÜ _____

Prof. Dr. Hasan Yazıcıgil
Geological Engineering Dept., METU _____

Prof. Dr. M. Zeki Çamur
Geological Engineering Dept., METU _____

Dr. Koray K. Yılmaz
Geological Engineering Dept., METU _____

Dr. Ahmet Apaydın
DSI 5. Regional Directorate _____

Date: 30/03/2010

I hereby declare that all information in this document has been obtained and presented in accordance with academic rules and ethical conduct. I also declare that, as required by these rules and conduct, I have fully cited and referenced all material and results that are not original to this work.

Name, Last name : Ayşe PEKSEZER

Signature :

ABSTRACT

ARTIFICIAL RECHARGE OF GROUNDWATER
IN THE KÜÇÜK MENDERES RIVER BASIN, TURKEY

Peksezer, Ayşe

M.S., Department of Geological Engineering

Supervisor: Prof. Dr. Hasan Yazıcıgil

March 2010, 113 pages

Küçük Menderes River Basin located in western Turkey has been facing continuous groundwater level decreases for the past 30 years. In dry periods, irrigation demand is completely met by pumping from groundwater system, which reduces water levels significantly. This provides enough storage to be recharged in wet seasons when streams are running. However, increased runoff in wet season are not utilized neither for irrigation nor for recharge and lost to the Aegean Sea without being infiltrated. Hence, surface artificial recharge methods can be useful to collect excess water in recharge basins, thus allowing infiltration to increase groundwater storage in wet seasons to be later utilized in dry seasons.

A 2-D groundwater model is set up by using SEEP/W software. The material functions and parameters used in the model for saturated/ unsaturated conditions are taken from previous studies. Calibration was done to check the accuracy of input data and to control the validity of model. The amount of excess water that will be collected in recharge basins was estimated from flood frequency analysis. Concerning different probabilities, different scenarios were simulated to observe the increase in groundwater levels. Simulation results suggest that significant increase

in groundwater storage could be achieved by applying artificial recharge methods. In addition to recharge basins, to reinforce the effect of artificial recharge, simulations were repeated with the addition of an underground dam at downstream side of the basin. Simulation results indicate that the increase in groundwater storage is not sufficient to warrant construction of the underground dam.

Keywords: Artificial recharge of groundwater, K. Menderes River basin, numerical modeling, SEEP/W, underground dam

ÖZ

KÜÇÜK MENDERES HAVZASI'NDA (TÜRKİYE)
YAPAY YERALTISUYU BESLENMESİ

Peksezer, Ayşe

Yüksek Lisans, Jeoloji Mühendisliği Bölümü

Tez Yöneticisi: Prof. Dr. Hasan Yazıcıgil

Mart 2010, 113 sayfa

Türkiye'nin batısında yer alan K. Menderes havzasında, son otuz yıldır, yeraltısu seviyesi düşümleri gözlenmektedir. Kurak zamanlarda, sulama ihtiyacının tamamı kuyular vasıtasıyla yeraltısu sisteminden karşılanmakta, bu da yeraltısu tablasında önemli düşümlere neden olmaktadır. Böylece yağışlı zamanlarda yeraltısuyu beslenmesi için yeterli depolama hacmi sağlanmaktadır. Ancak, yağışlı zamanlarda akarsularda oluşan akış, doğrudan Ege denizine karıştığından, sulama yada beslenim için kullanılamamaktadır. Bu durumda, yapay yeraltısuyu beslenimi metotlarının bu fazla suyun beslenme havuzlarında toplanıp, yeraltına süzdürülmesinde kullanılabileceği düşünülmektedir. Böylece, yağışlı mevsimlerde yeraltısuyu depolanmasının arttırılıp, kurak mevsimlerde kullanılması amaçlanmaktadır.

Bu çalışmada, sorunun çözümüne yönelik 2 boyutlu yeraltısuyu modeli SEEP/W programı aracılığıyla oluşturulmuştur. Modelde kullanılan doygun/ doygun olmayan ortamlara ait toprak özellikleri ve hidrolik parametreler, daha önceki çalışmalardan elde edilmiştir. Girilen verilerin doğruluğu ve modelin geçerliliği kararsız akım koşullarında yapılan kalibrasyon çalışmalarıyla kontrol edilmiştir. Beslenme havuzlarında toplanan su miktarının hesaplanmasında taşkın frekans analizi kullanılmıştır.

Elde edilen farklı olasılıklar için, yeraltısu seviyesindeki değişimleri gözlemlemek amacıyla farklı senaryolar oluşturulmuştur. Simülasyon sonuçları, yapay yeraltısuyu beslenmesi yöntemiyle yeraltısuyu depolanmasında belirgin bir artış olduğunu göstermiştir. Yapay yeraltısuyu beslenimi etkisini güçlendirmek için, beslenim havuzlarına ek olarak mansap tarafına yeraltı barajı da eklenerek simülasyonlar tekrar edilmiştir. Simülasyon sonuçları yeraltısu seviyesindeki artış miktarının baraj inşaatı için yeterli olmadığını göstermektedir.

Anahtar kelimeler: Yapay yeraltısuyu beslenimi, K. Menderes havzası, Nümerik modelleme, SEEP/W, Yeraltı barajı

TO THE VERY SPECIAL PEOPLE IN MY LIFE,

MY FAMILY

ACKNOWLEDGMENTS

I am very grateful to the supervisor of this thesis, Prof. Dr. Hasan Yazıcıgil, for his theoretical support, guidance, critism and trust during the preparation of the thesis.

I also would like to thank my family; my mother Sevgi Peksezer, my father İlker Peksezer and my sister Zeynep Peksezer for their patience, encouragement and love throughout my life. Sincere thanks are extended to other family members and my friends for their support and encouragement whenever needed.

Financial support of TÜBİTAK, which gave me the honor of being a scholar of such an institution devoted to science, is gratefully appreciated.

Finally, I want to express my deepest gratitude to a very special person in my life, Kaan Sayıt, for his support, love and patience in every aspect of my life.

TABLE OF CONTENTS

LIST OF TABLES

TABLES

LIST OF FIGURES

FIGURES

CHAPTER 1

INTRODUCTION

1.1.   Purpose and scope

Groundwater is the most important source of freshwater and widely used for agriculture, industry and domestic supply. The need for fresh water has increased in the past few decades due to growing population and increasing industrial activities. In addition, decreasing rainfall rates within the past decades have led to an increase in the demand on groundwater resources. To meet this demand, more wells have been drilled, which resulted in a significant decrease in groundwater storage. Although groundwater resources are renewable, it is not easy to replenish the groundwater storage. The rate of groundwater replenishment depends on several factors, such as climate and hydrogeology. When natural recharge processes become inadequate, artificial methods are used to accelerate the recharge process.

The purpose of this study is to assess the potential for artificial recharge of groundwater in the K. Menderes River Basin in Western Turkey. The K. Menderes River basin has been facing continuous groundwater level decreases for the past 30 years. Most of the groundwater in the basin is used for irrigation in the summer season when the K. Menderes River and its tributary streams are mostly dry. Streams in the basin generally run from October through April in response to precipitation received in this period. In the absence of surface water reservoirs, none of this water is stored but lost to the Aegean Sea. Thus, the extensive pumping in summer seasons reduces groundwater levels significantly, thereby allowing a groundwater storage potential to be recharged in the wet seasons when the streams are running. The groundwater storage is thought to be increased by utilizing this excess water obtained in wet periods to recharge the underlying aquifer. A reasonable way to achieve this is

to apply the methods of artificial recharge of groundwater. These methods aim to store water when water is available for later use when water is inadequate.

This study aimed at exploring the potential for artificial groundwater storage in one of the subbasins of the K. Menderes River Basin, known as the Eğri Creek Basin. For this purpose, surface artificial recharge methods in conjunction with underground dam construction are modeled and their contributions to the groundwater levels were investigated with the help of a numerical model.

1.2.   Location and Extend of the Study Area

The K. Menderes River basin is located to the south of Izmir, in western Turkey. It is surrounded by the Aegean Sea on the west, and steep mountain ranges on the north, east and south. Dağkızılca, Bayındır, Ödemiş, Kiraz, Beydağı, Ovakent, Tire, Selçuk and Torbalı are the main settlements in the K. Menderes plain (Figure 1.1). The mountain ranges at the margins of the plain are divided by streams and their tributaries; hence resulting in a rugged topography. The main area of interest is one of the subbasins of the K. Menderes River basin, named the Eğri Creek Basin.

The Eğri Creek subbasin is surrounded by the K. Menderes River in the north, and mountain ranges in the other directions. The main settlement in the area is the Gökçen village, which is located between the Tire and Ovakent villages. The catchment area of the Eğri Creek subbasin is calculated as 130.32 km^2. The altitude in the subbasin ranges between 100 m in the north and 1550 m in the south. The Eğri Creek originating at the mountains in the south drains the area. The most characteristic feature of the Eğri Creek Basin is the presence of thick alluvial fans. Presence of thick alluvial fan deposits which allows flow of water; and locating close to the source water, i.e. Eğri Creek, where excess flows can be used to artificially recharge the aquifer, make Eğri Creek Basin be a suitable area for artificial recharge of groundwater applications along the K. Menderes River Basin.
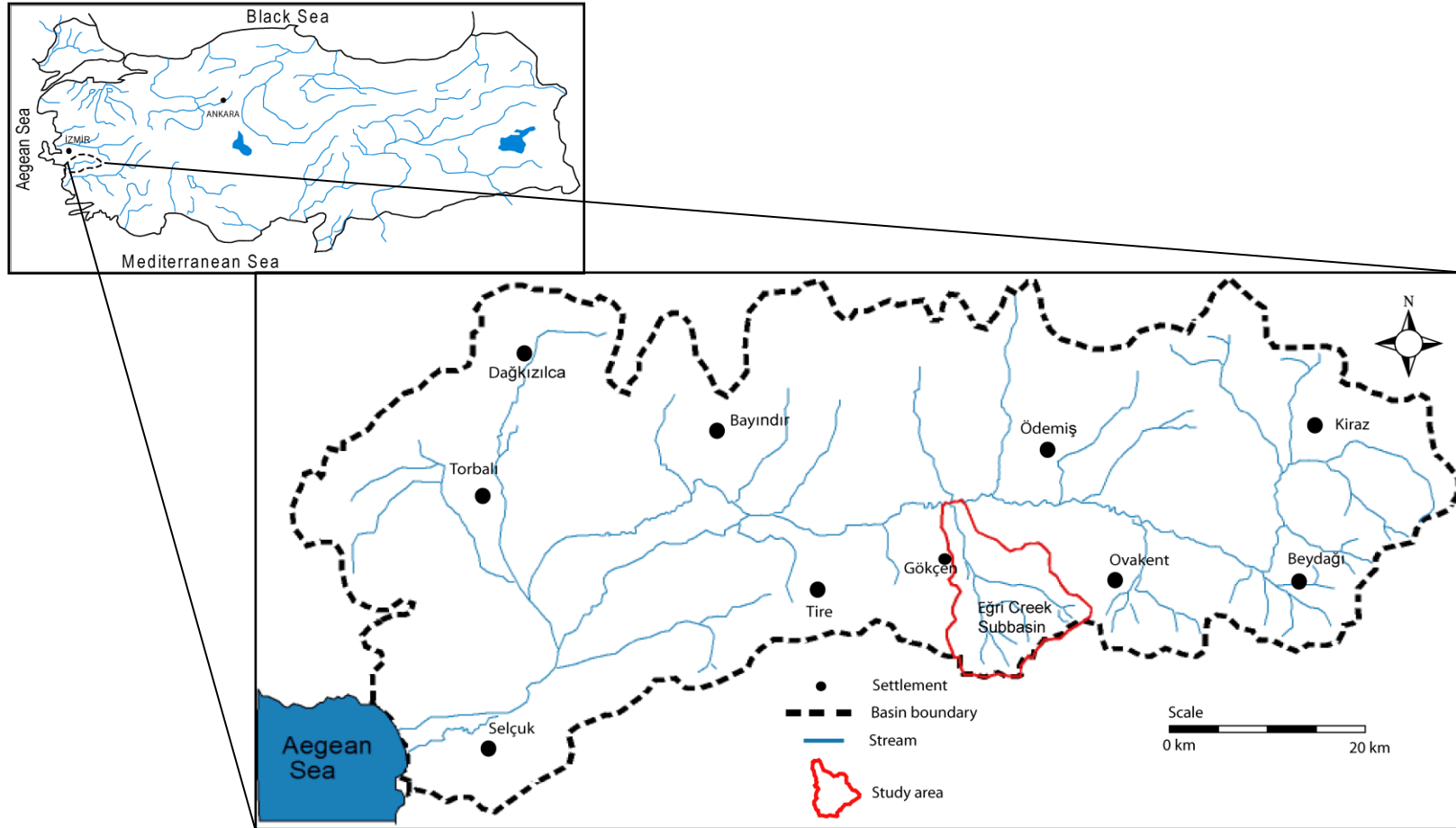
Figure 1.1. Location map of the K. Menderes River Basin and the Eğri Creek Subbasin.

CHAPTER 2

LITERATURE REVIEW ON ARTIFICIAL GROUNDWATER RECHARGE

2.1.   Introduction

Artificial recharge of groundwater is defined by Reddy (2008) as an engineered system designed to introduce and store water beneath the ground. In other words, it refers to the increase in the amount of water that is introduced into the ground, artificially (Philips, 2003). In the world, artificial recharge of groundwater has been used for the improvement of both water quality and quantity.

Groundwater management, improving water quality, reducing flood flows, storing stream waters during periods of water surplus, preventing salt water intrusion and reclaiming waste water are some examples that can be achieved by artificial recharge of groundwater (Lehr, 1982).

Artificial recharge system design considerations involve hydrogeological considerations, source water considerations, operation-maintenance considerations and legal and regulatory issues. The factors that should be taken into account for locating, designing and operating artificial recharge projects are summarized by Banks et al. (1954). Selecting a suitable location with respect to geology, specifying soil textures in recharge area, acquisition of sufficient lands, silt control, maintenance of percolation rates, quality of recharged water, degree of necessary prior treatment can be given as some examples. From hydrogeological point of view, type of the aquifer, permeability of geologic formations overlying the aquifer, characteristics of unsaturated zone and heterogeneity are the factors that affect recharge rate and design of artificial recharge system (Bouwer, 2002). If the vadose zone is thin,

groundwater mounding will occur during the recharge and cause pooling, leading to a decrease in recharge rate. On the other hand, if the vadose zone is too deep, vertical transit time to aquifer may be too long. Heterogeneous soils increase lateral dispersion of recharge water, and therefore increase time and distance; however, very uniform soils increase air entrainment in vadose zone, thus reducing recharge (Reddy, 2008). In addition, temperature of water can affect the recharge rate. Since cold water is more viscous, its recharge rate will be lower than warm water (Lytle, 1994). Therefore, in the recharge system design, climate conditions should be taken into consideration.

Sources of recharge water include surface water from streams or lakes, reclaimed wastewater, rainfall and storm runoff, imported water from other areas, groundwater from other aquifers and treated drinking water. Water quality plays a critical role in direct injection methods. For water spreading, since unsaturated zone and the material in the aquifer act as natural filters and clean the water, additional treatment is not necessary (Peters, 1994).

The annotated bibliographies by Todd (1959) and Signor et al. (1970) can be given as the basic references on the subject of the artificial recharge of groundwater. Recently, the interest on artificial recharge has increased due to growing population, decreasing rainfall rates and increasing demand for freshwater.

The first applications on the artificial recharge were started in 1810 in Scotland, where water was pumped from a filter gallery. In the 1820s, in France, basins were constructed to collect percolating waters from the river. Later, artificial recharge studies were carried out in Germany, Hungary, United States and Sweden (Jansa, 1952). Today, from Brazil and United States to Taiwan and Japan, many countries in the world use these methods. Especially in Germany and Sweden, artificial recharge of groundwater has become a standard procedure (Connorton and McIntosh, 1994).

Generally the demand for the water is not uniform; i.e., it increases in dry seasons, while decreasing in wet seasons; resulting in fluctuations of water table. The studies

conducted in France suggested that the success of artificial recharge projects depends mainly on these fluctuations (Soyer, 1947).

In this chapter, a brief outline will be given, regarding the research and developments of artificial recharge of groundwater on the basis of the applications of different methods. The methods of recharging the aquifer artificially can be summarized under two headings; namely, water spreading and direct injection methods. Besides, underground dam is also considered as an artificial recharge method. Modeling of artificial recharge of groundwater will also be discussed in this chapter.

2.2. Water Spreading

The most common method of artificial recharge of groundwater is water spreading, where recharge water is allowed to infiltrate down to the water table from natural or man-made depressions (Philiphs, 2003). The aquifer should be unconfined in order to give response to the infiltrated water. Based on the permeability of the underlying units in the unsaturated zone, water spreading methods can be divided into two subgroups; surface spreading and subsurface spreading methods. Spreading basins and recharge pits are some examples of surface spreading methods, whereas infiltration galleries can be classified as subsurface spreading methods (Figure 2.1). In subsurface spreading, a layer that prevents recharge (such as clay layer) exists near ground surface, hence recharge water is introduced at some depth beneath the land surface but above the water table (within vadose zone) and then allowed to infiltrate into the unconfined aquifer.

In the USA, water spreading studies were started in 1889, majority of which were performed in California (CA) and the eastern states located along the coast (Harrell, 1935). In the USA, one of the most significant recharge project (Central Arizona Project, CAP) have been conducted in Arizona, where water from Colorado River, Salt River and effluent were used to recharge the aquifer. For this purpose, recharge basins were constructed and operated in Arizona, Phoenix and Tucson (Jacobs and Holway, 2004).
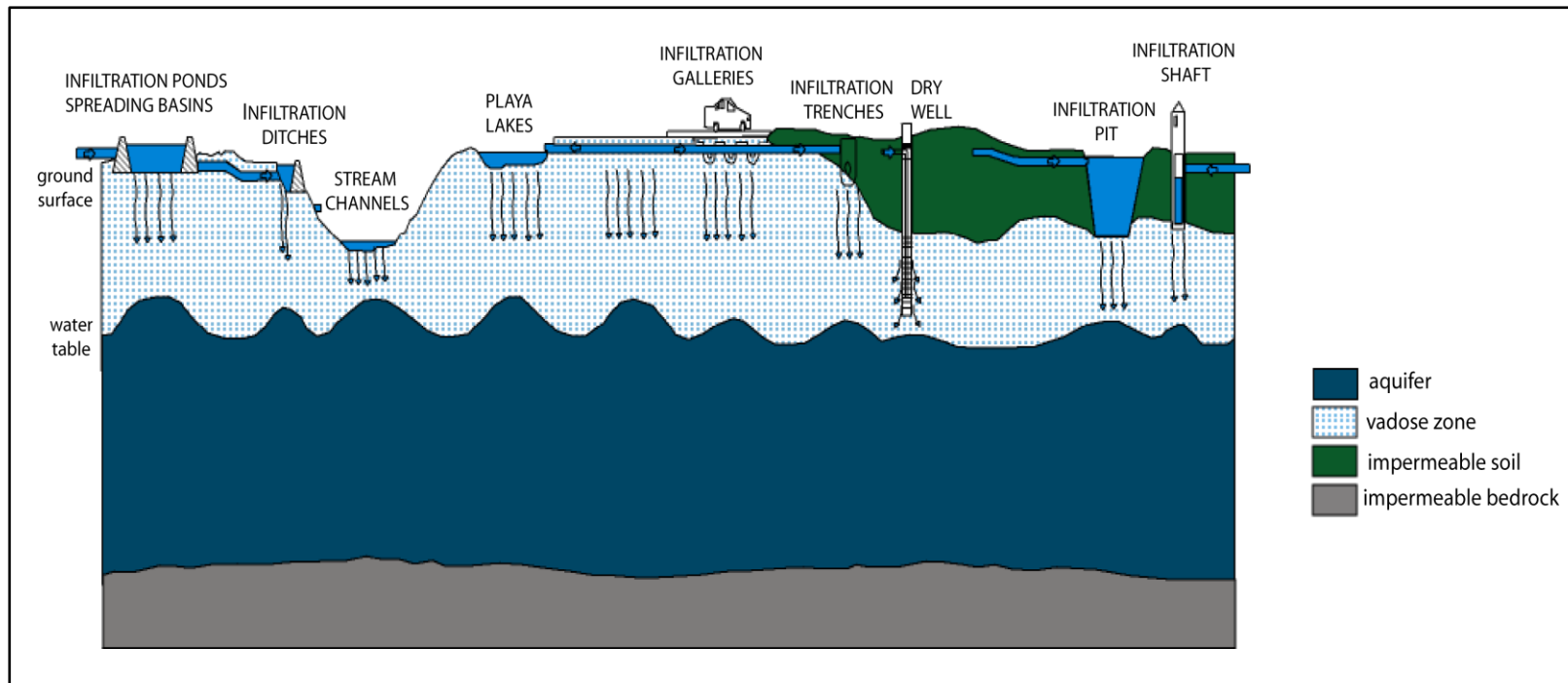
Figure 2.1. Examples of water spreading structures (Reddy, 2008).

Maximizing the infiltration rate beneath structures is the main concern in water spreading. Infiltration rates are closely related to the physical and chemical characteristics of soil and subsurface conditions. Ground shape, surface soils and physiography can be used as a guide for prediction of these conditions (Richter and Chun, 1959; Schiff and Dyer, 1964). In order to determine the groundwater recharge capacity of the sites, it is necessary to construct test ponds before constructing any recharge facilities (Flanigan et al., 1994). An average infiltration rate of 2 feet per day (~ 0.6 m/d) is regarded as optimal (Lane, 1934). Houk (1951) and Laverty (1952) suggest that an average rate of 1 foot per day (~ 0.3 m/d) can also be used in artificial recharge systems.

The prevailing factor that descends the infiltration rate is clogging. The presence of suspended mineral matter that leads to formation of an impervious film on soil surface is an example of clogging. To overcome this situation, desilting of floodwater before spreading is recommended (Berend, 1967). Also, draining and rinsing the infiltration basins have been used for the removal of clogging since 1897 (Jansa, 1952). Another method is to use chemicals for removing the suspended material, such as Separan 2610 (Imbertson, 1959). Based on the water spreading experiments, the success of rapid infiltration of dried basin surfaces before spreading was proved by Jans (1959).

Water spreading used for sewage disposal by spreading the sewage over large areas and letting the liquid to recharge the ground water has been a common method in Europe since the sixteenth century (Winslow and Phelps, 1906). The unsaturated zone and the material in the aquifer act as natural filters and clean the wastewater, hence unreliable surface water can be turned into a safe source by water spreading (Bouwer 1994; Peters, 1994). In the Middle East, since 1977, Israel has used the spreading basins for recharging the aquifer by tertiary effluent (Ishaq et al., 1994).

For floodwater conservation, water spreading methods were found to be economical and beneficial (Blaney, 1936). The examples of conservation of flood water by spreading methods can also be observed, starting from 1895 in the USA (Banks et al., 1954). A deflatable-inflatable rubber dam was also used for collection of the

floodwaters. These collapsible dams redirect the storm runoff for treatment and infiltration. Across the Los Angeles and the Santa Ana Rivers, these dams were constructed to meet the water demand (Imbertson, 1959 and Markus et al., 1994).

Surface spreading methods require extensive land areas, permeable surface materials with high vertical permeability, periodic maintenance to prevent clogging, and little or no water pretreatment (Kimrey, 1989). On the other hand, high evaporation losses and groundwater vulnerability to surface contamination make these methods inapplicable for nearby land use. In the case of subsurface spreading, evaporation losses and required land area are minimized but initial costs are increased. Besides, it is difficult to clean these structures (Reddy, 2008).

2.3. Direct Injection

Another method of artificial recharge is direct injection. Recharge wells and aquifer storage and recovery (ASR) wells are examples of direct injection methods, where water is injected into the aquifer (Philiphs, 2003). Figure 2.2 shows examples of both recharge and ASR wells.

The recharge well and its purpose were briefly described with equations derived from idealized boundary and permeability conditions by Thiem (1923). Simpson (1948) described the factors affecting recharge rates in wells. Dewey (1933) summarized the conditions where recharge wells can be used successfully. In the USA, well recharge methods were first conducted in 1927 in Los Angeles.

The feasibility of recharge from the wells should be tested in artificial recharge applications (Engler et al., 1945). Muckel (1945) explained the reasons for the decline of recharge rate with time in direct injection methods, such as clogging, incrustation by chemical actions in metal cased wells, and effect of organic matters. The test on a recharge well at Manhattan Beach, CA showed that if the flows are not stabilized by dosing recharge water with chloride, clogging occurs (Laverty et al., 1951). Clogging of the infiltration wells can partly be reduced by back flushing (Stakelbeek et al., 1994). Another factor that influences injecting well performance is

water temperature. Lytle (1994) suggested that in Denver basin, injecting colder, more viscous water into warm water reservoir results in decline of recharge rates.

Based on the position of well-bottom being above or below the water table, the recharge wells can be grouped as wet and dry wells, respectively. The studies proved the success of wet wells, since dry wells are subjected to intense clogging (Brashears, 1946).

In Arcadia, CA, it was observed that the presence of nearby pumping wells raises the recharge rate (Irwin, 1931). According to Brashears (1953), mixing of recharged and pumped waters below ground can be avoided by locating wells at different depths, since horizontal permeability exceeds the vertical one.

The ASR wells are the other type of direct injection methods, where water is stored and recovered from the same well. The benefits of the ASR wells were introduced by Pyne (1994). Requirement of small land area, frequent maintenance and monitoring, need of pretreatment are the characteristics of direct injection methods (Kimrey, 1989). In US, the first ASR wells were used in 1968.

Pros and cons of water spreading and direct injection methods are summarized in Table 2.1.

2.4. Underground Dam

Underground dams are also considered as an artificial recharge method, which prevent groundwater flow and store water beneath the ground (Nilsson, 1988). They are used where surface storage becomes impractical owing to high evaporation rates, reservoir siltation, pollution risks, etc (Boochs and Billib, 1994). Although this technology is not new, its efficiency and simplicity has revived interest (Foster and Tuinhof, 2004).
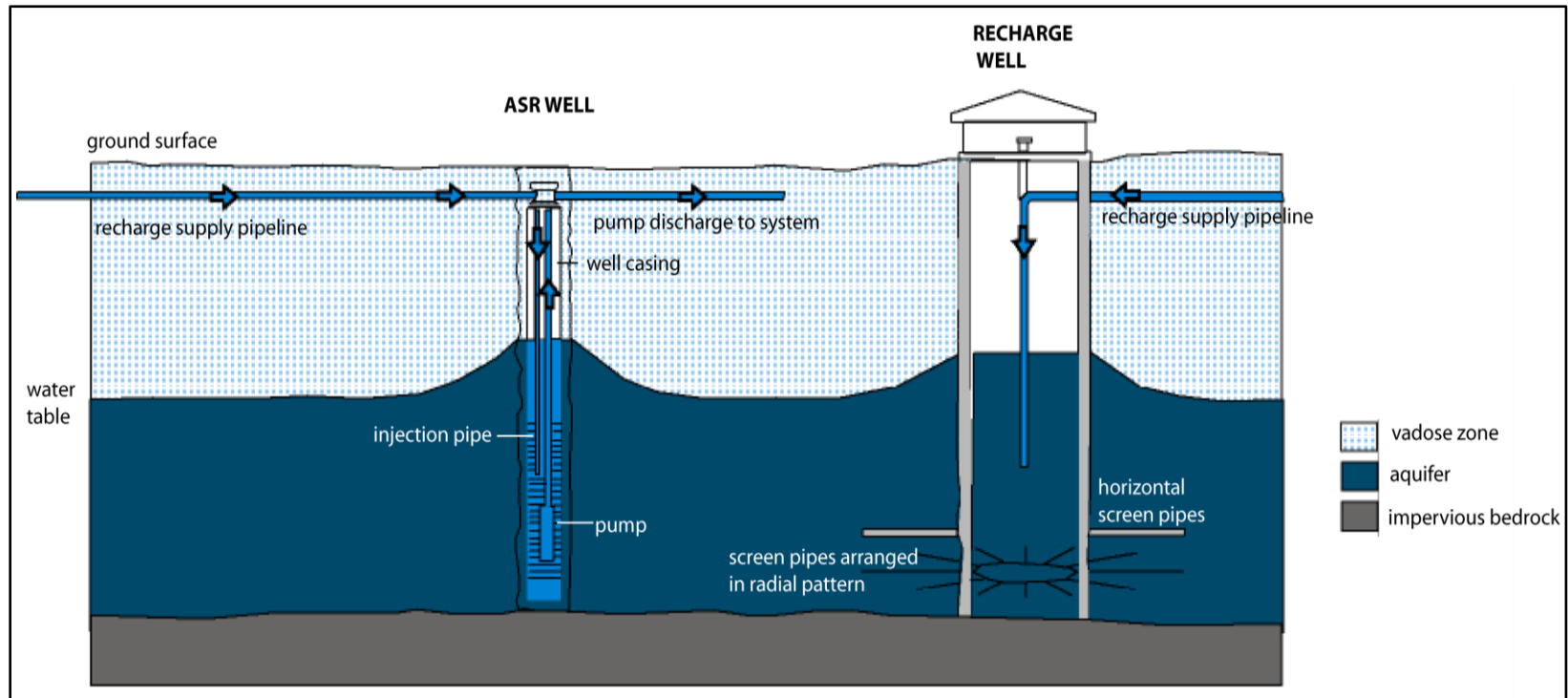
Figure 2.2. Examples of direct injection methods (Reddy, 2008).

Detailed information about physical conditions, design and construction of underground dams are given by Nilsson (1988). Underground dams are usually constructed in arid regions, where irregular rainfall is observed. Well defined and narrow valleys, natural dikes are preferred for locating underground dams. In hydrogeological point of view, the river beds consisting of sand and gravel are considered as best localities, where suitable storage and flow characteristics are observed.

In Turkey, studying underground dam construction is a new topic. The first large-scale underground dam was constructed in Çeşme, İzmir to prevent salt water intrusion and store groundwater. Other than Çeşme, experiments on the underground dams were conducted in Yahşihan, Kırıkkale and Malıboğazı, Ankara (Apaydın, 2009; Apaydın et al., 2005).

2.5.   Modeling of Artificial Groundwater Recharge

Optimization techniques are widely used in artificial recharge of groundwater for the determination of the optimal recharge rates. Generally, the objective is to determine the maximum infiltration volume, whereas the constraints are flow continuity, infiltration, groundwater flow and the ones describing a physical environment, such as, a recharge basin (Mushtad and Mays, 1994). Numerical models, on the other hand, are used for determining the wet-dry schedules or multi-period operations (Mushtad and Mays, 1994).

The main step in recharge from a basin is to determine the infiltration from the basin after water ponding. The Green-Ampt model is widely accepted and used in the artificial recharge projects for calculating the infiltration (Al-Muttair and Al-Turbak, 1991).

Table 2.1. Advantages and disadvantages of artificial recharge methods.

	WATER SPREADING METHODS		DIRECT INJECTION METHODS
	SURFACE SPREADING METHODS	**SUBSURFACE SPREADING METHODS**	
ADVANTAGES	❖ Initial low capital cost ❖ Simple maintenance ❖ Low operation and maintenance costs	❖ Used where surface layers of low permeability preclude surface infiltration ❖ Co-exists with other surface urban uses ❖ Minimize evaporation losses	❖ Used where vertical permeability is limited ❖ Occupy small surface areas ❖ Fit in most land patterns ❖ Utilize existing water supply infrastructures
DISADVANTAGES	❖ Require: ➢ Near surface aquifer ➢ Permeable soil profile with high vertical permeability ➢ Frequent maintenance to prevent clogging ❖ High evaporation losses and groundwater vulnerability to surface contamination	❖ Higher initial capital cost ❖ Limited aerial extend ❖ Difficult to clean/ maintain	❖ High: ➢ Capital cost ➢ Energy requirements ➢ Operation and maintenance costs ❖ Require: ➢ Frequent pumping to remove clogging ➢ Pretreatment prior to recharge

Since each recharge site is unique in terms of its hydrogeology, it requires a careful investigation prior to modeling. Light (1994) summarized the steps required to analyze the system. On the other hand, all the parameters required to define the system cannot be usually obtained. The previous studies conducted in similar areas with similar soils can be used as best references to provide preliminary estimates about the artificial recharge potential (Munevar and Marino, 1999).

The use of MODFLOW, which is a block centered finite difference software, in the area of surface water and groundwater interaction is common throughout the world. Mainly, direct injection methods are modeled by MODFLOW, where aquifer is confined to semi- confined, and wells are used for artificial recharge. Good examples can be found in Wiese and Nutzmann (2007) and Brothers et al. (1994)

Water spreading methods involve the simulation of unsaturated zone, since the infiltration process mainly takes place in this zone and the aquifer is unconfined. For construction of the vadose zone representations and extrapolation of soil material hydraulic properties, a complex 2D modeling of fluid flow is necessary. To achieve this, numerical codes like TOUGH2, VS2D, SUTRA etc. can be used, which are able to simulate fluid flow under both saturated and unsaturated conditions.

Munévar and Marino (1999) set up a model for estimating potential of artificial recharge on alluvial fans in Salinas Valley, CA via recharge basins. In the model, soil surveys, geologic investigations, seasonal groundwater response to rainfall and runoff were first identified. For the representation of vadose zone, driller's logs were used to correlate material types in this zone. In the unsaturated zone modeling, the key parameter is determination of soil properties. The hydraulic properties of vadose zone were determined from the previous works conducted in similar areas, and after several model tests, the one which best represents the area was chosen. VS2D was selected for modeling the unsaturated zone, which is a modular, block centered, 2D finite difference model capable of handling fluid flow problems in porous media. Since the main concern of the study was to show the applicability of artificial recharge of groundwater, exact representation of subsurface was not essential.

Izbicki et al. (2007) modeled the Oro Grande Wash area to test its feasibility for artificial recharge from ponds. In that study, a water table monitoring well and unsaturated zone instrumentation were installed at a site one year before the recharge pond was constructed. Depth to water, matric suction and quality of water in the unsaturated zone were examined one year prior to application and four years after the application. For the simulation of flow of water in vadose zone, as a numerical code, TOUGH2 was selected, which can simulate 2D flow of water, heat and air under both saturated and unsaturated conditions. The results suggested that infiltration from properly sited ponds can be used to recharge aquifers, even if clay layers exist.

CHAPTER 3

STUDY AREA

3.1. Physiography

The study area, namely the Eğri Creek subbasin, is one of the subbasins of the Küçük Menderes River Basin. It is bounded by the K. Menderes River in the north and steep mountain ridges in the other directions. The relief map of the K. Menderes River Basin and location of the Eğri Creek subbasin is shown in Figure 3.1. The altitude of the area ranges between 100 m and 1550 m. Most characteristic feature in the area is the presence of alluvial fans at the front of the mountains, which is the case for north and south margins of the K. Menderes River basin. The Eğri Creek, which originates at the mountains in the south of Gökçen, drains the area. The Eğri Creek watershed covers an area of 130.32 km^2.

3.2. Climate

The study area is under the influence of Mediterranean (Aegean) climate, where summers are hot and dry, while winters are mild and rainy. Two types of rainfalls are observed in the area; convective type at depressions in the inlands, and orographic type at high elevations (Yazıcıgil et al., 2000).

In Turkey, meteorological data is obtained from DMİ (State Meteorological Works). Meteorological stations located throughout the country measure different parameters such as precipitation, evaporation, temperature, relative humidity, wind and radiation values. In the K. Menderes River Basin, there are 10 meteorological stations; however only three of them is located adjacent to the study area; namely Tire,
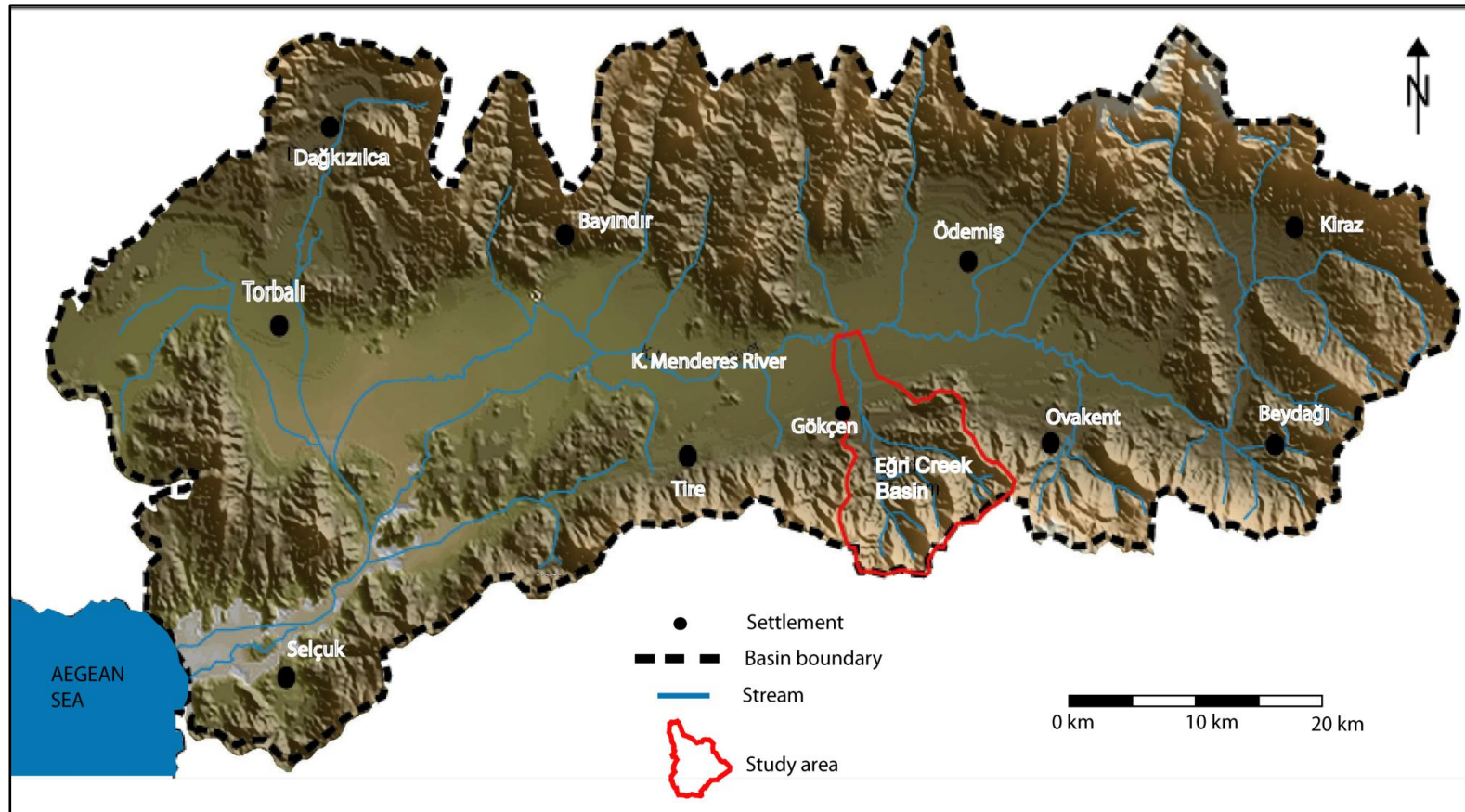
Figure 3.1. Relief map of K. Menderes River Basin and location of Eğri Creek subbasin (after Yazıcıgil et. al., 2000).

Ödemiş and Ovakent stations. Ödemiş Station is the closest station to the model area (about 12 km) and topographically at the same elevation as the model domain. Therefore meteorological data used in this work have been obtained from Ödemiş Station, which is still operated and best represents model area.

In the Ödemiş Station, from May to September, measured monthly temperatures are above the average. The maximum temperature is measured as 30 °C, whereas the minimum temperature is measured in January as about 3 °C. The annual average temperature is about 16 °C. Monthly average, maximum and minimum temperature values obtained for the years 1945 - 2007 are shown in Figure 3.2.

	Jan	Feb	Mar	Apr	May	Jun	Jul	Aug	Sep	Oct	Nov	Dec
■ average	7.2	8.0	10.6	14.8	20.1	24.9	27.7	27.0	22.5	16.9	12.0	8.7
■ minimum	3.2	4.5	6.7	10.9	17.3	22.9	25.1	23.7	19.8	14.1	9.0	4.0
■ maximum	10.8	10.8	14.6	18.4	23.3	27.1	29.7	30.0	26.3	20.1	15.3	12.3
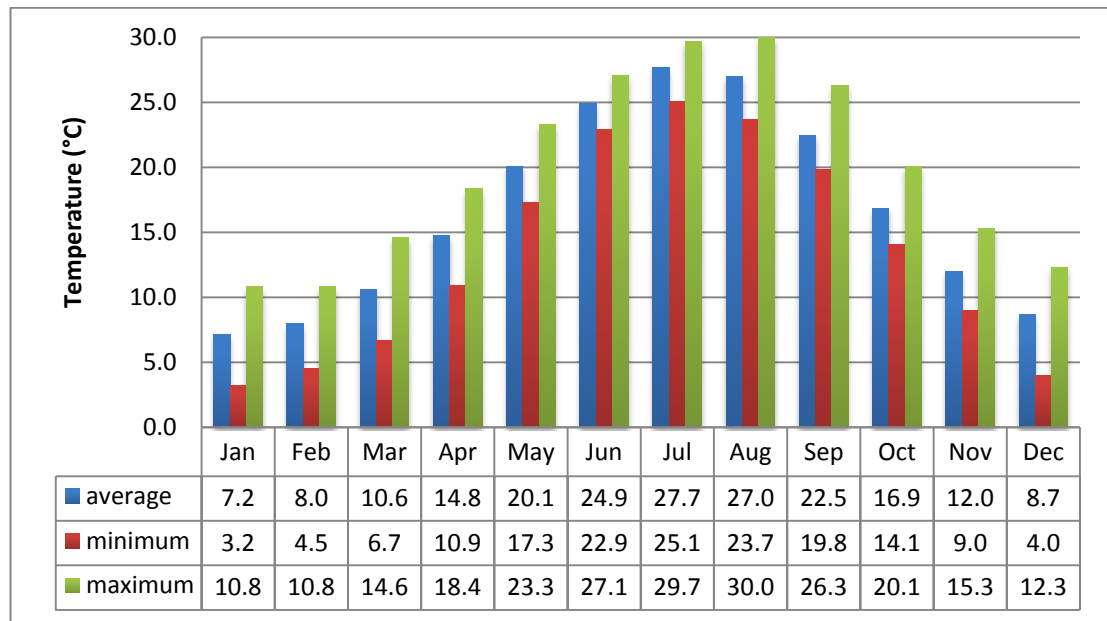
Figure 3.2. Average, minimum and maximum monthly temperature values for Ödemiş station.

As a characteristic of Mediterranean climate, precipitation is high in winter, but low in summer. Seasonal distribution of average annual precipitation is given in Figure 3.3. The average monthly precipitation is about 52 mm. Based on the long term data from the Ödemiş station, the maximum and minimum monthly precipitations are measured as 333.7 mm and 0 mm, respectively. Figure 3.4 illustrates the monthly

average maximum and minimum precipitation results obtained for the years 1945 - 2007. On the annual basis, the Ödemiş station receives a 592.4 mm of precipitation.
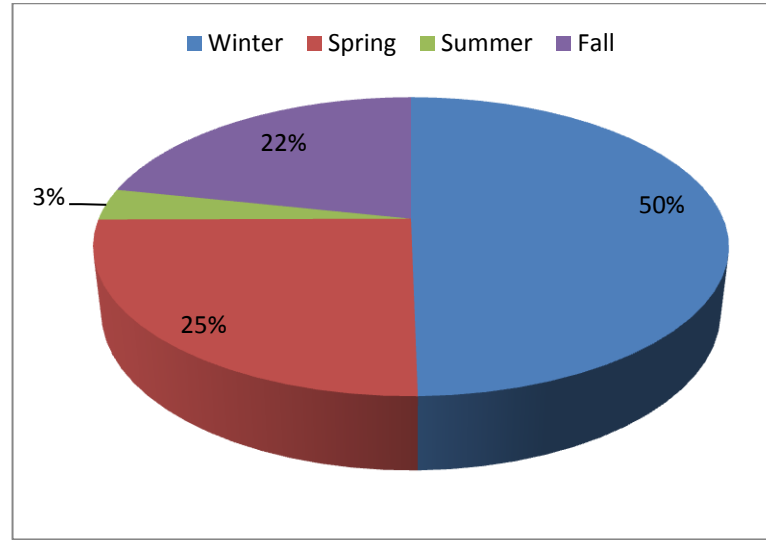
Figure 3.3. Seasonal distribution of average annual precipitation for Ödemiş Station.

	Jan	Feb	Mar	Apr	May	Jun	Jul	Aug	Sep	Oct	Nov	Dec
average	101.5	87.9	72.1	51.1	33.6	13.6	5.4	2.4	17.5	38.3	79.0	120.1
mimimum	10.0	8.3	8.5	7.6	2.0	0.0	0.0	0.0	0.0	7.4	12.5	19.1
maximum	257.1	225.5	173.7	144.3	102.5	71.0	42.6	17.9	103.1	124.7	227.4	333.7
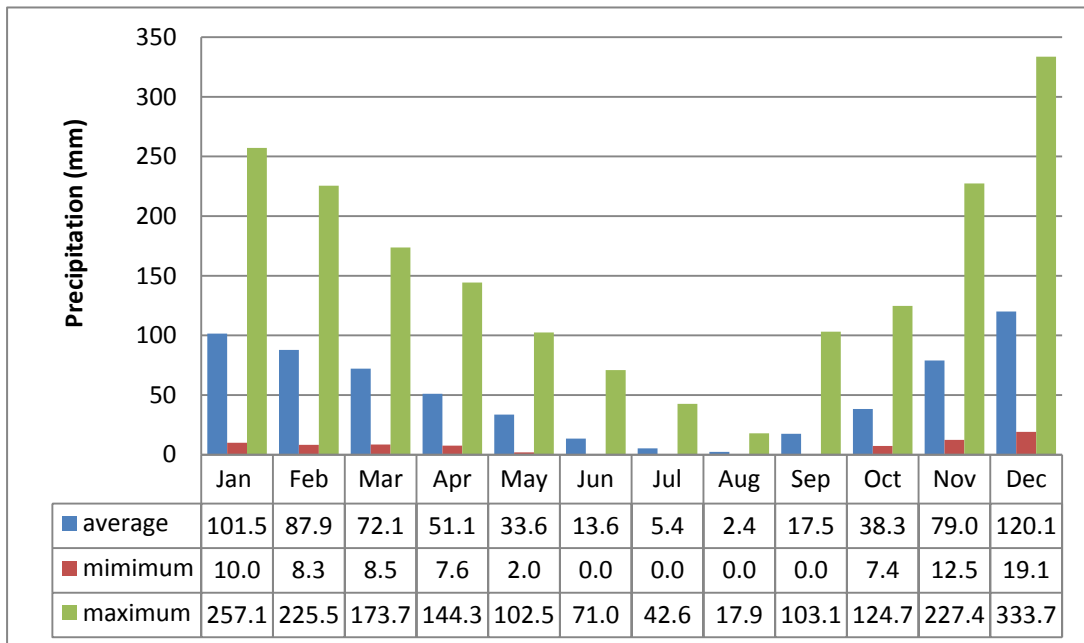
Figure 3.4. Average, minimum and maximum monthly precipitation values for Ödemiş Station.

Measurements indicate that from April to December, evaporation data can be monitored. From January to March, due to the freezing, measurements cannot be performed. The missing data were completed by correlating the measured monthly evaporation data with the average monthly temperature data obtained from the Ödemiş station. The monthly maximum evaporation value is measured as 415.4 mm in July, which is the hottest month. The long term data indicate that the annual total evaporation is measured as 1509.3 mm. The monthly average, and minimum and maximum evaporation data obtained for the years 1945 - 2007 are shown in Figure 3.5.

In addition, to obtain dry and wet periods, graph of cumulative departure from the average annual precipitation and distribution of precipitation was drawn for the Ödemiş station (Figure 3.6). Based on the graph, the periods between 1961-1967 and 1977-1981 are classified as wet periods, whereas periods between 1971-1977 and 1981-2007 are described as dry. It is clear that a long-term dry period persisted in the study area for the past 25 years.

	Jan	Feb	Mar	Apr	May	Jun	Jul	Aug	Sep	Oct	Nov	Dec
■ average	18.3	26.8	57.8	101.9	166.3	231.0	263.8	246.0	187.5	117.8	65.1	32.5
■ mimimum	0.0	0.0	11.6	59.5	114.7	196.3	221.4	206.5	144.0	11.6	33.0	0.0
■ maximum	60.1	58.4	121.5	159.0	235.6	327.0	415.4	359.6	243.0	156.4	108.5	72.0
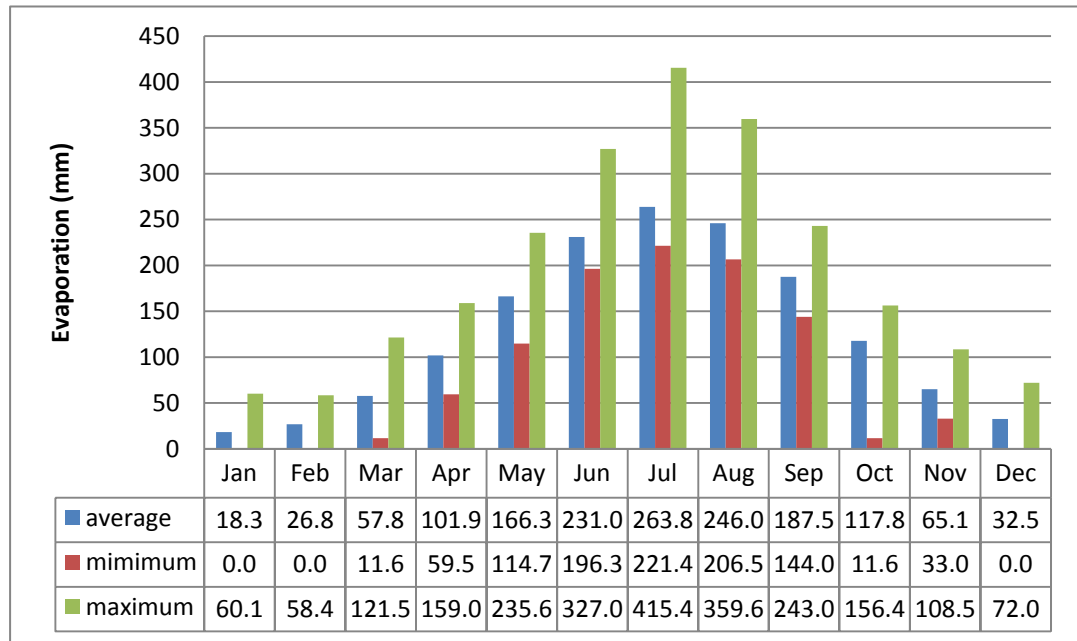
Figure 3.5. Average, minimum and maximum evaporation values for Ödemiş Station.
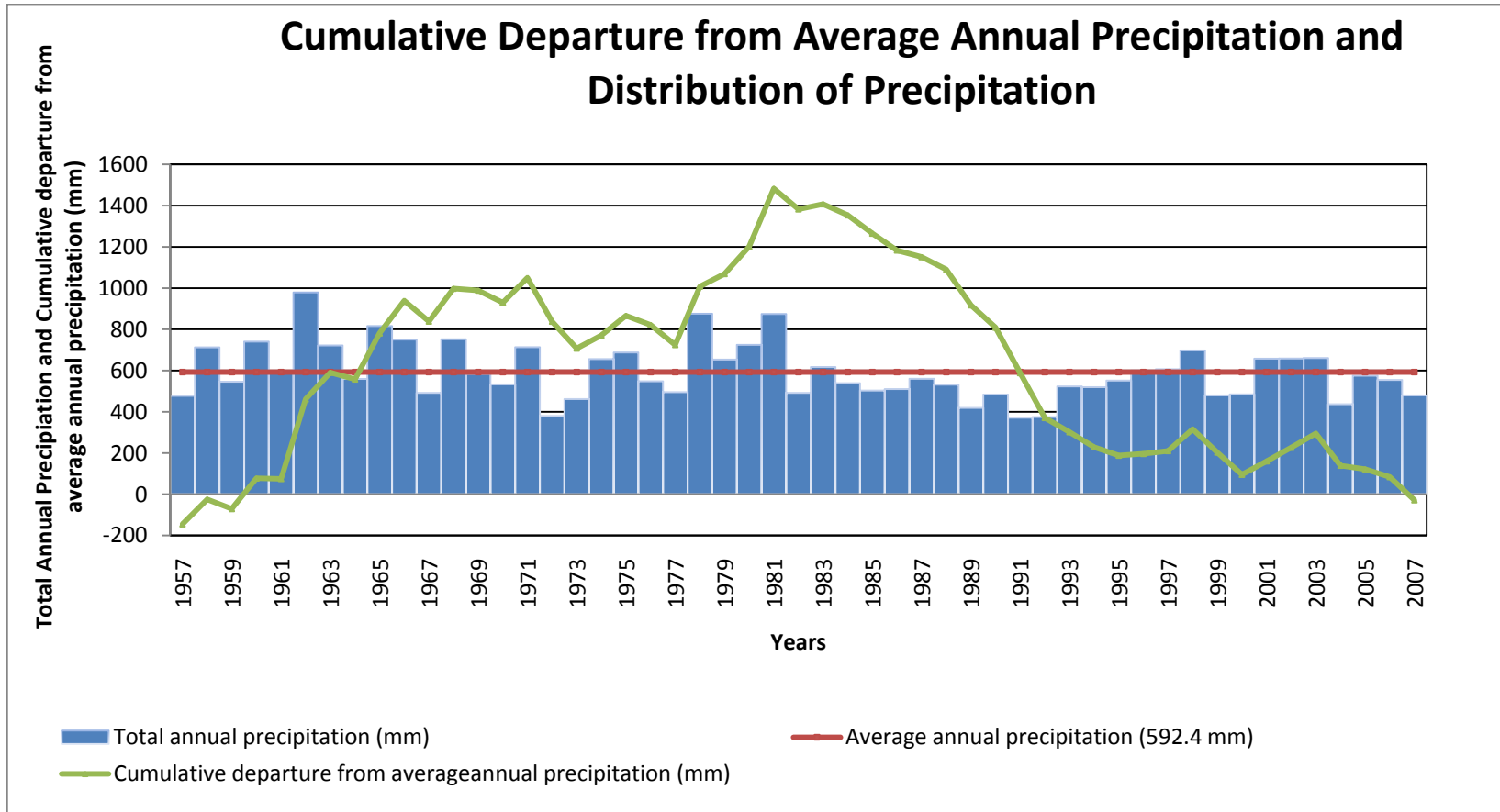
Figure 3.6. Cumulative departure from the average annual precipitation and distribution of precipitation for Ödemiş station.

3.3. Geology

The geological information related to the K. Menderes River Basin and the Eğri Creek subbasin were synthesized from the final report of "Investigation and Management of Groundwater Resources In K. Menderes River Basin Under the Scope of Revised Hydrogeological Studies" by Yazıcıgil et al (2000).

3.3.1. Regional Geology

Western Anatolia is a region characterized by approximately N-S directed continental extension. E-W and WNW-ESE grabens and their related active normal faults are the most distinctive neo-tectonic features in the region. The K. Menderes River Basin is one of the grabens stretching in the east-west direction. It is surrounded by the Gediz and the B. Menderes Grabens in the north and south, respectively (Figure 3.7). In Western Anatolia, metamorphic rocks of Menderes Massif and Neogene sediments are widely observed.

The K. Menderes River Basin includes metamorphic assemblages of the Menderes Massif as the basement rocks, and it is overlain by the Late Cretaceous- Paleocene Bornova flysch that is represented by limestone blocks, Neogene units and Quaternary sediments. Generalized columnar section and geological map of the Küçük Menderes River Basin after Yazıcıgil et al. (2000) is shown in Figure 3.8 and 3.9, respectively.

Northern and southern ridges of the K. Menderes Basin are characterized by the Menderes Massif metamorphics. The Menderes Massif is tectonically surrounded by the İzmir-Ankara-Erzincan Suture Belt to the north and by Likya Nappes to the south.

The Bornova Flysch is observed in the western part of the Küçük Menderes River Basin. From bottom to top, it is made up of dark colored greywacke - conglomerate and massive dolomitic limestone. Limestone blocks are generally seen in a greywacke-dominated matrix. The contacts between the Menderes Massif - flysch and flysch- Neogene unit is marked by an unconformity.

The Neogene sedimentary sequence is characterized by alternation of conglomerate- sandstone- mudstone and clayey limestone, and it is mainly observed in the western part of the study area. The volcanics are rarely seen in the Küçük Menderes basin. Quaternary alluvium and talus unconformably overlie these volcanics.

Quaternary alluvium, alluvial cone, talus, Plio-Quaternary river deposits and red pebbles characterize the Plio-Quaternary unit. The contact between the Plio-Quaternary units and the underlying units is defined as an angular unconformity.

Alluvial fans, which are composed mainly of boulder, gravel and sand alternating with clay, are widely observed, especially in the margins of the K. Menderes Plain. Thickness of these fans generally exceeds 90 m. Their great thicknesses and steep slopes are considered as fault indicators. Alluvial fill is another deposit that covers most of the plain. It is composed of alternation of gravel, sand, silt and clay. Changes in discharge rate and migration of the river channel are responsible for the deposition of different lithologic units. Faults located in the northern and southern margins of the plain control deposition of the alluvial fills.

The K. Menderes River Basin is characterized by E-W trending normal faults due to N-S extension of the Western Anatolia. The most evident E-W trending normal fault can be observed along the Beydağı- Gökçen- Tire- Belevi belt. Foliation measurements performed in the basin reveal the presence of a syncline. The axis is of the syncline passes through the Beydağı- Gökçen- Tire- Belevi belt, and is parallel to the longitudinal axis of the basin.

3.3.2. Local Geology

The study area is located near the Gökçen region, which lies between Tire in the west, and Adagüme in the east. As seen from the geological map of the study area represented in Figure 3.10, there are two main lithologic units; alluvial fan deposits and Menderes Massif metamorphics.
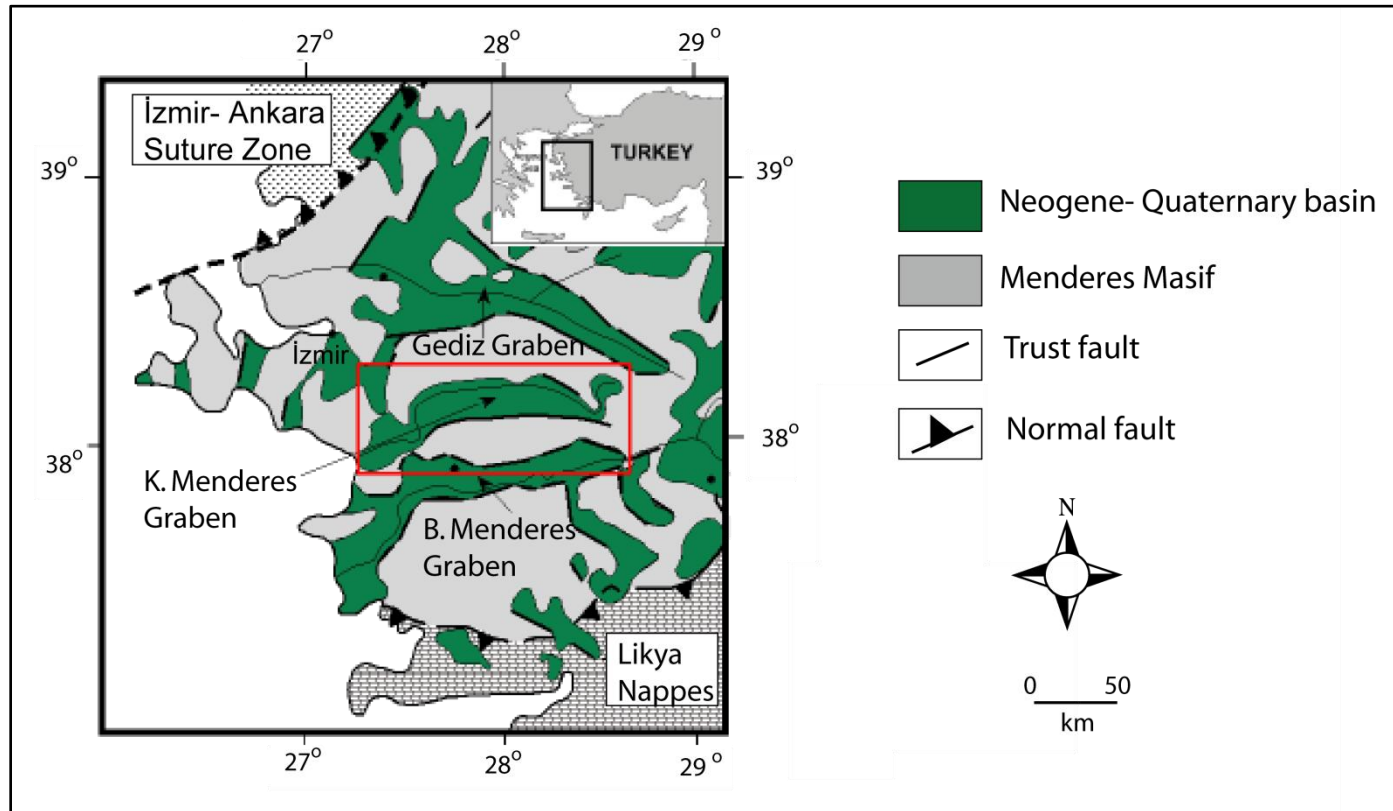
Figure 3.7. Regional location of the K. Menderes River Basin (after Yazıcıgil et. al., 2000).
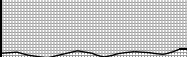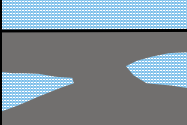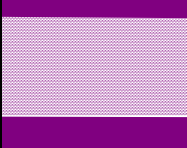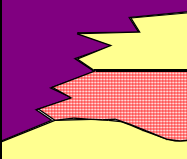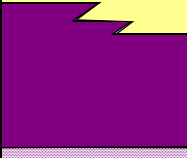
AGE	FORMATION	LITHOLOGY	EXPLANATION
QUA.			Alluvium, alluvial cone, talus
			Clayey limestone
NEOGENE	NEOGENE UNITS		Conglomerate, sandstone, mudstone, andesitic intrusions
			(Unconformity)
UPPER CRETACEOUS	BORNOVA FLYSCH		Sequence of conglomerate- graywacke- limestone with calcareous blocks of Jurassic age
			(Unconformity)
			Marble- calcschist alternation
			(Tectonic)
			Meta- ultramafics
			(Tectonic)
PALEOZOIC	MENDERES GROUP METAMORPHICS		Micaschist, calcschist and marble alternation
			Augen gneiss, granitic gneiss, migmatitic-syngenetic granite, micaschist and metagabbroic metamorphics
			Micaschist, garnet bearing schist, phyllite; marble interbedded

Figure 3.8. Generalized columnar section of Küçük Menderes River Basin   (after Yazıcıgil et. al., 2000).
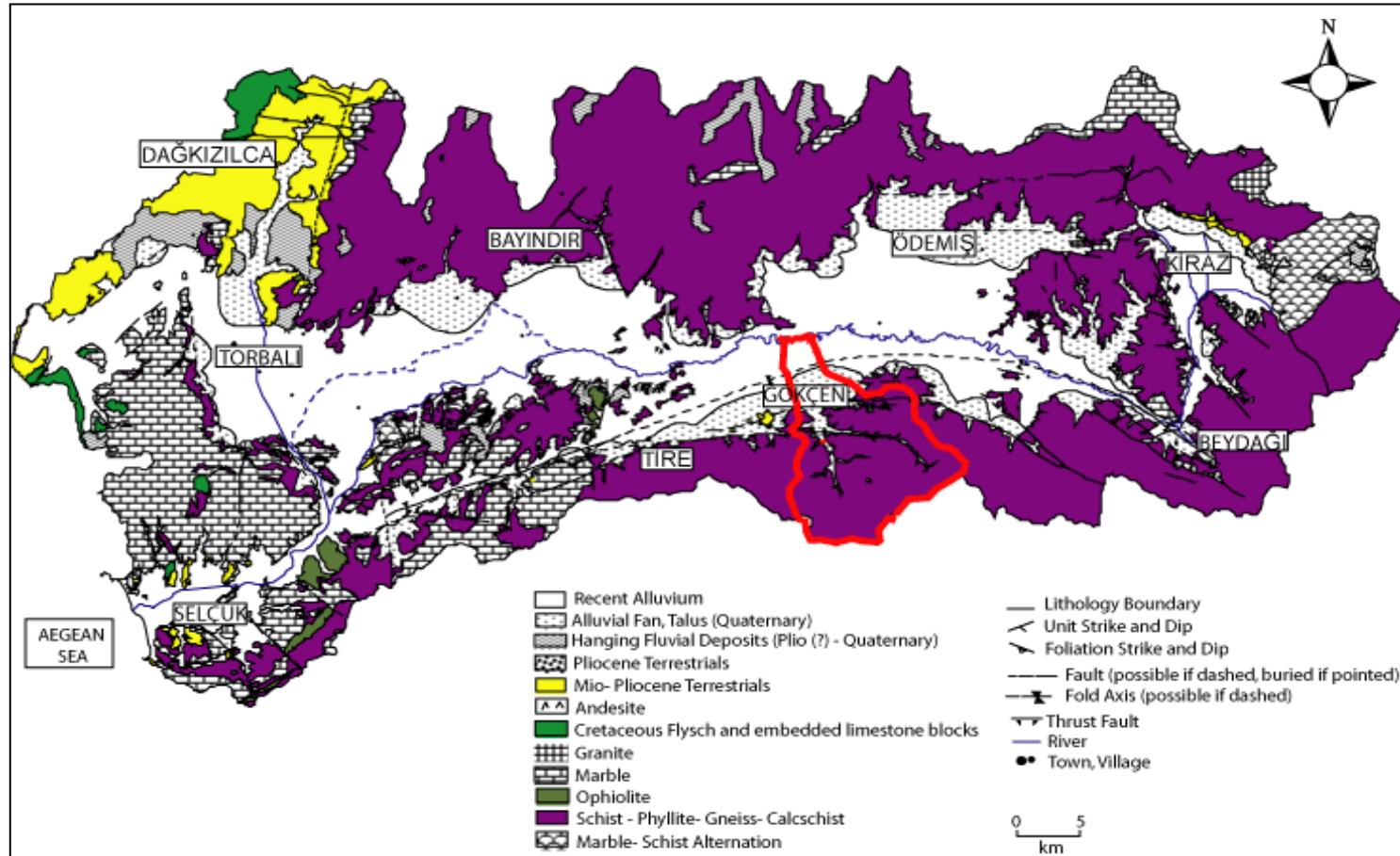
Figure 3.9. Geological map of the Küçük Menderes River Basin and study area (after Yazıcıgil et. al., 2000).
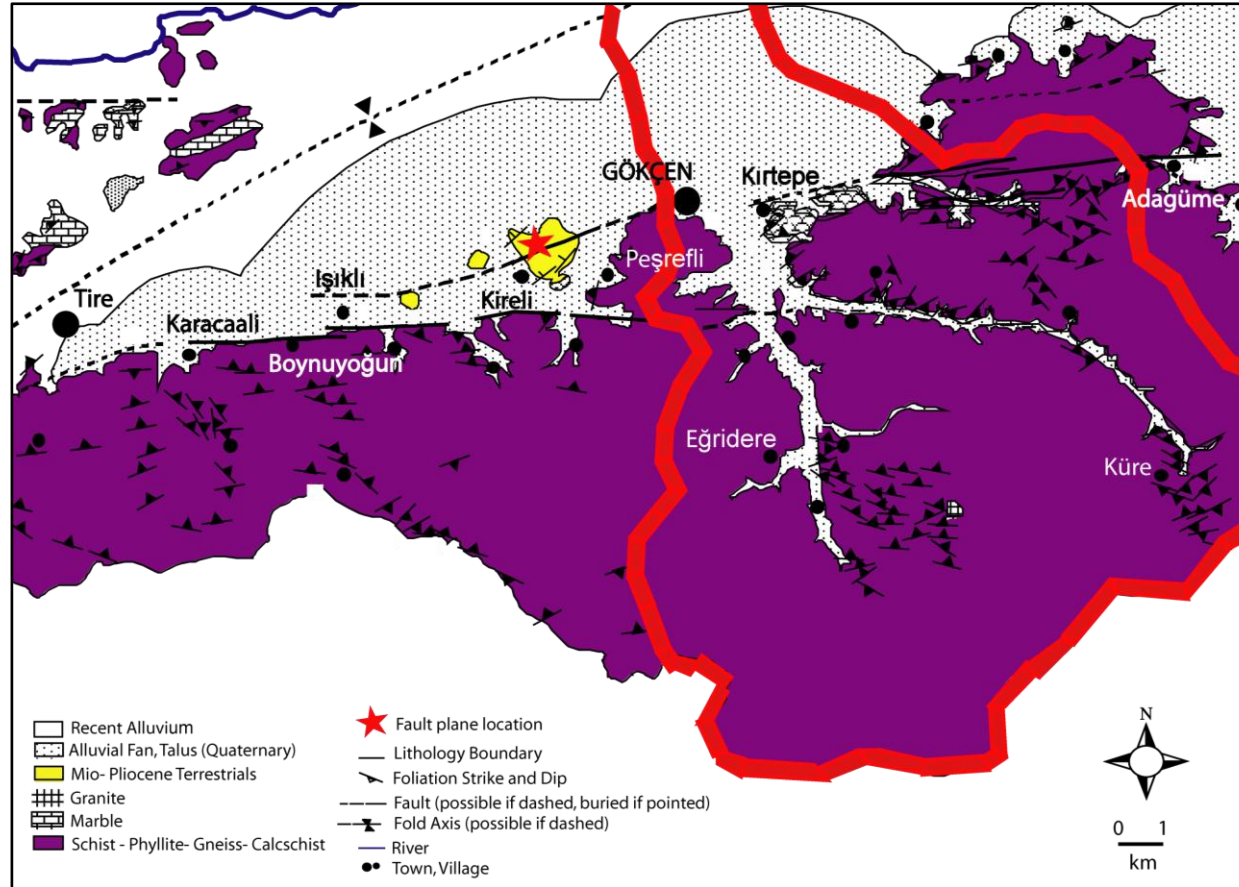
Figure 3.10. Geological map of Gökçen region, study area (after Yazıcıgil et. al., 2000).

The most characteristic feature in the area is the presence of alluvial fans. Thickness and slope of the fans seem to increase from Tire towards the eastern parts. The thickness appears to be about 180 m. In addition, the fan material has been transported over long distances into the plain. The main mechanism controlling the formation of the alluvial fans is the faulting.

Along the margins of the area, the Menderes Massif metamorphics are widely observed. Especially in the Gökçen region, alternation of schists and gneiss are dominant, whereas marble is not found.

In the Gökçen region, 160 foliations were measured, and two foliation directions were determined on the basis of the analyses. The dominant foliation direction; i.e. south of Belevi- Tire; belongs to the southern part of the synclinal. The synclinal axis passes through the Beydağı- Gökçen- Tire- Belevi belt. The other direction also belongs to the same part of synclinal, but it seems to have grown differently owing to the effects of faults in E-W direction, and secondary folding in the synclinal.

The faults examined in the Gökçen region stretch in the E-W direction. The largest fault can be followed along the Çamlıca, Sarılar, Işıklı, Boynuyoğun and Karacaali villages, not continuously but discretely. To the west, this joins with another fault that reaches to Belevi. Fault steepness, the presence of thick alluvial deposits and Neogene units are the main indicators for the occurrence of the fault. Based on the lineation studies, the fault appears as a left-lateral normal fault.

3.4.   Hydrogeology

3.4.1. Surface Water Resources

The K. Menderes River basin is drained by the K. Menderes River and its tributaries. One of these tributaries, the Eğri Creek drains the study area. Eğri Creek flows in northerly direction and joins the K. Menderes River at the north.

In artificial recharge projects, the aim is to utilize excess water (that is lost to the sea without being infiltrated) as a source to recharge the aquifer. Hence, potential

volume of water that can be collected should be first determined from flow measurements.

In the K. Menderes River basin, stream gauging stations operated by DSİ (State Hydraulic Works) and EİEİ (General Directorate of Electrical Power Resources Survey and Development Administration) measure flow data. Along the basin, there are eight stream gauging stations, where seven stations belong to DSİ and one station belongs to EIEI. The distribution of the stations in the basin is given in Figure 3.11.

It is observed that neither DSI nor EIEI has a stream gauging station in the study area, i.e. along the Eğri Creek. The two DSI stream gauging stations operating adjacent to Eğri Creek, namely the Aktaş and Rahmanlar stations, were used to determine the discharge pattern in the study area. Average monthly flow rates for both stations are given in Figure 3.12. Maximum discharge occurs in winter months, whereas a significant decrease is seen in summer. In the case of the Eğri Creek, a similar situation is also expected.

In order to determine the Eğri Creek flow data, a correlation analysis is conducted. Correlation analysis is started with comparing measured daily flow rates of the Aktaş and Rahmanlar creeks (Figure 3.11) to obtain a relation between the flow data for the period between 1982 and 2001, where both stations were operating. However, a reasonable correlation coefficient cannot be determined (Figure 3.13). Then, geomorphologic characteristics of the basins, such as slope, area, elevation, etc., are compared to obtain a relation among the flow rates (Table 3.1). When the watersheds of the Aktaş, Rahmanlar and Eğri creeks are investigated, it is observed that the mean basin slopes, elevation of the basins and stream lenghts are similar, whereas the catchment areas of the basins are quite different. Thus, this suggests that the differences in measured flow rates of Aktaş and Rahmanlar creeks are related to the differences in catchment areas. The catchment areas of the Aktaş, Rahmanlar and Eğri Creeks are approximately 103 km^2, 80 km^2 and 130 km^2, respectively. Estimated discharge rates of the Eğri Creek is determined by multiplication of measured flow rates of both Aktaş and Rahmanlar Creeks with an areal factor corresponding to the basin area ratio.
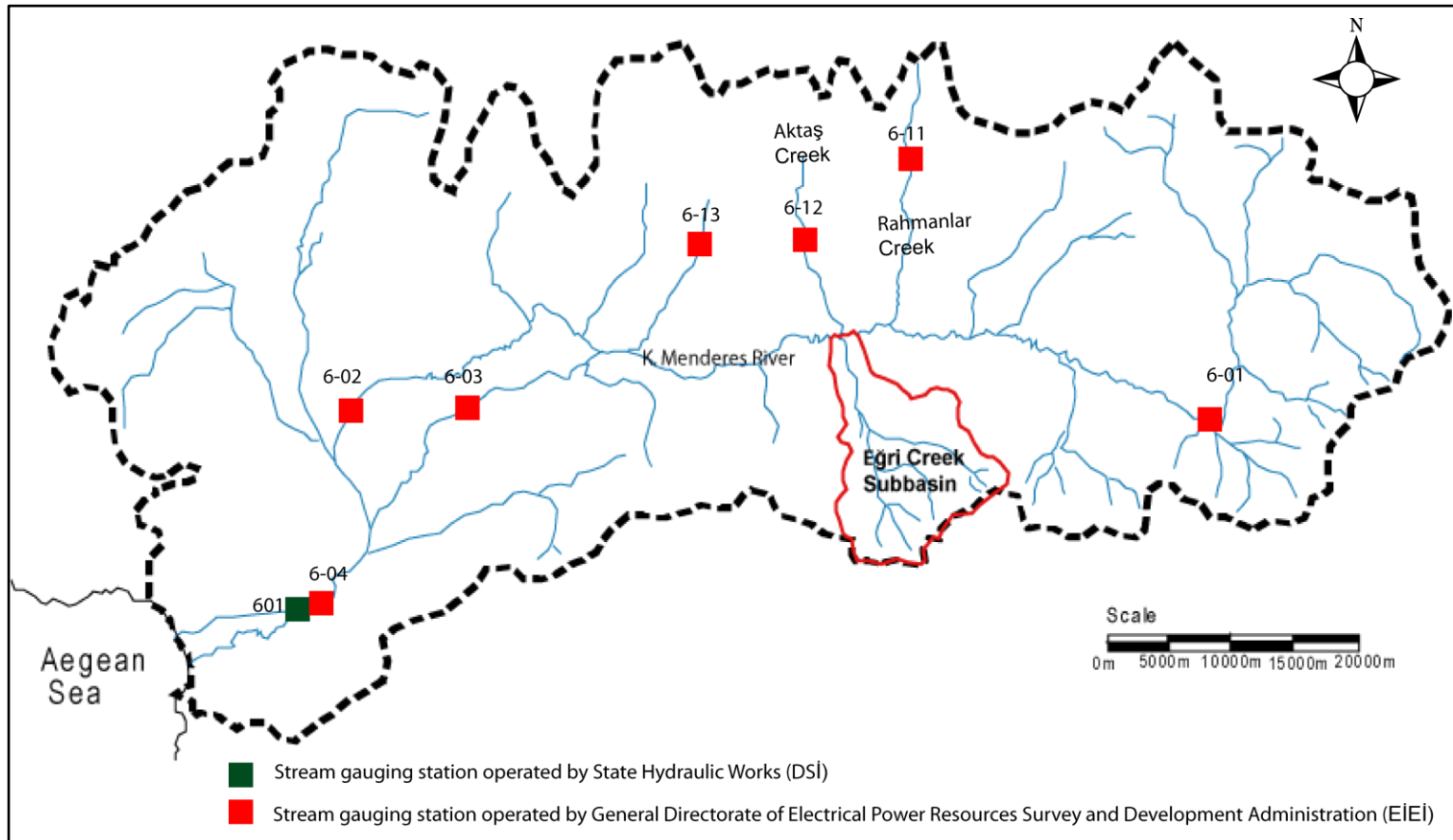
Figure 3.11. Flow measurement stations in the K. Menderes River Basin.
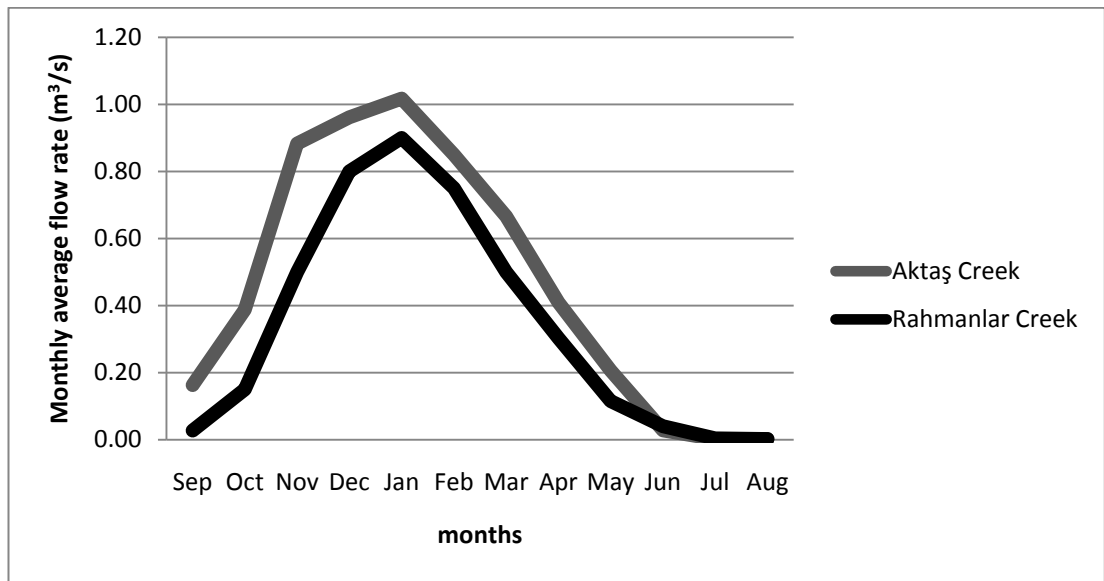
Figure 3.12. Average monthly discharge rates for the Aktaş and Rahmanlar Creeks.
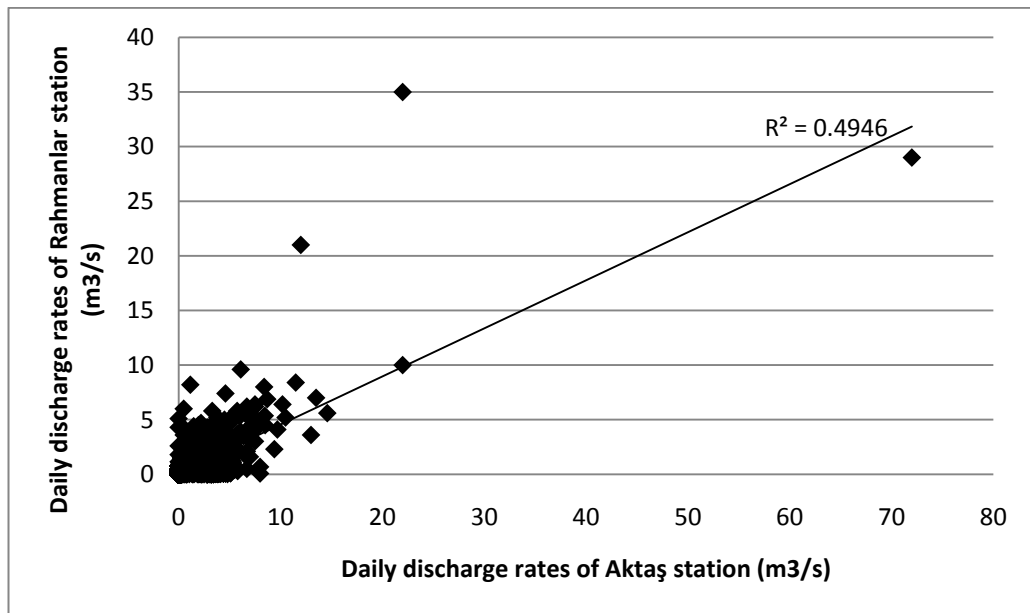
Figure 3.13. Daily discharge relation between the Aktaş and Rahmanlar station.

Table 3.1 Geomorphologic characteristics of Rahmanlar, Aktaş and Eğri Creeks

	RAHMANLAR CREEK	AKTAŞ CREEK	EĞRİ CREEK
ELEVATION	50-1000 m	50-1050 m	50-1550 m
SLOPE	0.042	0.040	0.047
STREAM LENGTH	22.8 km	25.3 km	27.5 km
AREA	80.4 km^2	103.5 km^2	130.32 km^2

Discharge rates of the Eğri Creek is computed to determine maximum flow rates obtained for each year, which in turn were used in flood frequency analysis to compute potential volume of water that can be collected to recharge the aquifer artificially. The maximum flow rates of the Eğri Creek determined from discharge rates of both Aktaş and Rahmanlar Creeks are very close to each other. Estimated average monthly discharge rates of the Eğri Creek are given in Figure 3.14. Computed peak annual runoff volumes of Eğri Creek for the period from 1982 to 2001 is shown in Table 3.2.

3.4.2. Flood Frequency Analysis

Flood frequency analysis is conducted for estimating probable floods that can be used as a source water to recharge the aquifer. The analysis include obtaining some statistical information by using observed annual peak discharge rates. The statistics, then, were used to construct frequency diagrams, where various discharge rates are described as a function of exceedence probability.

In the application of artificial recharge methods in the study area, the recharge basins were thought to be constructed to store flood waters along the Eğri Creek. Therefore, it is essential to calculate the volume of flood waters that will be stored in the recharge basins to determine the applicability of the artificial recharge project. For this purpose, estimated daily discharge rates of the Eğri Creek were plotted for each

year, from 1982 to 2001 to determine annual peak discharge volumes. In the graph, the area below the discharge versus time curve gives the volume of water for a single flood event. Calculated annual peak runoff volume, then, was ranked in a decreasing order. The calculation of exceedence probability is formulated as:

$$p = \frac{m}{N+1}$$ (3.1)

where m: runoff volume rank

N: number of years of record

p: exceedence probability
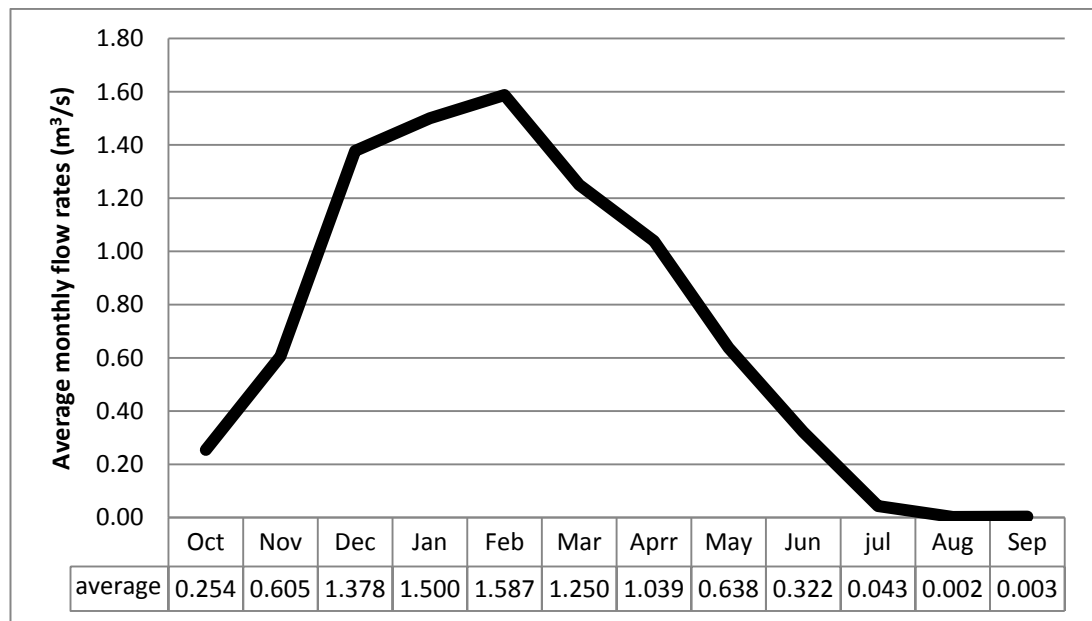
Figure 3.14. Estimated average monthly flow rates of Eğri Creek.

The total number of classes is obtained as 16 and each class is equally probable. The exceedence probabilities computed for the Eğri Creek is given in Table 3.2. Frequency curves can be plotted on normal, log- normal or Gumbel distribution papers to determine a suitable relation between data points. The flood frequency analysis of the Eğri Creek shows a normal trend (Figure 3.15). By using this relation,

the volume of water that can be stored in recharge basins is determined for different probabilities as shown in Table 3.3.

In addition, exceedence recurrence interval (return period) for Eğri Creek was also determined (Table 3.3). The recurrence interval is an estimate of the average time between past occurrences of random events, which are statistically used to estimate the probability of the occurrence. The recurrence interval was computed by:

$$T = \frac{N+1}{m} \qquad (3.2)$$

where m: runoff volume rank

      N: number of years of record

      T: exceedence recurrence interval

Table 3.2. Exceedence probability of Eğri Creek.

RANK (m)	RANKED RUNOFF VOLUME (10^6 m^3)	EXCEEDENCE PROBABILITY	
		p	%
1	4.267	0.0625	6
2	3.824	0.125	13
3	3.500	0.1875	19
4	3.482	0.25	25
5	2.635	0.3125	31
6	2.331	0.375	38
7	2.095	0.4375	44
8	1.864	0.5	50
9	1.528	0.5625	56
10	1.462	0.625	63
11	1.455	0.6875	69
12	1.035	0.75	75
13	0.529	0.8125	81
14	0.488	0.875	88
15	0.437	0.9375	94
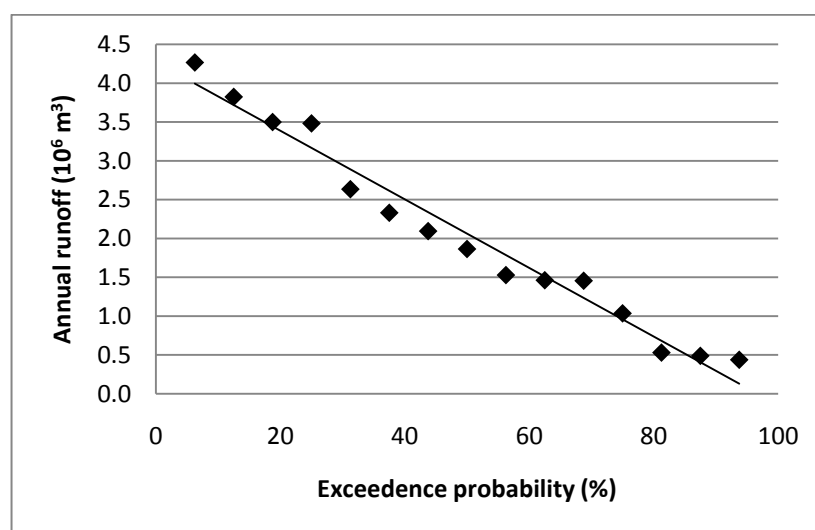
Figure 3.15. Cumulative frequency curve of annual flows of Eğri Creek.

Table 3.3. Volume of water that can be obtained for each exceedence probability.

EXCEEDENCE PROBABILITY (%)	RUNOFF VOLUME (10^6 m^3)	EXCEEDENCE RETURN PERIOD (year)
90	0.2952	1.1
80	0.7372	1.3
70	1.1792	1.4
60	1.6212	1.7
50	2.0632	2.0
40	2.5052	2.5
30	2.9472	3.3
20	3.3892	5.0
10	3.8312	10.0

3.4.3. Water Bearing Units

The lithologic units observed in the area show different characteristics in hydrogeological point of view. In the study area, main lithologic units can be divided into two subgroups; alluvial fan deposits and the Menderes Massif metamorphics. The cross sections drawn for the characterization of the subsurface lithological units indicate that the basement rocks are composed of gneiss and schist, which are overlain by talus, gravel, sand and silt with alternation of clay.

Alluvial fan, the most characteristic feature in the area, is of fluvial origin and observed along the foothills of the mountain ranges surrounding the basin. Alternation of talus, sand, silt and gravel define the alluvial fan material. Due to their high porosity, they provide an ideal environment for groundwater storage. Schist and gneiss define the mountain ranges in the study area. Due to the poor water storage and transmitting capacities, and absence of fractures, they are regarded as impervious (Yazıcıgil et al. 2000).

3.4.4. Hydraulic Parameters

Estimation of hydraulic parameters is a critical issue and directly affects the characterization of the system. Since hydrogeological models usually deal with aquifer simulations, estimation of saturated zone parameter is generally sufficient. However, in artificial recharge models, both saturated and unsaturated parameters should be taken into consideration.

3.4.4.1. Saturated Zone

Hydraulic parameters of the saturated zone include determination of specific yield, saturated hydraulic conductivity and storativity values, as well as the aquifer top and bottom elevations and water table elevations. Detailed maps, well logs and pumping test results are used for estimation of the parameters. The previous studies conducted by Yazıcıgil et al. (2000) were used for obtaining the saturated zone parameters.

Saturated hydraulic conductivity values derived from pumping test results performed in previous studies vary from 3.7 m/d to 20.4 m/d, with a geometric mean of 9.6 m/d in the study area. The 26 irrigation wells drilled by State Hydraulic Works (DSİ) were used to determine the areal extent of the hydrogeological units and saturated parameters. In the study area, saturated thickness of the aquifer varies from 5 m to 215 m.

3.4.4.2. Unsaturated Zone

The unsaturated zone is characterized by alluvial fan materials, which consist of alternation of talus, gravel, sand, silt and clay. Since the aquifer is unconfined in the study area, movement of recharged water in the unsaturated zone is directly controlled by the parameters of the unsaturated zone.

Depth of the unsaturated zone is observed to decrease from north to south. The depth ranges from 60 m to 20 m throughout the Eğri Creek subbasin, with an average depth of 45 m. Hydraulic parameters for the unsaturated zone is not available in the previous studies performed in the K. Menderes River Basin. Therefore, saturated hydraulic properties of the region determined from Yazıcıgil et al. (2000) and the unsaturated zone parameters of similar lithologies obtained from literature surveys were used to determine unsaturated hydraulic conductivity and volumetric water content functions of the Eğri Creek subbasin.

In the Eğri Creek basin, there are 26 wells drilled by State Hydraulic Works (DSİ). The distribution of the wells in the study area is shown in Figure 3.16. A 2D representation of unsaturated zone characteristics and subsurface environment is determined by cross sections drawn from well logs, whose locations are illustrated in Figure 3.17. The cross sections drawn from three locations along the basin are shown in Figures 3.18-3.21. The subsurface geology mainly consists of alternation of gravel, talus, sand and silt. This formation sometimes includes small amount of clay content but not in the form of thick bands or lenses. The bottom of the study area is composed of schist and gneiss. As seen from the cross sections, majority of the wells cannot reach the base rock. The bedrock elevation map obtained from Yazıcıgil et.
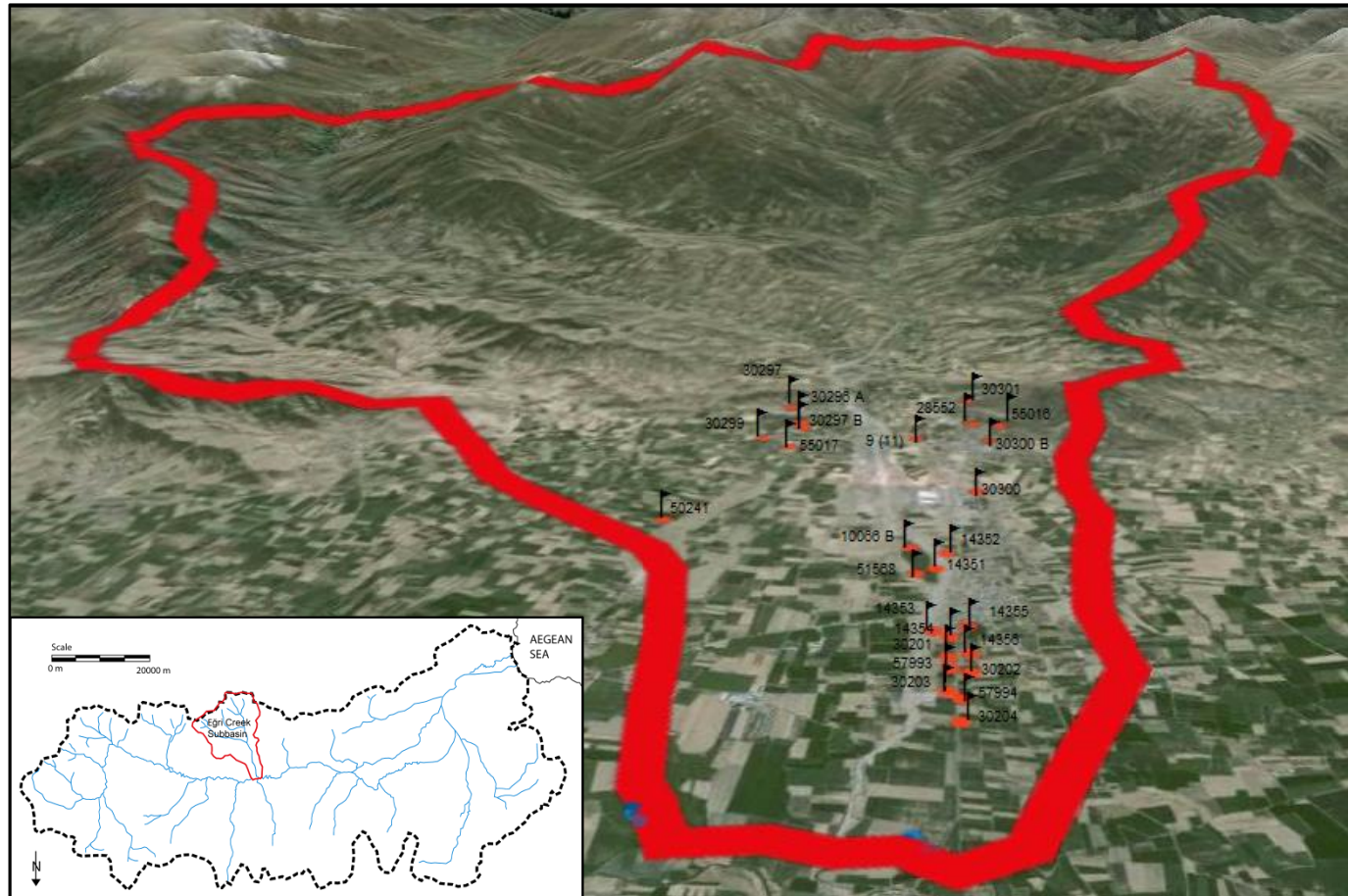
Figure 3.16. Distribution of wells drilled by DSİ in the Eğri Creek Basin (satellite map is taken from Google Earth).
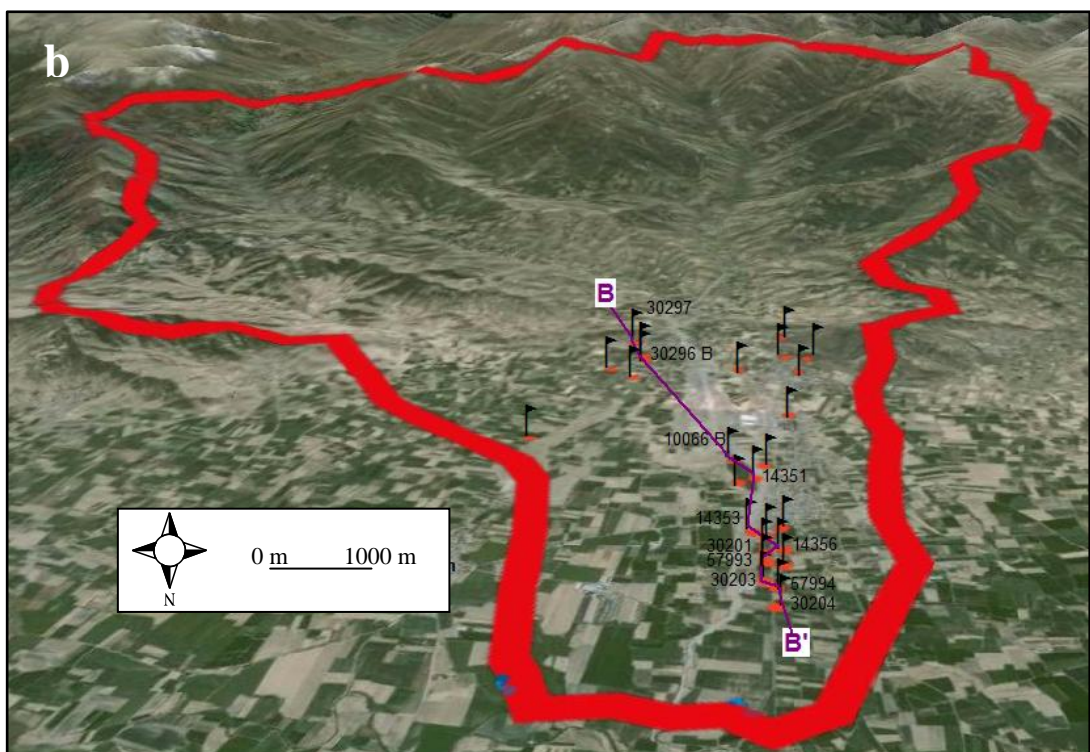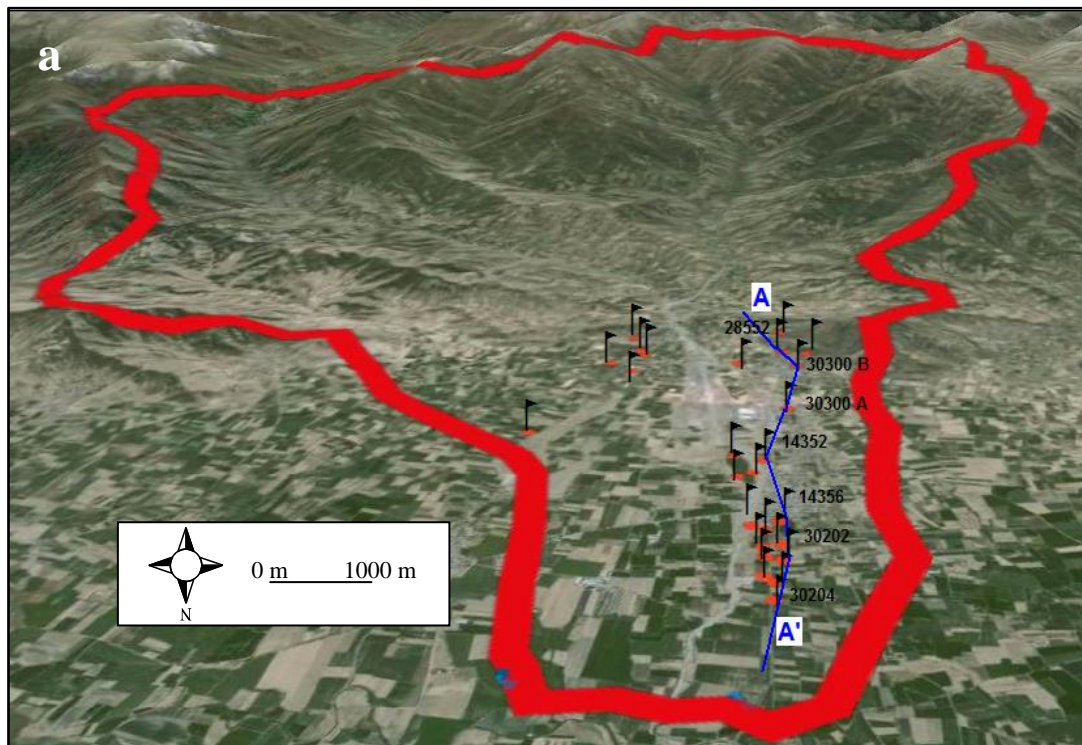
Figure 3.17. Cross section locations (the map from Google Earth): (a) for A-A' section; (b) for B-B' section; (c) for C-C' section.
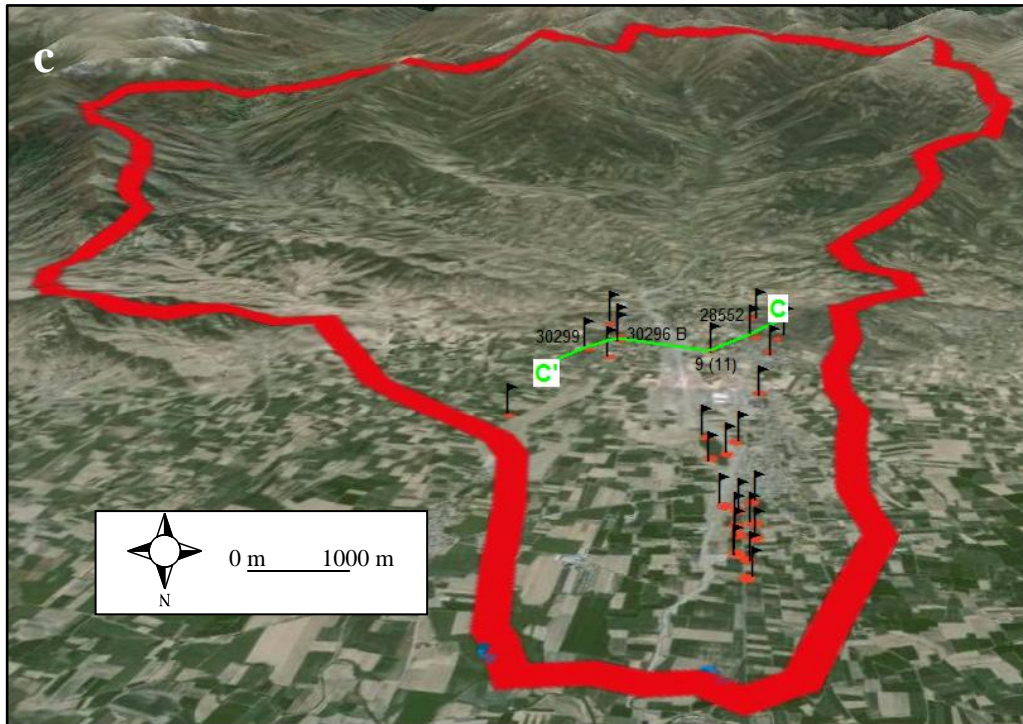
Figure 3.17. continued

al. (2000) based on geophysical surveys and boreholes was used to determine the location of the boundary between the schist-gneiss and the overlying alluvial fan deposits. It can be concluded that subsurface environment is dominated by highly porous materials, which is suitable for the applications of surface artificial recharge methods. A detailed explanation for the determination of unsaturated hydraulic properties can be found in the chapter entitled "Model Parameters and Calibration".
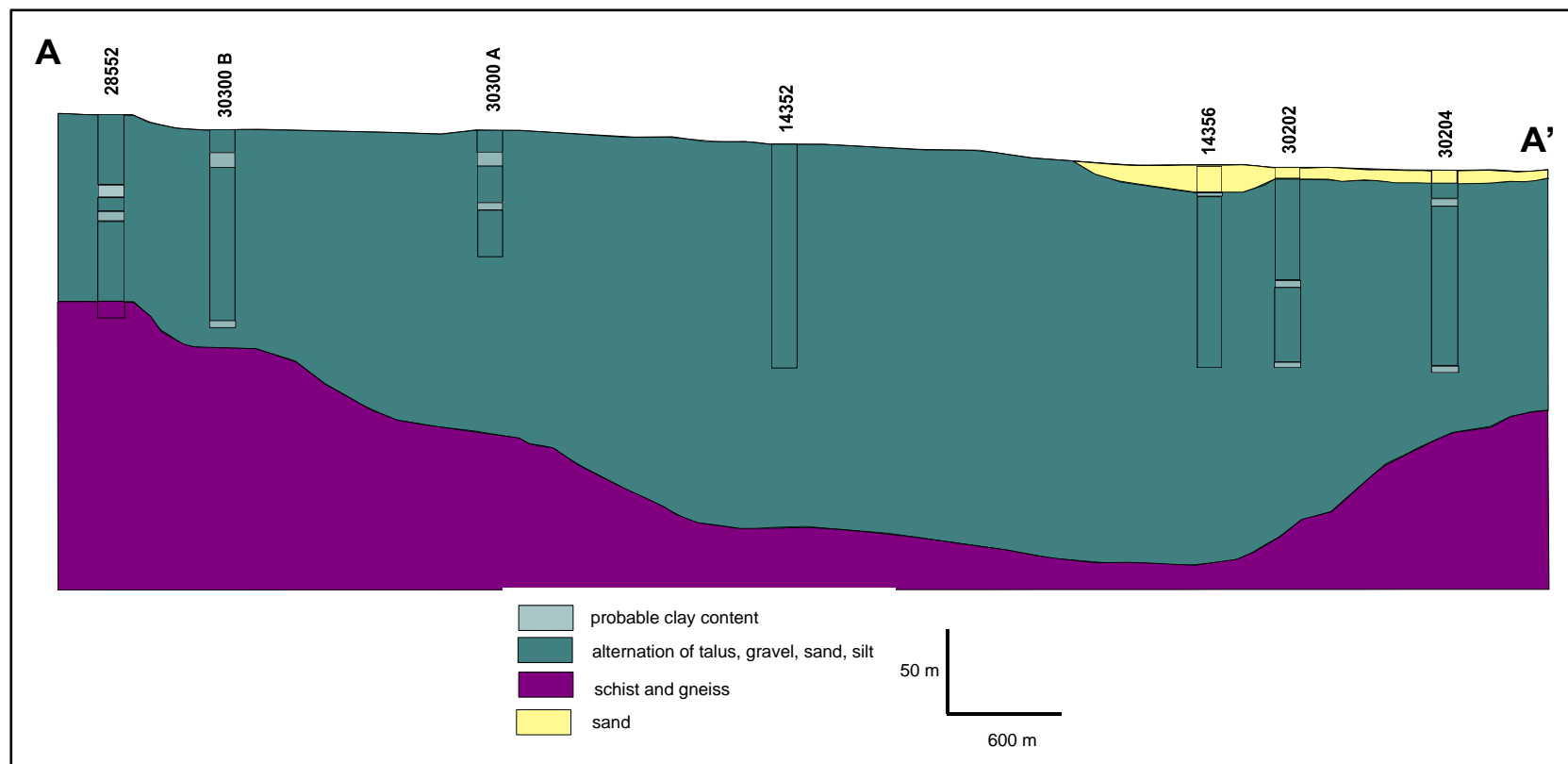
Figure 3.18. Cross section drawn from A-A'.
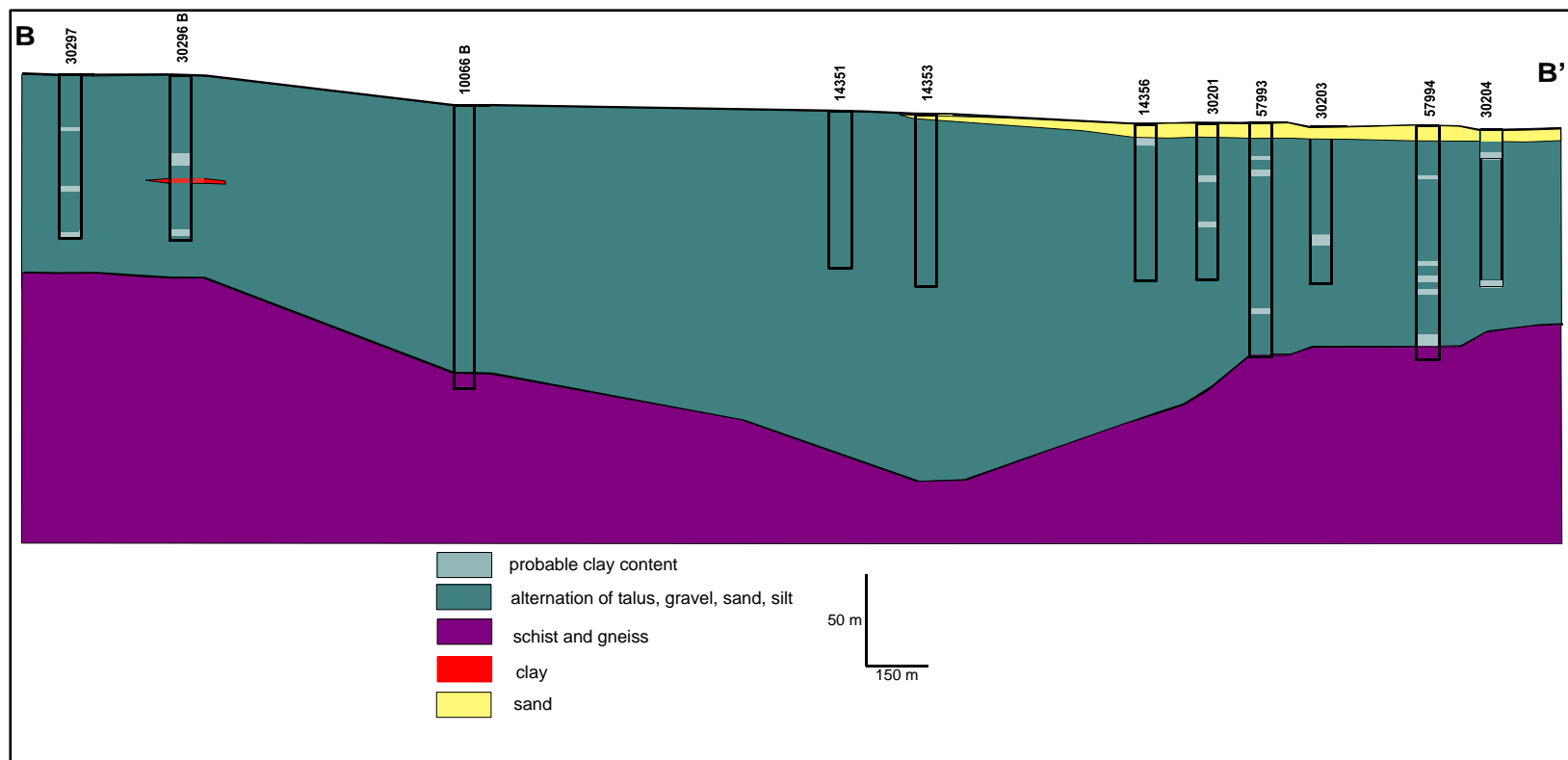
Figure 3.19 Cross section drawn from B-B'.
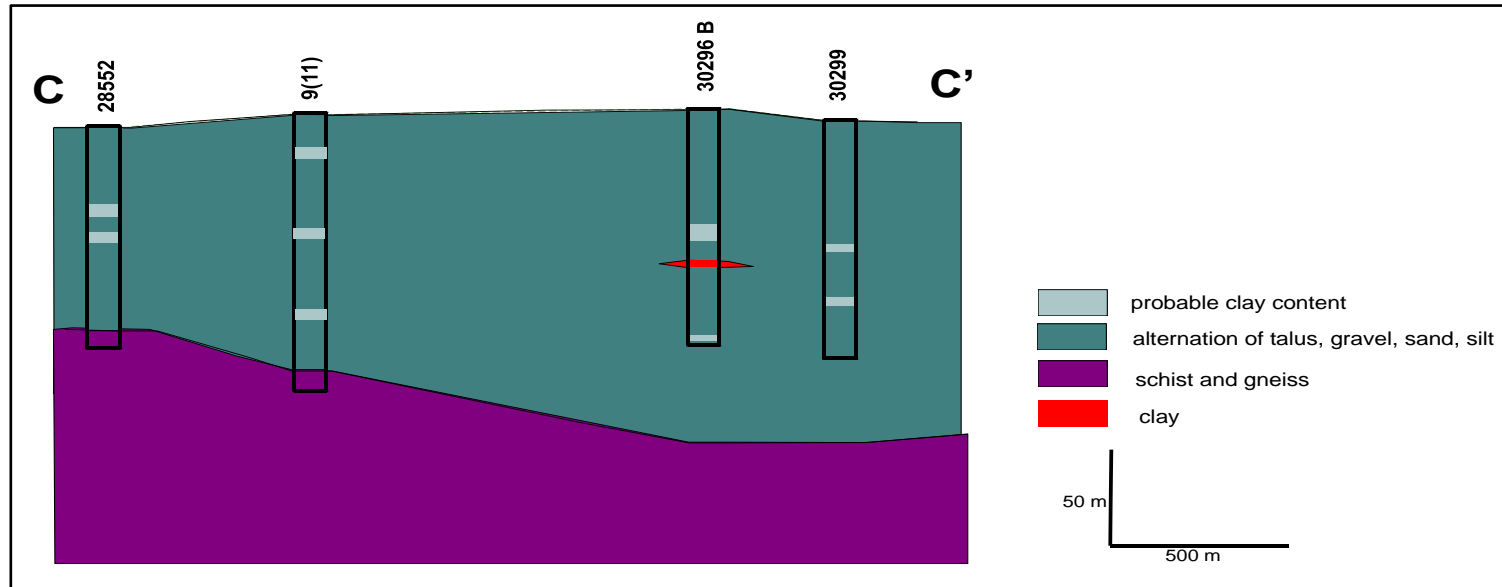
Figure 3.20. Cross section drawn from C-C'.

CHAPTER 4

MODELING METHODOLOGY

4.1.   Introduction

Model is a simplified representation of the real world by using mathematical equations (Wang and Anderson, 1982). The success of a model depends on the degree of how closely the mathematical equations approximate the physical system being modeled. A systematic approach should be followed in the modeling procedure.

The methodology of the recharge system design is defined by American Society of Civil Engineers (Reddy, 2008). The recharge system design starts with preliminary activities such as data collection, determination of processes involved in the system and conceptual model development. Then, in order to gain a better understanding of the system, field investigations and tests are performed. In the design phase; recharge system design, groundwater modeling, economic analysis and environmental assessments are completed. Design phase is followed by construction, operation and maintenance.

This study aims to show applicability of artificial recharge methods in the K. Menderes River Basin. Therefore, it includes preliminary activities and recharge system modeling. Before implementation of any recharge system, more detailed characterization of the site supported with field and laboratory tests are required.

4.2.   Unsaturated Zone Flow

Unsaturated zone is defined as the portion of subsurface above water table, which contains both air and water in the pores. It is used in many parts of hydrology, such

as infiltration, evaporation, groundwater recharge and soil erosion (Nielsen et al., 1986). Unsaturated zone flow is quite different and complex compared to saturated zone flow. Unlike saturated zone where the primary driving force is the gradient of a positive pressure potential; in unsaturated zone negative pressure (i.e. matric) potential is the primary driving force. Flow paths in unsaturated flow are tortuous since some pores are filled with air. Table 4.1 compares the main aspects of both saturated and unsaturated flows (Lal and Shukla, 2004).

Table 4.1. Summary of differences between saturated and unsaturated flows.

PARAMETER	SATURATED FLOW	UNSATURATED FLOW
Water content	constant	Variable over space and time
Air content	zero	Variable over space and time
Potential gradient	Positive and constant	Negative and variable
Hydraulic conductivity	Maximum, constant	Low and variable
Flow paths	continuous	Tortuous
Continuity equation	Inflow=outflow	Inflow = outflow + source/ sink
Flow parameter	K_s	$K(\Theta)$
Flow description	Darcy's law	Darcy- Buckingham equation Richards equation

4.2.1. Unsaturated Flow Equation

Darcy's equation, which is originally derived for flow of water in saturated conditions, also adapted in unsaturated conditions with some provisions. In unsaturated conditions, hydraulic conductivity is no longer constant but varies with changes in water content and indirectly varies with changes in pore-water pressures. The conversion of Darcy's law in unsaturated zone flow is known as Richard's equation, which is obtained from combination of Darcy-Buckingham equation with continuity equation (Kim et al., 1996).

Vertical flow in unsaturated zone is described by Darcy-Buckingham equation as:

$$q(\psi) = -k(s)\left[\frac{\partial \psi}{\partial z} + 1\right]$$

(4.1)

where q: unsaturated water flux

    k: hydraulic conductivity

    s: degree of saturation ($0 \leq s \leq 1$)

    ψ: soil matric head (≤ 0)

    z: vertical coordinate (positive upward)

Continuity relation can be expressed as:

$$\theta_s \frac{\partial s}{\partial t} = -\frac{\partial q}{\partial z}$$

(4.2)

where s: degree of saturation and equals to Θ / Θ_s

    Θ_s: saturated value of moisture content

    Θ: moisture content

Richard's equation is obtained by combining (4.1) and (4.2):

$$\theta_s \frac{\partial s}{\partial t} = \frac{\partial}{\partial z}\left(k(s)\left[\frac{\partial \psi}{\partial z} + 1\right]\right)$$

(4.3)

The same equation can also be expressed as follows:

$$\frac{\partial \theta}{\partial t} = \frac{\partial}{\partial z}\left[K(\theta)\left(\frac{\partial \psi}{\partial z} + 1\right)\right]$$

(4.4)

where K: unsaturated hydraulic conductivity and depends on water content

    Ψ: matric suction

    Θ: moisture content

The dependence of both water content and hydraulic conductivity on matric suction in unsaturated zone is resulted in nonlinearity, which leads to the numerical methods for the solution of flow equation.

4.2.2. Unsaturated Soil Hydraulic Properties

Flow of water in unsaturated zone is controlled by two factors; unsaturated hydraulic conductivity and volumetric water content of the soil. Their accuracy determines the accuracy of flow in the soil.

4.2.2.1. Unsaturated Hydraulic Conductivity

When the soil is saturated, all pores are water filled and conducting. The water phase is continuous and conductivity is at maximum. When the soil desaturates, some pores become air filled, thus the conductive portion of the soil's volume diminishes, and tortuosity increases. When the suction develops, the first pores to be emptied are the largest ones, which are the most potentially conductive. Therefore, unsaturated hydraulic conductivity is less than saturated conductivity, and it is a function of matric suction and also related to water content (Hillel, 2008). Unsaturated hydraulic conductivity mainly depends on soil textures.

Direct measurement of unsaturated hydraulic conductivity is difficult, time consuming, expensive and requires simplified assumptions. To overcome this situation, mathematical models are formed by using measured or predicted volumetric water content function (Neilsen et al., 1986). The closed form equations derived by Fredlund et al. (1994), Green and Corey (1971) and Van Genuchten (1980) are widely used for the estimation of unsaturated hydraulic conductivity. In the literature, Van Genuchten (1980) closed form equation is the most common method.

Van Genuchten equation estimates unsaturated hydraulic conductivity function from saturated hydraulic conductivity and two curve fitting parameters. The equation is expressed as:

$$k_w = k_s \frac{\left[1-(a\psi^{(n-1)})(1+(a\psi^n)^{-m})\right]^2}{\left(((1+a\psi^n))^{\frac{m}{2}}\right)} \tag{4.5}$$

where k_s: saturated hydraulic conductivity

a, n, m: curve fitting parameters

n=1/(1-m)

ψ: required suction range

4.2.2.2. Volumetric Water Content (VWC) Function (Soil Moisture Characteristic Curve)

In saturated soils, since all pores are filled with water, volumetric water content (VWC) of soil equals to its porosity. In unsaturated soils, volume of water stored in the voids varies due to matric suction (i.e. negative pore water pressure) within pore-water. VWC function is used to determine the capacity of soil to store water under changes in matric pressures. Since water content changes with time and space, it is defined by a function (Hillel, 2008).

Soil moisture characteristic curve is described by two inflection points: Air-entry suction and residual water content. When a slight suction is applied to a saturated soil, the suction reaches a point where the largest surface pore begins to empty, and its water content is displaced by air. This critical point is known as air-entry suction. Air entry suction is generally small in coarse- textured and well aggregated soils having large pores, whereas relatively large in fine- textured, poorly aggregated soils. The point where the increase in suction causes no more decrease in water content is defined as residual water content (Geo-slope international, 2007).

VWC is influenced by the size of individual soil particles and distribution of particle sizes in the soil. Materials with uniform pore sizes drain under a small range of matric suction, thus resulting in steep functions.

The VWC function can be obtained by two ways; desorption (i.e. starting from a saturated soil and applying increasing suction to gradually extract water while taking continuous measurements of remaining soil moisture) or sorption (i.e. by gradually wetting an initially dry soil while reducing the suction). Both methods result in continuous curves which are not identical, known as hysteresis (Figure 4.3). Generally, equilibrium soil wetness at a given suction is greater in desorption than sorption. Since the pores in the soil are irregular in shape and connected by narrow necks, the process of sorption and desorption do not follow the same pattern (Hillel, 2008). In practice, only the main drying curve is often used to describe the relation between water content and matric suction.
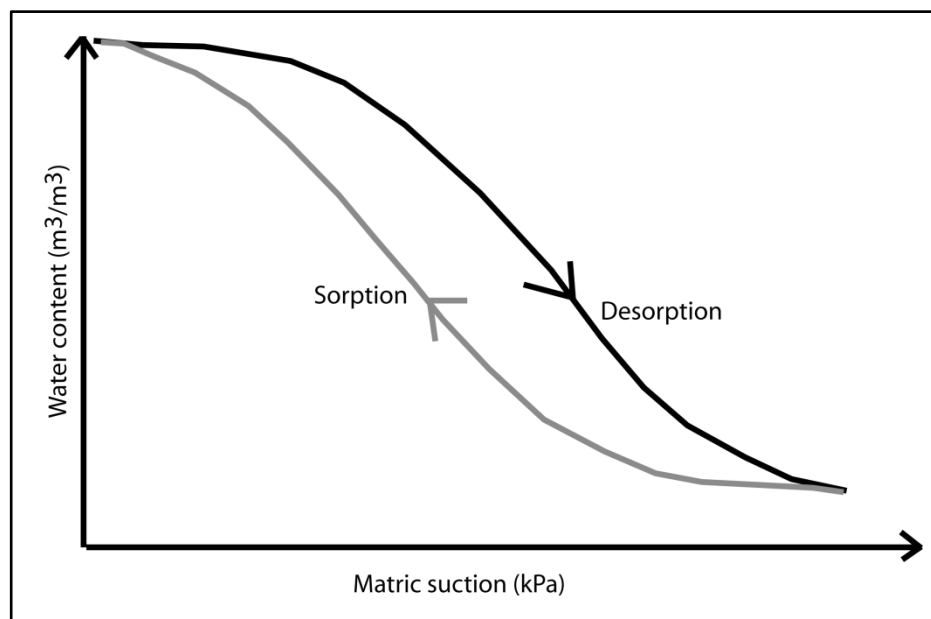
Figure 4.1. Hysteresis effect.

Field measurements require the use of tensiometers for the measurement of hydraulic gradients. Gravimetric methods (by taking a soil sample and determining its moist and dry weights, by weighting at the time of sampling and after dried in an oven for 24 hours, respectively), neutron or gamma ray techniques (Nielsen et al., 1986) are examples of some methods to carry out these measurements. On the other hand,

laboratory measurements are quite expensive and time consuming. As an alternative, estimation methods are used to obtain VWC function based on basic material properties or curve fitting parameters. Aubertin et al. (2003), presented a method to compute VWC by using basic material properties (from grain size analysis). Fredlund and Xing (1994) and Van Genuchten (1980) developed a closed form solution to predict the function.

For the prediction of VWC function, Van Genuchten solution is mostly preferred. The governing equation is as follows:

$$\theta_w = \theta_r + \frac{\theta_s - \theta_r}{\left[1 + \left(\frac{\psi}{a}\right)^n\right]^m} \tag{4.6}$$

where Θ_w: volumetric water content

Θ_s: saturated volumetric water content

Θ_r: residual volumetric water content

Ψ: negative pore water pressure

a, n, m: curve fitting parameters

where a: inflection point of the VWC function and slightly larger than air-entry value ($a = \psi_i$)

m: controls the residual water content

n: controls slope of VWC function

In the literature, the curve fitting parameters can be found for most of the soil types.

4.3. Subsurface Flow Model

4.3.1. Model Description

Model is the simplified version of a physical system and the key advantage of using a model is enhancing engineering judgment. Since hydrogeological relations within a

system is defined in the form of mathematical equations, a mathematical model is used to describe the flow process. A set of partial differential equations together with determination of system geometry, parameters and boundary and/or initial conditions are required for the modeling (Chapuis, 2001).

Numerical solutions are used for more complex situations, which is usually the case in real world. In unsaturated zone, dependence of both water content and hydraulic conductivity on matric suction results in highly nonlinear conditions, which requires numerical methods for the solution of flow equation.

Numerical methods involve subdividing the domain into small, finite pieces, which is known as discretization. Each sub-domain is called an element, and they are composed of a series of nodal points. The overall solution is achieved by describing the behavior of individual pieces, subsequently solving them and reconnecting all pieces. In numerical models, governing equations can be solved by either finite difference or finite element methods. Finite difference method uses rectangular elements, which restricts its usage in irregular, complex systems. It is simple and efficient in treating time derivatives. Finite element method, on the other hand, has the ability to describe irregular boundaries and non-homogeneous systems. A variety of element types result in more accurate description of the system.

4.3.1.1. Computer Code Selection

In this study, the modeling of recharge basins for the applicability of artificial recharge of groundwater in the K. Menderes River Basin was achieved by using SEEP/W software.

SEEP/W is a 2D finite element software developed by Geo Studio (2007). It is used to analyze groundwater seepage (which refers to the movement of water through soil regardless of the source of driving force or flow being saturated or unsaturated) and problems concerning excess pore water pressure distribution within porous media. SEEP/W can be applied for a wide range of problems; from simple saturated steady

state problems to complex saturated-unsaturated time dependent problems. Typical examples include:

- Dissipation of excess pore pressure after reservoir drawdown
- Changes in pore-water pressure conditions within earth slopes due to infiltration of precipitation
- Mounding of the groundwater table beneath water retention structures
- Effect of subsurface drains and injection wells
- Drawdown of water table due to pumping from an aquifer
- Seepage flow quantities into excavations

In this study, feasibility of artificial recharge methods in the Eğri Creek subbasin was investigated. The recharge water is expected to infiltrate below the ground surface, reach water table and consequently increase groundwater levels. The problem involves unsaturated-saturated, time dependent flow with complex material functions and boundary conditions. Besides, 2D representation of the system provides complete understanding of the processes. Thus, SEEP/W can be thought to be a comprehensive tool for artificial recharge modeling.

4.3.1.2. Mathematical Model

SEEP/W is formulated on the basis of Darcy's law, which can be used for saturated as well as unsaturated conditions with some provisions. In unsaturated soils, hydraulic conductivity is related to water content and the changes in pore water pressures.

The general governing differential equation for 2D seepage is expressed as follows:

$$\frac{\partial}{\partial x}\left(k_x \frac{\partial H}{\partial x}\right) + \frac{\partial}{\partial y}\left(k_y \frac{\partial H}{\partial y}\right) + Q = \frac{\partial \theta}{\partial t} \qquad (4.7)$$

where H: total hydraulic head

k_x, k_y: hydraulic conductivity in x and y directions, respectively

Q: applied boundary flux

Θ: volumetric water content

t: time

Changes in volumetric water content depend on the change in stress state and soil properties. The stress state can be described as $(\sigma - u_a)$ and $(u_a - u_w)$ for both saturated and unsaturated conditions, where σ is total stress, u_a and u_w are pore- air and pore-water pressures, respectively. SEEP/W is formulated for conditions of constant total stress and assumes pore-air pressure remains constant at atmospheric pressures under transient conditions. Thus, the changes in volumetric water content depending only on the changes in pore water pressures, which can be shown as:

$$\partial\theta = m_w \partial u_w \tag{4.8}$$

where m_w: slope of the storage curve

u_w : pore water pressure where $u_w = \gamma_w (H-y)$

Thus, SEEP/W finite element equation can be formed as:

$$\frac{\partial}{\partial x}\left(k_x \frac{\partial H}{\partial x}\right) + \frac{\partial}{\partial y}\left(k_y \frac{\partial H}{\partial y}\right) + Q = m_w \gamma_w \frac{\partial H}{\partial t} \tag{4.9}$$

4.3.1.3. Numerical Solution

In an abbreviated form, finite element seepage equation can be expressed as:

$$[K]\{H\} + [M]\{H\}, t = \{Q\} \tag{4.10}$$

where   [K]: element characteristics matrix

[M]: element mass matrix

{H}: nodal head vector

{Q}: element applied flux vector

t: time

SEEP/W applies Galerkin method of weighed residual to the governing equation to derive 2D finite element seepage equation, which is:

$$\tau \int_A ([B]^T [C][B]) dA\{H\} + \tau \int_A (\lambda < N >^T < N >) dA\{H\}, t = q\tau \int_L (< N >^T) dL$$

(4.11)

where [B]: gradient matrix

[C]: element hydraulic conductivity matrix

{H}: vector of nodal heads

<N>: vector of interpolating function

q: unit flux across the edge of an element

τ: thickness of an element

t: time

λ: storage term for a transient seepage equals to $m_w\gamma_w$

A: a designation for summation over the area of an element

L: a designation for summation over the edge of an element

The solution of finite element equation is conducted by iterative numerical techniques to match computed primary variable and material properties. Solution will be executed until a maximum number of iterations is obtained or the nodal head vector between two successive iterations becomes less than the specified tolerance. If the difference is greater than the tolerance, the iteration process continues until it reaches a maximum number of iterations.

4.3.2. Conceptual Model

Conceptual model development is the main and most important step in modeling procedure. Conceptual model enables a detailed characterization of the system, extent of the model geometry and distribution of materials.

As indicated in previous chapter, the study area consists of two main geological units; the basement rocks of schist and gneiss, and the overlying alluvial fan deposits. In terms of water bearing capacities, the alluvial fan deposits are the main unit which allow flow of groundwater due to high porosity. The other unit, that is composed of schist and gneiss form an impervious boundary, where no flow is observed. Hence, the flow takes place within alluvial fan deposits which consist of combination of coarse and fine materials, i.e. gravel, talus, sand, silt alternation. Cross sections drawn from well logs indicate that the subsurface geology does not contain any impeding clay layers with significant thickness or extend. The aquifer in the study area is defined as unconfined. The flow in the area is northerly directed, towards the K. Menderes River.

Conditions of a thick unsaturated zone, the presence of alluvium and permeable material, as well as existence of an unconfined aquifer suggest that artificial recharge of groundwater can be achieved via surface spreading methods (see Table 2.1). With the implementation of a numerical model, the success of artificial recharge of groundwater in the K. Menderes River basin will be discussed.

4.3.3. Numerical Model

4.3.3.1. Model Domain

Hydrogeological investigations reveal that the Eğri Creek subbasin is suitable for surface artificial recharge applications. An optimally suitable site would be one that consists of highly permeable soils, have the capacity for horizontal flow at the aquifer boundary, and is lack of impeding layers and a thick unsaturated zone. Since SEEP/W uses a 2D representation of the subsurface, in this study a section with a

length of about 5.1 km and thickness of 1 m along Eğri Creek bed was selected to model.

In selection of the model domain, some factors were taken into consideration. As a source of recharge water, excess flows of the Eğri Creek were chosen. Therefore, the model domain should be located at the downstream side, along a gentle topography to collect and infiltrate water. Also, the model area should be away from settlements to make construction of recharge basins possible. Besides, the area should not contain any confining layers.

The model domain was selected based on these conditions and with the help of Google earth maps (Figure 4.2). The hydrological parameters in the domain were interpreted from the cross section, which was drawn from projection of well logs located near the section (Figure 4.3). Projected well locations along the model domain were represented by numbers from 1 (referring to well number 30301) to 16 (referring to well number 30204), in order to avoid confusion. The model domain contains projections of sixteen wells and their logs were used to determine unsaturated and saturated parameters. Schematic view of the subsurface material based on the projection of well logs is given in Figure 4.4.

4.3.3.2. Finite Element Grid

Discretization or meshing is a critical step in numerical modeling. Discretization involves division of the system that is being modeled into small pieces where the governing equations are solved to obtain the overall solution. In terms of finite element method, the model domain is divided into small parts, known as elements, the shape of which can be rectangular, triangular or quadrilateral. In each element block, hydrogeological parameters are assumed to be uniform.

The number of finite equations to be solved is equal to the number of nodes located along element edges. Although smaller elements result in more accurate simulations, more time and computer memory is required to obtain the solution.

Determination of size and shape of elements depends on the model geometry and aim of the study. In order to obtain the most suitable mesh size and shape, trial and error method was used, where the effect of each mesh type on the solution was investigated. As a result, the quads and triangular type gave the best results, and hence was selected. The element size in the model was assigned as 10 m with a width of 1 m, which resulted in 6967 nodes and 6498 elements (Figure 4.5). Since the flow equations are highly nonlinear and the respond of water table to recharge is critical, smaller mesh size was used.

4.3.3.3. Boundary Conditions

One of the important parts of numerical modeling is assigning boundary conditions. It is not an easy task to convert real processes that take place on the boundary into mathematical relations. In order to obtain realistic results, boundary conditions should be assigned carefully.

The model boundaries were determined from both geological and hydrogeological characteristics of the study area. Based on the data obtained from geological and hydrogeological investigations, and cross sections; the model domain can be defined by the schist and gneiss in the southern edge and at the bottom; while the alluvial fan materials are in the other directions. Since the flow of recharge water is modeled in 2D by surface recharge methods, the upper part of the domain is represented by ground surface. Basically the schist and gneiss are represented by no flow boundary, and thus they were not included in the solution of the flow equation. Hence, the bottom and southern edge of the area is represented by no flow condition. Since the ground surface is exposed to meteorological events, a flux-type boundary condition was chosen to represent recharge. The northern part of the study area is the part where groundwater flow is directed to the K. Menderes River. The northern boundary is expressed with a flux-type boundary condition, which represents flow of water out of the system (Figure 4.6).
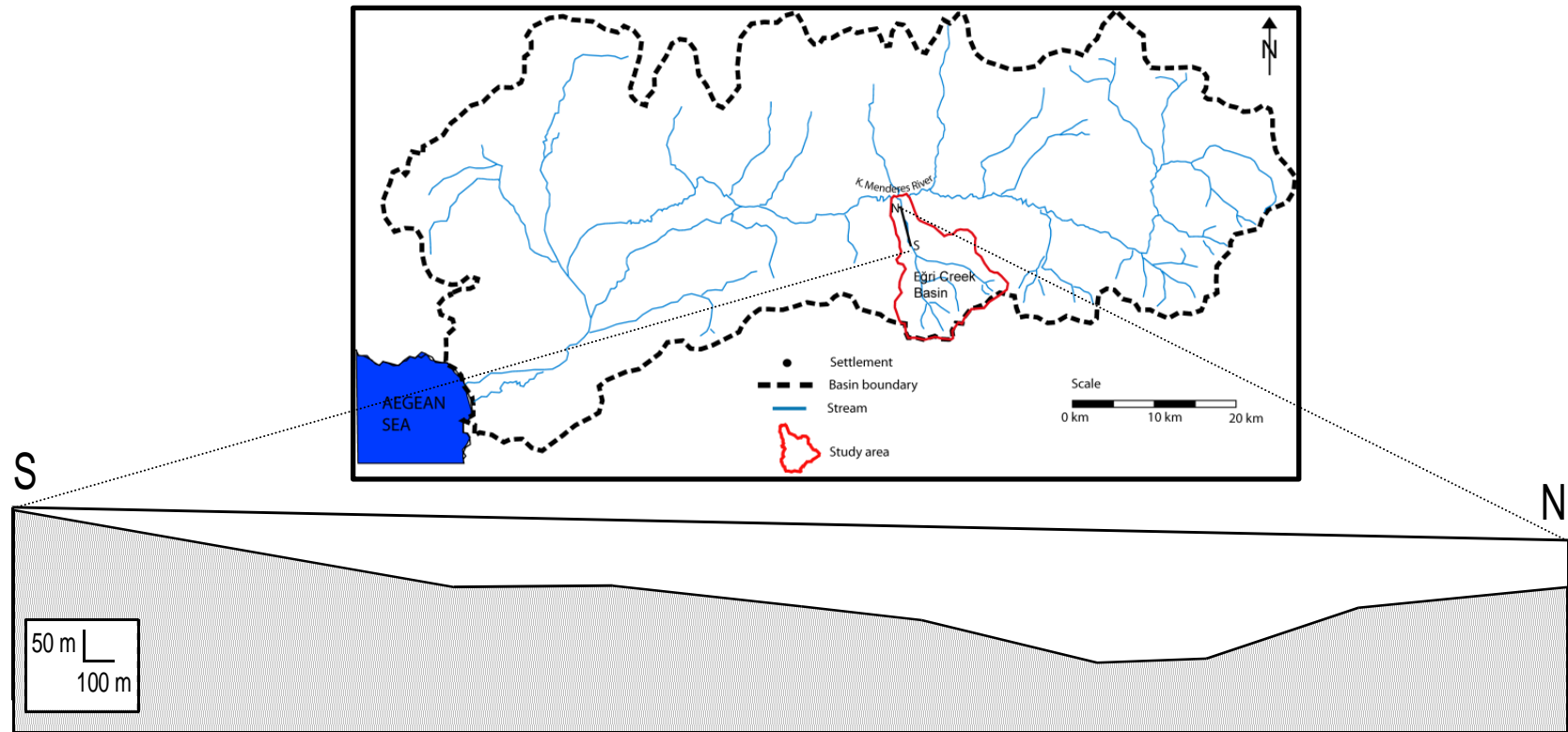
Figure 4.2. Configuration of model domain in Eğri Creek subbasin.
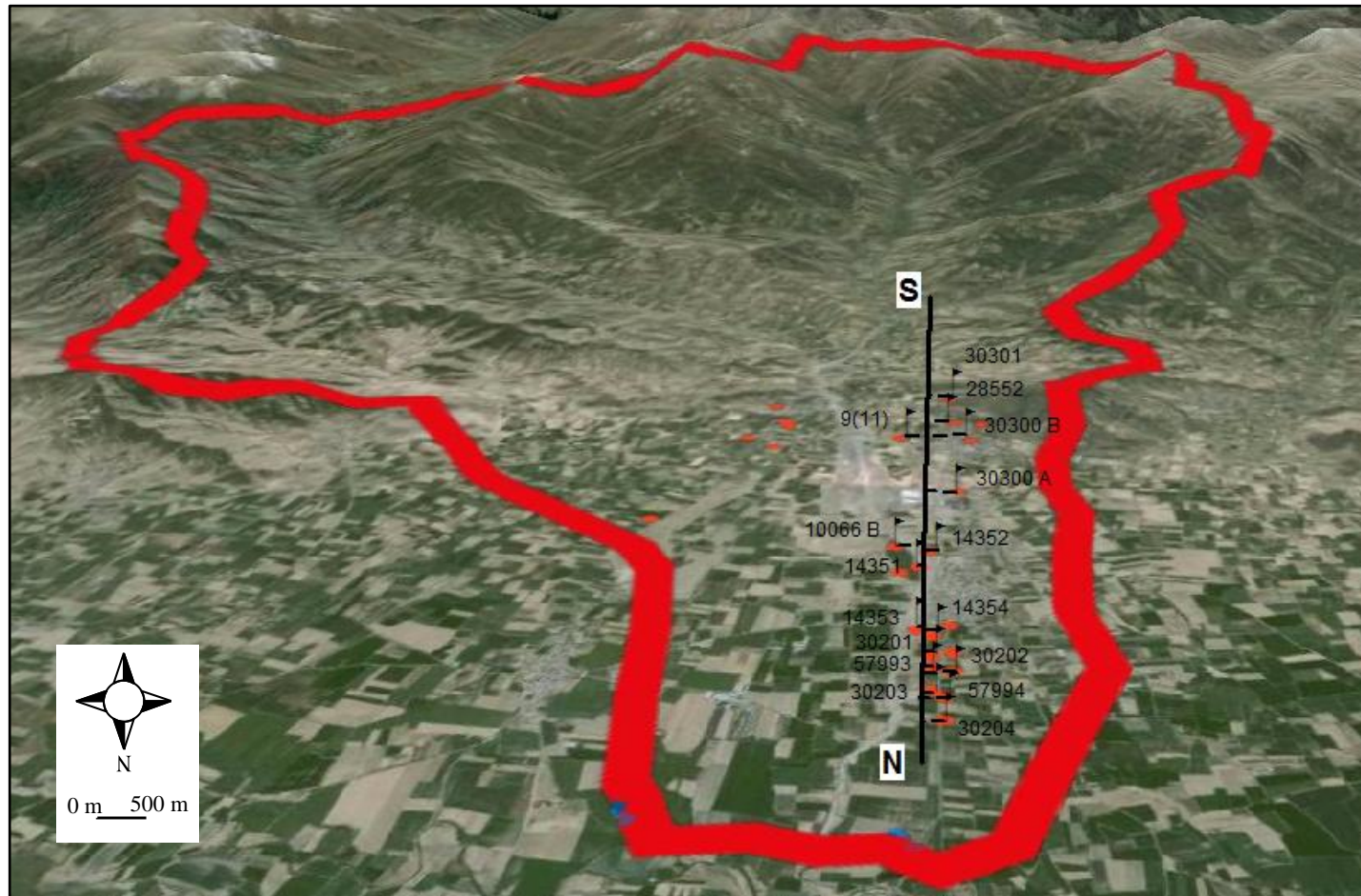
Figure 4.3. Model domain showing projected wells (the map from Google Earth).

59
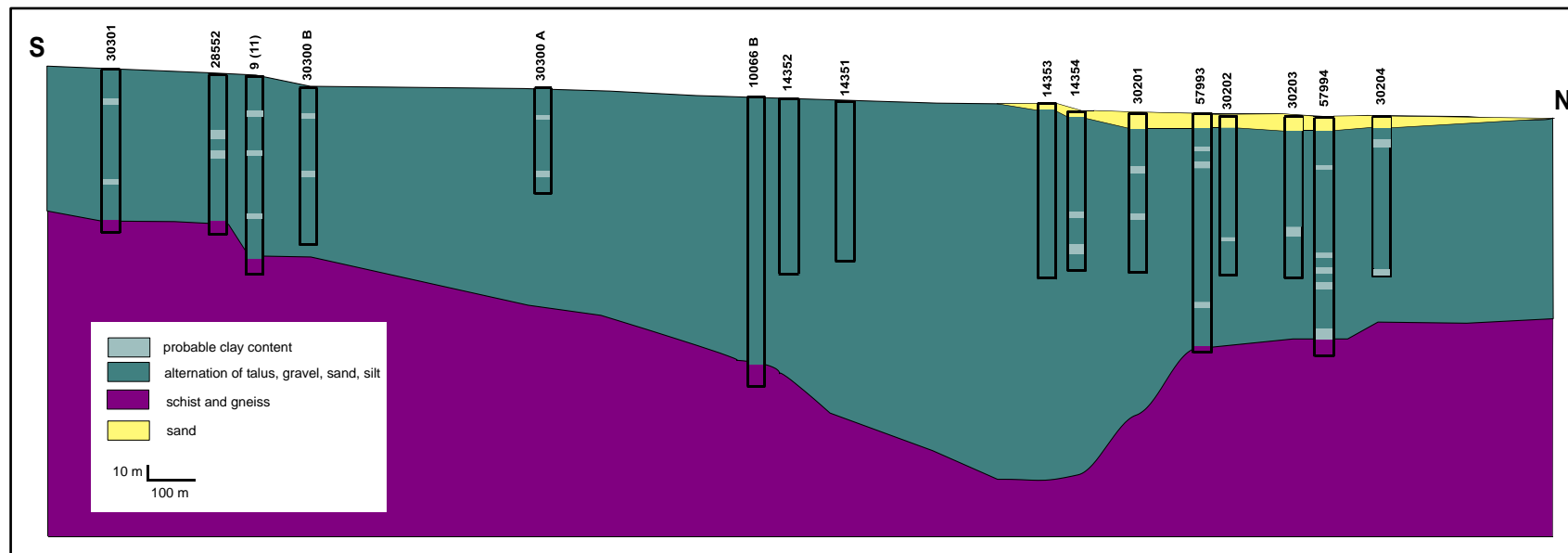
Figure 4.4. Schematic view of subsurface material types in the model domain.
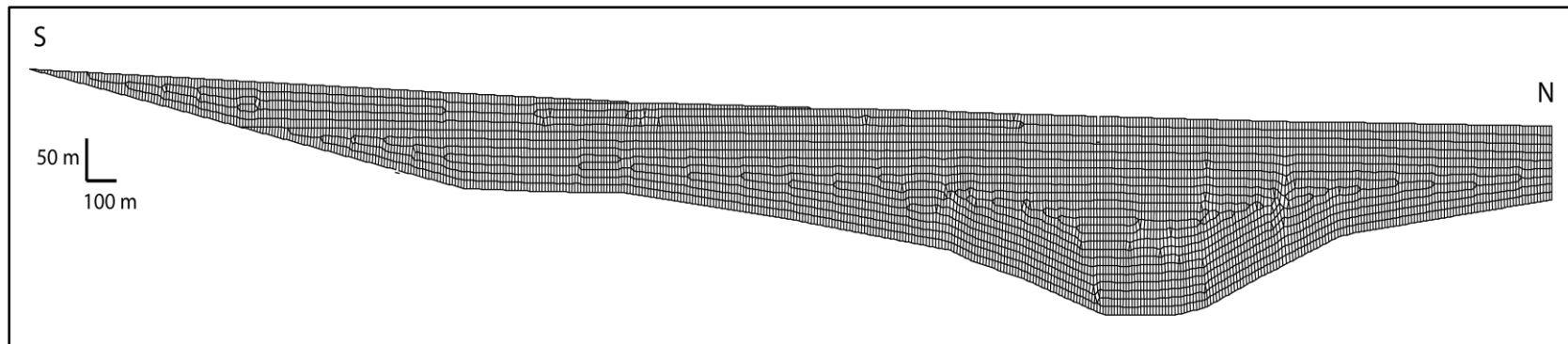
Figure 4.5. Distribution of finite element mesh along the domain.
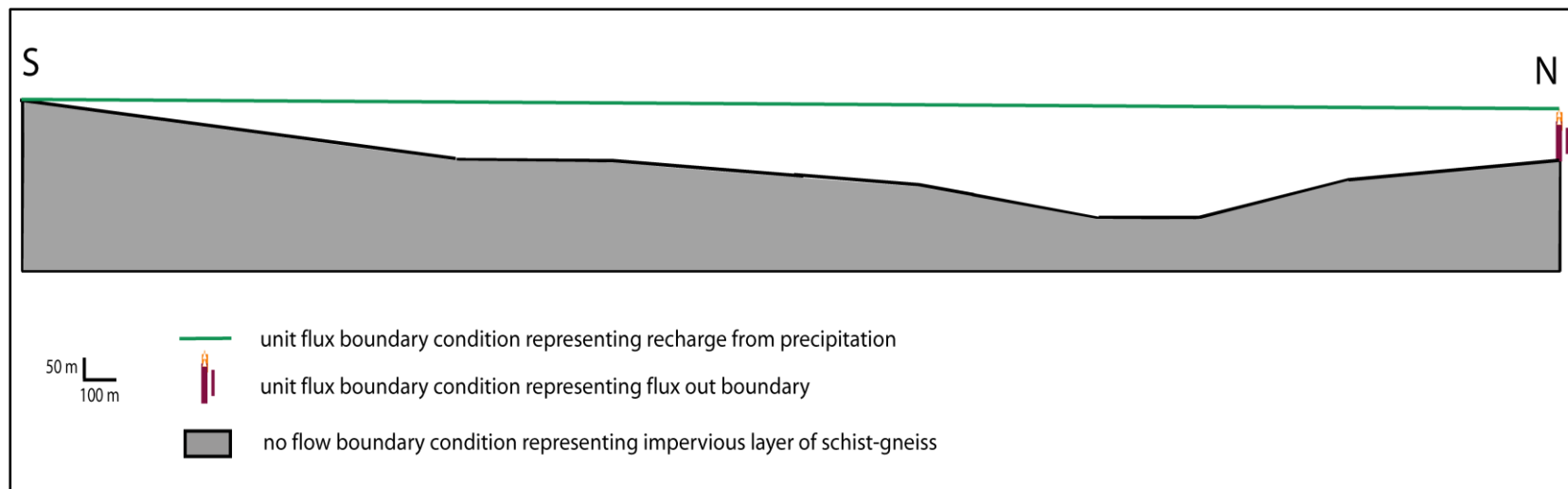
Figure 4.6. Boundary conditions used in the model.

CHAPTER 5

MODEL PARAMETERS AND CALIBRATION

5.1. Model Parameters

The modeling procedure includes basically three main parts; discretization, applying suitable boundary conditions, and assigning material properties. Geological and hydrogeological mapping, well log data, field and laboratory tests are some methods where material properties can be gathered. Saturated- unsaturated flow modeling requires determination of both unsaturated and saturated hydraulic conductivities, and volumetric water content function as hydraulic parameters. In addition, the recharge and discharge parameters have to be added to complete model set up. Since each site is unique in terms of its hydrogeology, the determination of model parameters is based on the response of assigned properties to the field observations.

5.1.1. Hydraulic Parameters

5.1.1.1. Saturated Hydraulic Conductivity

The saturated hydraulic conductivity value is present for eight out of 16 wells that are used to represent model domain. These values range from 3.7 m/d to 20.4 m/d with a geometric mean of 9.6 m/d. An average value was initially assigned to the model, assuming that the subsurface material is uniform within the domain. However, the calibration results were not successful with uniform material property. Thus, the domain was divided into two regions based on the distribution of measured conductivity values. The saturated hydraulic conductivity value of each region was obtained from geometric mean of the measured data. The saturated hydraulic conductivity values measured for projected wells along the domain are shown in

Table 5.1. In addition, resultant saturated hydraulic conductivity distributions within the model are illustrated in Figure 5.1.

5.1.1.2. Volumetric Water Content Function

Volumetric water content (VWC) function is an important factor for the modeling of subsurface flow. It describes soil capacity to store water under changes in matric pressure. Grain size analysis, in-situ and laboratory tests can be conducted to obtain the function. However, in the absence of site specific analysis, the initial volumetric water content function in the model was determined by examining literature and gathering the related information from the analyses performed on similar soil types.

Volumetric water content functions for various soil types are available in the literature. Figure 5.2 shows some examples of published functions. These functions are obtained experimentally by measuring the water content of different soil types. Some estimation methods are also available to determine these functions. These formulations use saturated volumetric water content (i.e. porosity) and some parameters determined from actual measurements of similar soils to produce a continuous curve. SEEP/W uses Van Genuchten estimation method to draw the VWC curves. As mentioned earlier in the modeling methodology, Van Genuchten estimation formula uses saturated and residual water contents plus curve fitting parameters to obtain the change in water volume with respect to changes in matric suction. The curve fitting parameters are observed from soil-water retention data and referenced in the literature (Osman and Bruen, 2002; Al-Yahyai, R. et. al., 2006; Mallants, D. et. al., 1999).

Table 5.1. Saturated hydraulic conductivity values present in the model domain.

Well numbers	1	2	3	4	5	6	7	8	9	10	11	12	13	14	15	16
Saturated hydraulic conductivity, K_{sat} (m/d)	6.5	5	3.7	-	-	-	-	15.1	-	-	13.6	-	11.8	11.8	-	20.4
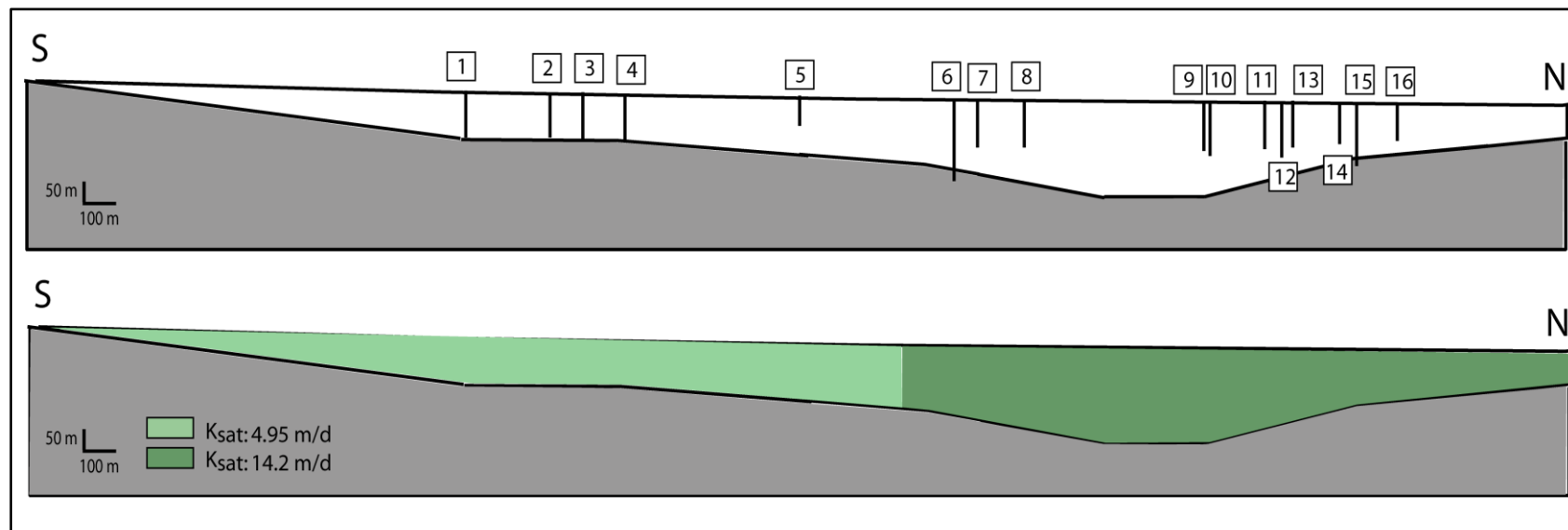
Figure 5.1. Saturated hydraulic conductivity distribution in the model domain.
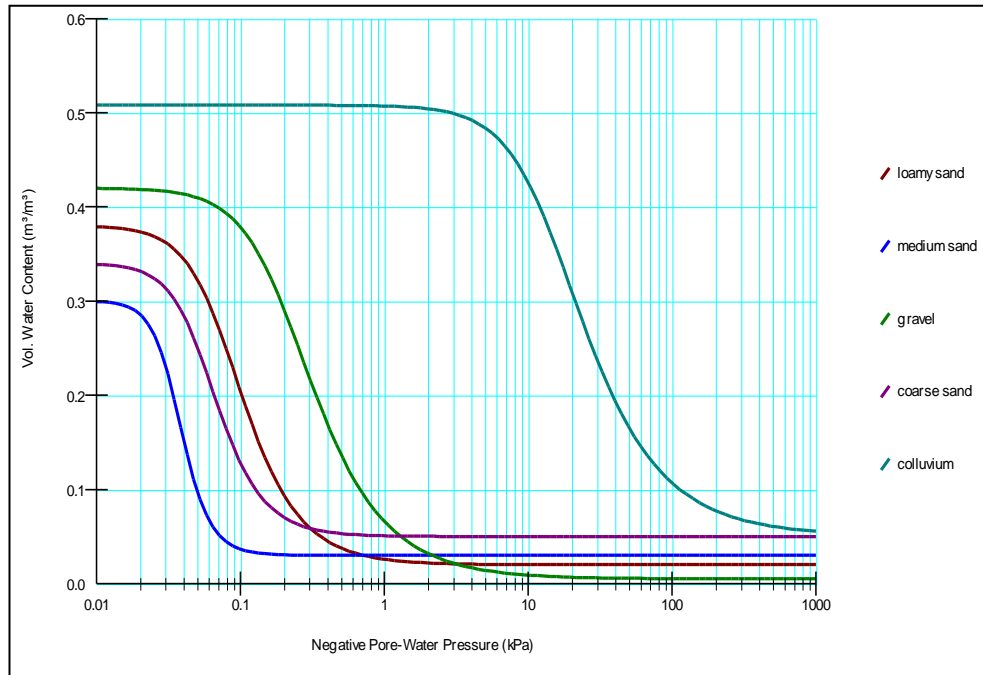
Figure 5.2. Volumetric Water Content functions from literature.

Initially, the model domain was assumed to be made up of single soil type, since the only lithologic unit in the domain is the alluvial fan deposits. Since the alluvial fan deposits are composed of coarse and fine materials, the function is expected to lie between colluvium and medium sand graph. In the model, sandy loam function was selected first, since it best describes the combination of coarse and fine particles. Then, the modeling was conducted under transient conditions for the period between October 1998 and April 1999 using the October 1998 measured water levels as initial conditions. The model was calibrated against the measured water levels in April 1999. However, it was impossible to match the measured groundwater table profile of April 1999 when sandy loam function was used in the model. In the unsaturated flow equation, volumetric water content function is represented by its slope.

Therefore, by modifying the slope of volumetric water content curve of the sandy loam, the runs were repeated. It is seen that steeper slope reflects the material properties better than gentler slope. Although changing the slope of the function gave a relatively better match between the measured and observed groundwater levels, the

66

match was poor in some parts of the model domain. The reason for this poor match is attributed to the assumption of a uniform distribution of materials in the domain.

The sixteen well logs that are used to represent the subsurface lithology of the domain reveal that throughout the domain, minor differences are present in the material types. The southern part of the model (i.e. zone 1) indicates the presence of clay, which are not in the form of lens or bands. The middle part (zone 2) consists of gravel, talus, and sand alternation. In the northern part of the model (zone 3), in addition to alluvial fan deposits, sand layers are observed (Figure 5.3). Based on these varieties in the subsurface materials, the model domain was divided into three zones. Each zone requires a volumetric water content graph that reflects the ability of that soil to store water under changes in matric pressure. For each zone, the initially assigned sandy loam graph was modified on the basis of the dominant lithologic unit.

Consequently, the response of water table to these altered functions was observed. The best combination of graphs was selected as a result of model calibration, where measured groundwater level of April 1999 was best represented (Figure 5.4). The volumetric water content function is the basic parameter, since unsaturated hydraulic conductivity function is estimated from volumetric water content graph.

5.1.1.3. Unsaturated Hydraulic Conductivity Function

Although measuring saturated hydraulic conductivity is simple and can be achieved by measuring the quantity of water that passes through a fixed head gradient under steady state conditions, determination of unsaturated hydraulic conductivity is a fairly complex task. There are some methods that can be used to predict the shape of the function with respect to the saturated hydraulic conductivity. In order to achieve this, volumetric water content function must be determined, since unsaturated hydraulic conductivity calculations are based on the slope of volumetric water content graph.
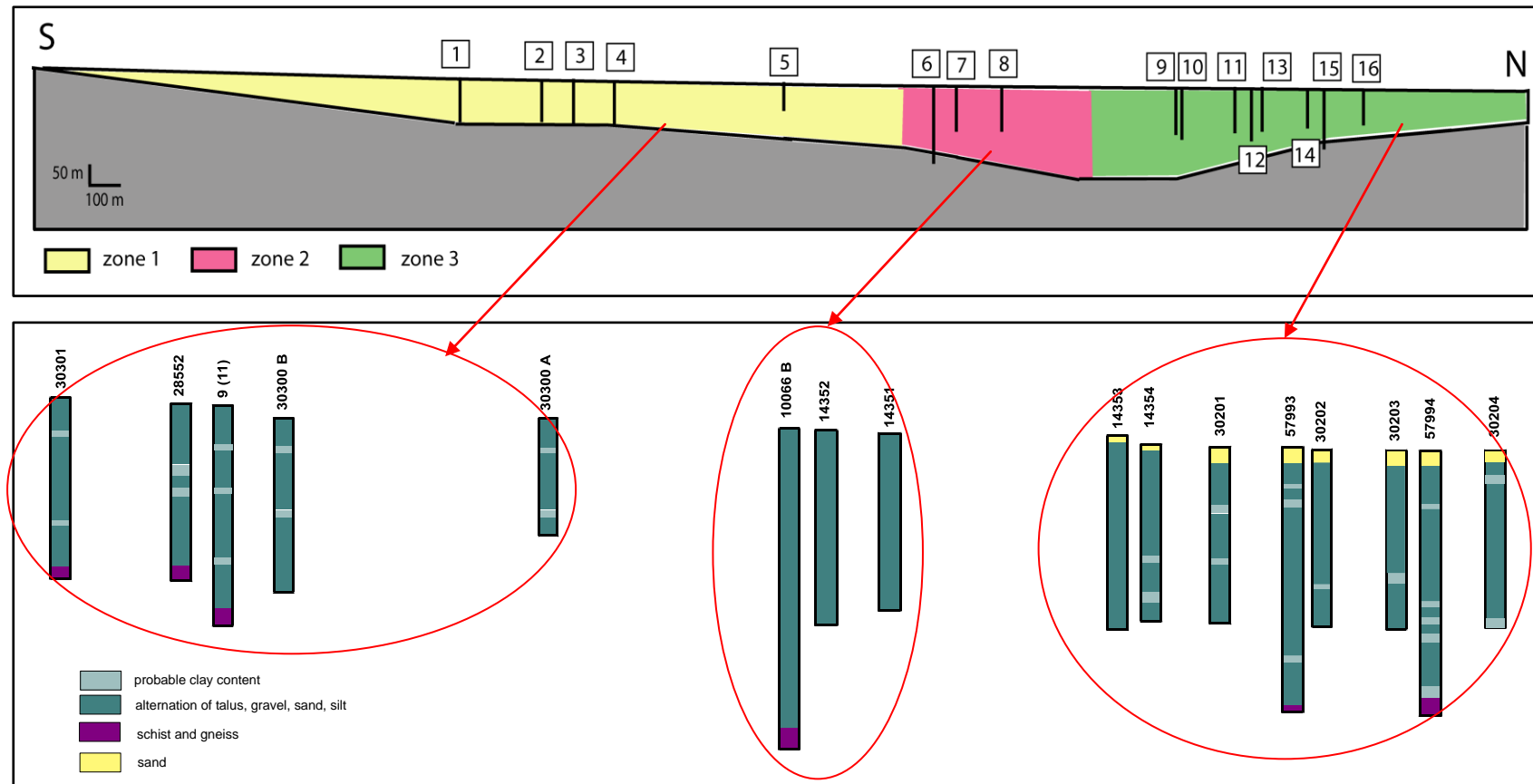
Figure 5.3. Distribution of material properties and zones.
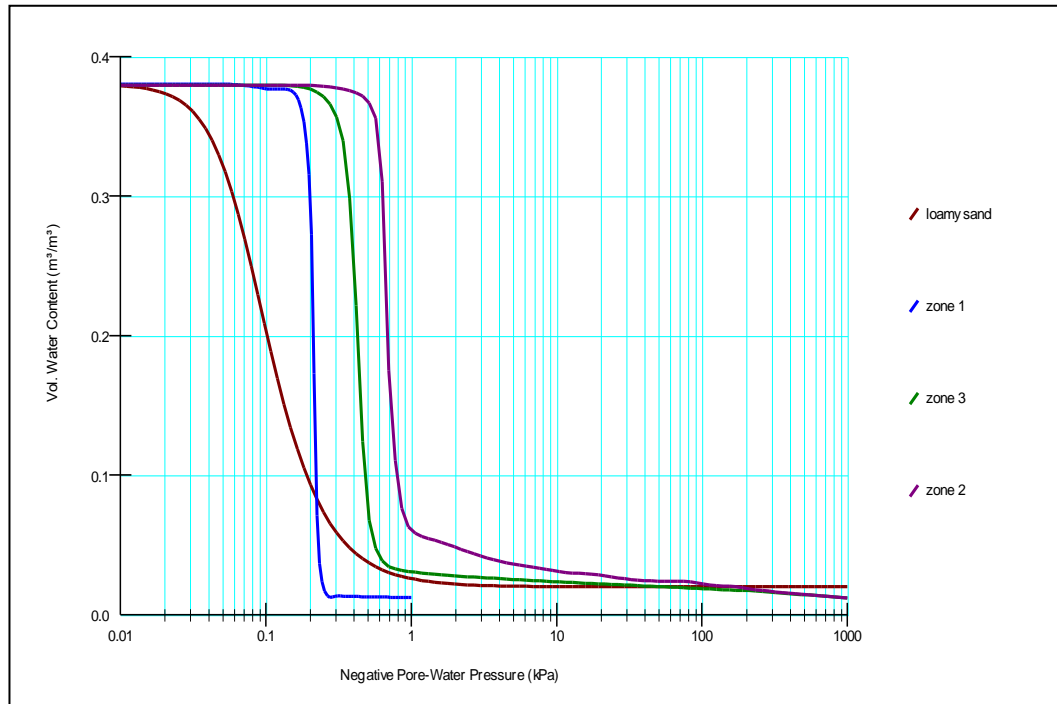
Figure 5.4. Volumetric water content function of materials in the domain.

Due to the absence of site-specific data, unsaturated hydraulic conductivity functions were estimated from measured or predicted volumetric water content functions, which are listed in the published papers. The most common estimation method is the one made by Van Genuchten (1980). In this method, saturated hydraulic conductivity and residual water content of the soil are required. The curve fitting parameters are determined graphically from the volumetric water content function. The unsaturated hydraulic conductivity functions obtained from the literature survey for different soil types (Osman and Bruen, 2002; Al-Yahyai et. al., 2006; Mallants et. al., 1999) are shown in Figure 5.5.

As a first step, since the model domain is assumed to be a single unit and soil type is determined as sandy loam, a single function which is derived from sandy loam volumetric water content curve was assigned in the model. As the model was divided into two regions based on the saturated hydraulic conductivity values, unsaturated hydraulic conductivity functions of sandy loam was assigned for each zone in the model with two different saturated hydraulic conductivity values. However, this

single function gave poor calibration results as well, confirming the heterogeneous character of the subsurface materials.

During calibration studies, as volumetric water content graphs are modified, unsaturated hydraulic conductivity functions are also modified, since the VWC function is used to determine curve fitting parameters of the estimated hydraulic conductivity function. Besides, the iterative process of solver also enables to determine the slope of unsaturated hydraulic conductivity function. In the iterative process, unsaturated hydraulic conductivity function drawn for groundwater pressures obtained from the last iteration and the current iteration are compared. In the case of real convergence, two functions should coincide. Thus, after each run, the slope of the functions for each zone is modified to provide convergence. The representative unsaturated conductivity functions in the model domain, which were determined after several calibration runs are shown in Figure 5.6.
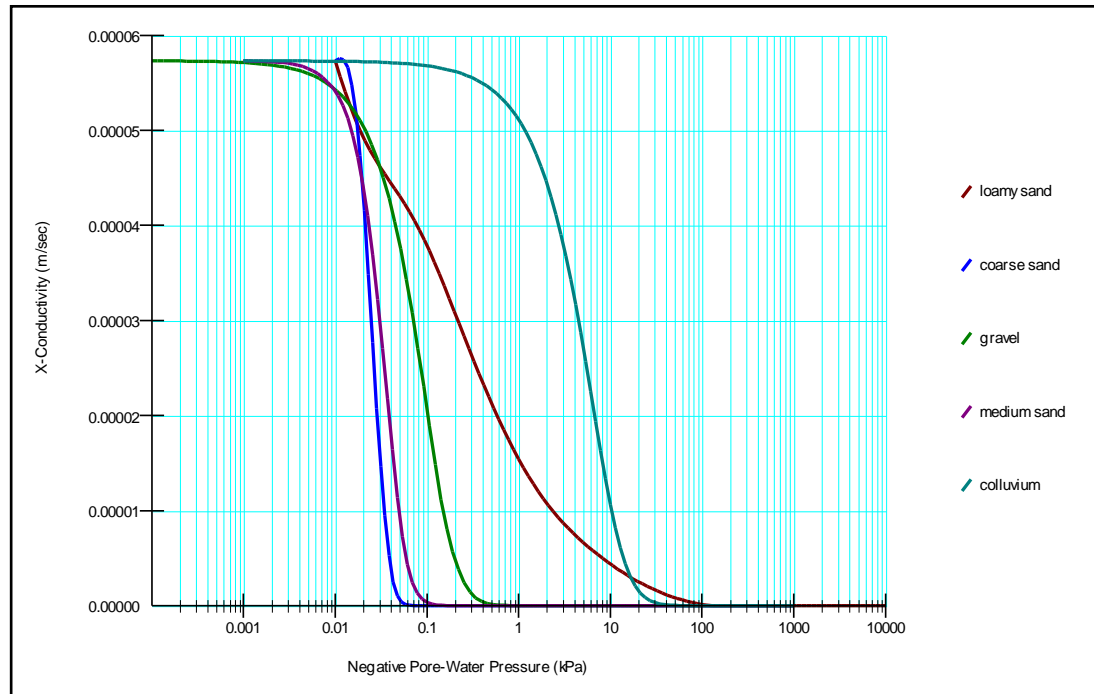
Figure 5.5. Unsaturated hydraulic conductivity functions from the literature (where K_{sat} is assigned as 5.73e-5 m/s).
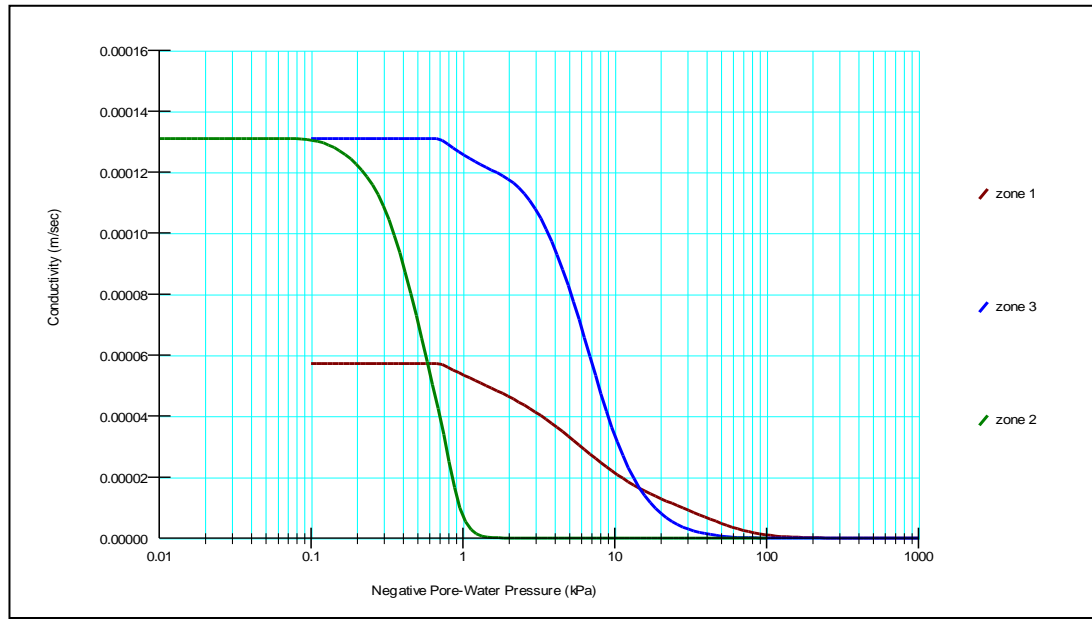
Figure 5.6. Unsaturated hydraulic conductivity function for each zone in the model.

The unsaturated hydraulic conductivity value is also not same in all directions, since natural systems are generally anisotropic. The ratio of anisotropy, i.e. ratio of vertical conductivity value to horizontal was assumed as 0.1 in the model.

5.1.2. Recharge Parameter

Since some of the precipitation is lost by evapotranspiration, it is necessary to compute the amount of water that percolates into the ground and recharges the groundwater. Recharge from precipitation into the model domain was determined by using Thornthwaite method. In this method, an empirical equation is used to determine monthly evapotranspiration amount. The amount of groundwater recharge is obtained by subtracting the amount of water lost by evapotranspiration from precipitation. The average monthly precipitation and monthly temperature values recorded at the Ödemiş station were used to calculate amount of groundwater recharge for each month. Annual groundwater recharge was determined as 174 mm/year based on the long-term data, while for a specific period of October 1998 – April 1999, it was determined as 314 mm/year. Thus, the groundwater recharge for

71

the calibration period was almost doubled as compared to the long-term recharge. Figure 5.7 shows recharge graph for the period between October 1998 and April 1999, which is the period chosen for the model simulations. The corresponding values of recharge were determined from Thornthwaite equation by using the average monthly temperature and precipitation values measured in the Ödemiş station, for the October 1998 -April 1999 period.

The recharge value can be assigned in the model by using flux type boundary condition, either as a constant value or in the form of a function. For transient analysis, the recharge value was defined by a temporarily changing function as shown in Figure 5.7. In the recharge graph, monthly average recharge values were converted to daily values and assigned as unit flux versus time boundary condition over the model top surface.
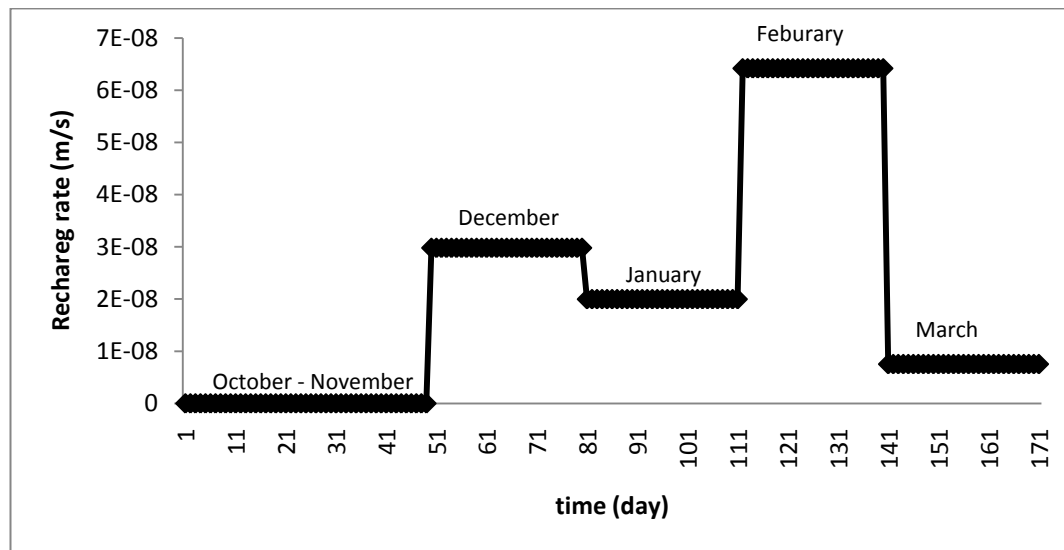
 Figure 5.7. Recharge graph from October 1998 to April 1999 (a period of 171 days).

5.1.3. Discharge Parameter

In the model domain, groundwater flow is directed from south to north, where it reaches the K. Menderes River. The amount of flow discharging from the northern part of the domain was unknown at the beginning. In order to obtain a complete representation of the study area, the flow rate along the northern part should be specified as a boundary condition. For this purpose, an analytical calculation was performed for a steady state flow in an unconfined aquifer (eq. 5.1), to approximate the amount of flow.

$$q = K \frac{h_1^2 - h_2^2}{2L} + w \left(x - \frac{L}{2} \right) \qquad (5.1)$$

where q: unit groundwater flow

      K: hydraulic conductivity

      h: hydraulic head

      L: flow length

      w: recharge per unit area

From the equation 5.1, a $5.67*10^{-7}$ m/s flux rate was computed. This value was also checked in the steady state analysis, where the material in the domain was assumed to be uniform. This value was later utilized in transient analysis.

The flow that goes out of the system through the northern boundary was assigned as a flux type boundary condition. To allow water level fluctuations with respect to time in transient analysis a potential seepage face condition was also assigned in the northern part boundary of the model. A potential seepage face boundary was used for conditions where neither the flux nor the head is known. It describes the situation where seepage surface may develop in the domain from time to time, and the exact value of flow amount is unknown. In the model, since the initial flux value is known in the northern boundary, potential seepage face has been useful to represent actual conditions during the analysis.

5.2.   Model Calibration

Calibration of the model is used to check whether the system inputs reflect the actual field conditions. In the calibration analysis, trial and error method was used to modify input parameters, such as hydraulic conductivity values for both saturated and unsaturated conditions, volumetric water content functions, etc. These parameters were then adjusted within reasonable limits, until a good match between calculated and observed groundwater levels was obtained. The groundwater table profiles obtained from the field measurements of water levels in October 1998 and April 1999 were used in the calibration process (Yazıcıgil et al., 2000).

The model was calibrated under transient conditions for the period between October 1998 and April 1999. The simulation covered a period of 171 days. This period corresponds to a wet season during which no pumpage took place for irrigation purposes. Thus, one of the parameters belonging to the real system, i.e. groundwater pumpage through wells was eliminated in the calibration process. Starting with the end of dry season water table (October 1998), the aim was to match the observed water table profile at the end of wet-season (i.e., April 1999).

In order to conduct a transient analysis, initial conditions should be determined, where the system gets the soil pressures at the start of the period. In the model, the initial conditions were specified by drawing the initial water table, i.e. water table elevations of October 1998. Then, the system computed the necessary initial pore water pressures or head conditions from the assigned water table. The groundwater recharge for the corresponding period was assigned as a unit flux boundary condition, which is represented by a monthly step function from October 1998 to April 1999. The northern boundary was assigned as the unit flux boundary, whose value was calculated as $5.67*10^{-7}$ m/s, analytically.

The material functions initially assigned in the model were modified throughout the calibration. At first, the system was thought to be composed of single material, which was determined as sandy loam. During calibration, the shape and slope of the volumetric water content function corresponding to sandy loam were modified to

obtain the expected response in groundwater levels. Determination of volumetric water content function is of crucial importance, since unsaturated hydraulic conductivity function was estimated from the VWC curve. Thus, the change in volumetric water content function also resulted in the change in unsaturated hydraulic conductivity function.

Initially assigned unsaturated hydraulic conductivity function of sandy loam was modified during the calibration, as volumetric water content function was modified. The shape of the unsaturated hydraulic conductivity function was also controlled by the convergence analysis of the solver. In the convergence analysis, the conductivity functions were drawn by using two data sets, where conductivity values were obtained from the assigned function by using ground pressures at the end of the last iteration and the current iteration. In the case of a real convergence, two data sets should plot on top of each other. During the calibration, the shape of conductivity function for each zone was modified to make the solution converge.

For the initial model runs, material properties were assumed to be uniform and were represented by sandy loam soil type throughout the model domain. The corresponding parameters of sandy loam were assigned in the model. However, it was impossible to achieve a good calibration with a uniform material property. Consequently, the model domain was divided into three zones based on the differences in the subsurface materials, which resulted in three different volumetric water content and unsaturated hydraulic conductivity functions to be defined. Initially assigned sandy loam material was modified for each zone during calibration until a good match was obtained between the simulated and measured groundwater levels of April 1999.

Calibration of the model under transient conditions was carried out and goodness of fit was determined by comparing the simulated groundwater levels (h_s) with the measured groundwater levels (h_m). Moreover, three error statistics were also used as the goodness of fit between the simulated and measured water levels:

1. The root mean squared error (RMSE) or the standard deviation is the average of the squared differences in measured and simulated heads.

$$RMSE = \left[\frac{1}{n} \sum_{i=1}^{n} (h_m - h_s)_i^2 \right]^{0.5}$$

(5.1)

    where n is number of observations.

2. The mean error (ME) is the mean difference between measured heads (hm) and simulated heads (hs).

$$ME = \frac{1}{n} \sum_{i=1}^{n} (h_m - h_s)_i$$

(5.2)

3. The mean absolute error (MAE) is the mean of the absolute value of the differences in measured and simulated heads.

$$MAE = \frac{1}{n} \sum_{i=1}^{n} |(h_m - h_s)_i|$$

(5.3)

The simulated and the measured groundwater levels for April 1999 conditions were plotted for comparison purposes in Figure 5.8. The overall root mean square error (RMSE) equals to 1.36 m, mean error (ME) equals to 0.57 m and the mean absolute error (MAE) equals to 1.25 m. The 0.57 mean of differences indicates that the simulated heads are on the average 0.57 m lower than the mean of measured water levels in the wells used for comparison. The correlation coefficient between the simulated and the measured groundwater levels is 0.95.

The effect of change in mesh size and type in the model results were also investigated during the calibration by trial and error method. The best mesh properties appear to consist of quads and triangles with an element size of 10 m.
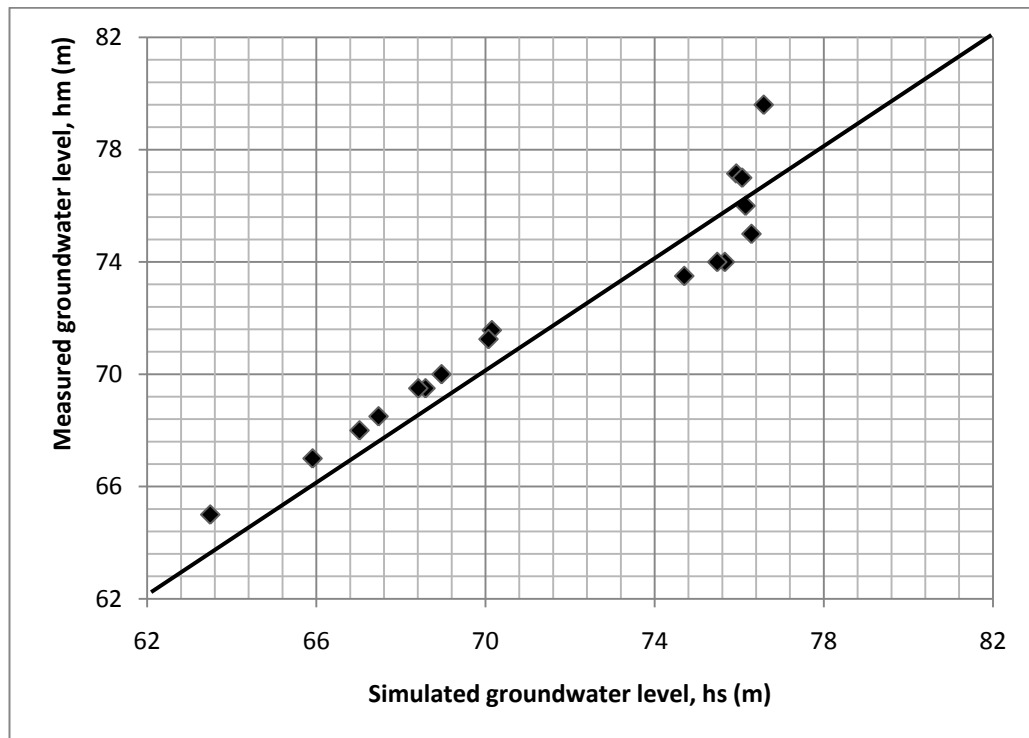
Figure 5.8. Relationship between the measured an simulated groundwater levels.

CHAPTER 6

ARTIFICIAL RECHARGE SCENARIOS

6.1.   Introduction

Once the model calibration is completed, the model is ready for further investigations, planning and operations. In the case of present study, the effect of recharged water on the water table elevation was simulated for various exceedence probabilities determined from the flood frequency analysis. In addition to recharge basins, an underground dam was simulated to test if the groundwater levels could be increased further. The calibrated model was taken as a reference to compare various scenarios.

The simulations were conducted for a period of 171 days between October 1998 and April 1999, where the initial and boundary conditions are known. Furthermore, this period corresponds to a wet season during which well discharge for irrigated agriculture did not take place. Hence, a maximum response from groundwater storage via artificial recharge was obtained.

Instead of steady state, a transient analysis was conducted, which best represents the changes in assigned parameters in the model domain. The use of transient analysis requires determination of the initial conditions, from which the system computes the ground pressures at the beginning of the period. Initial conditions were assigned by drawing water table elevation corresponding to October 1998. The simulation period ended in April 1999.

Since the domain is bounded by impervious schists and gneisses in the south and at the bottom, no flow boundary was assigned for those portions. The natural recharge from precipitation was represented by a function describing the monthly recharge

amount for the period between October 1998 and April 1999, for which values were calculated using Thornthwaite method. The northern boundary was defined by a unit flux boundary condition representing outflow, with the addition of potential seepage face to let excess water leave the system. The assigned unit flux value was determined from the model calibration stage.

The recharge basin method involves construction of rectangular basins along the Eğri Creek bed on the model domain. The amount of water collected in the basins was calculated from the flood frequency analysis and assigned as head type boundary condition along the bottom of basins. For simulating underground dam, an impervious structure was assigned along the northern boundary which prevents flow of water out of the system. It should be noted that since SEEP/W uses a 2D representation where the thickness of the system is assumed to be 1 m, the obtained solutions in the model results reflect the changes in storage, inflow or outflow for a unit thickness.

The model outputs of the calibrated model and each artificial recharge method corresponding to exceedence probabilities of 70%, 50% and 10% are illustrated in the Appendix.

6.2.   Recharge Basin Design

The recharge basin design involves construction of the basins along the Eğri Creek to collect the excess water calculated from the flood frequency analysis. The dimensions of the basin were determined by using Google earth maps to check the available space for construction, with a limiting factor that the depth of recharge basin should not exceed 6 m to provide stability. Based on the flood frequency analysis, and constraints of land availability and maximum depth of 6 m, it is concluded that two basins are required to store the calculated volume of flood water. The basins cover an area of 0.2 and 0.4 km^2, respectively. Locations of the recharge basins are shown in Figure 6.1.

The ground surface in the model slopes towards north. The construction of the basins was achieved by excavating one side with a maximum depth of 6 m and constructing impervious embankments on the other side, to obtain a rectangular basin. The recharge basins and their locations in the model domain are given in Figure 6.2.
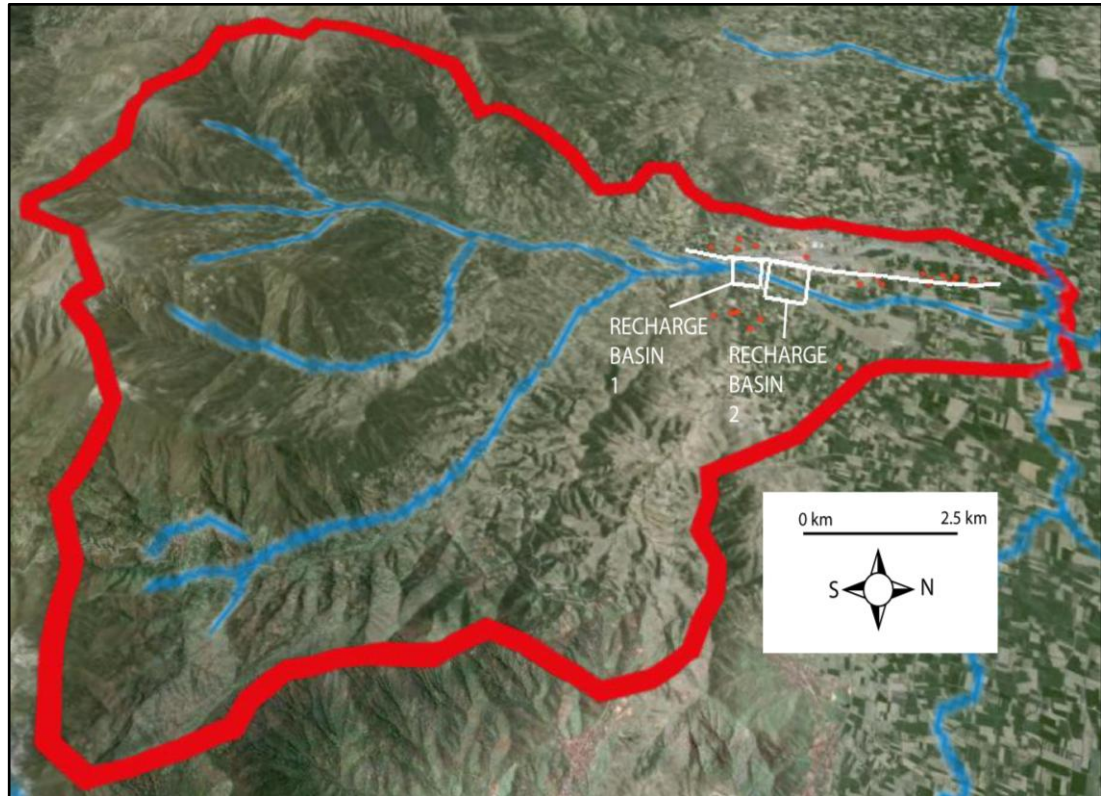
Figure 6.1. Location of the recharge basins (the map from Google Earth).

The amount of water that can be collected in the basins was calculated from the flood frequency analysis. Since SEEP/W uses a 2D representation of the domain where the thickness is determined as 1 m in the model, the volume of water that falls into unit thickness of the basin was simulated. This was achieved by dividing the computed volume by the width of the basins.

In the recharge basin simulations, the conditions simulated were chosen to represent realistic recharge basin operations. Recharge basins generally operated on a wet-dry

cycle, to prevent clogging and decline of infiltration rates. The boundary conditions that are thought to be most suitable are constant head boundary to represent wet conditions and zero flux boundary to represent dry conditions. The value of constant head refers to the total hydraulic head in SEEP/W and is calculated by summing elevation head (i.e. bottom elevation of the basin) and pressure head (water depth in the basin).

Table 6.1 shows the depth of the recharged water and the corresponding hydraulic heads in the recharge basins for various exceedence probabilities. It is obvious that as the exceedence probability becomes lower, the volume of water collected in the basins increases. Table 6.1 indicates that for the exceedence probabilities of 90, 80 and 70 percent, a single basin is sufficient to collect the floodwaters. For the remaining probabilities, however, operation of two basins are required to collect the computed volume of water. The latter situation is achieved in two parts. First, recharge basin 1 is filled with water until the maximum depth is reached. Then, as the flood water continues to flow, the recharge basin 2 is started to be filled with water in addition to the first basin.

6.2.1. Alternative Scenarios For Recharge Basin

Alternative scenarios for the artificial recharge of groundwater via recharge basins involve repeating the simulations for different exceedence probability amounts. The simulation period starts from October 1998 and ends in April 1999, where the calibrated model is closely compatible with actual field conditions.

The flood frequency analysis indicates that the highest runoff volumes are generally detected in February, whereas to a lesser extent, highest flow rates are also observed in October or April. In the model, the operation of recharge basins starts when the simulation time period starts, i.e. October 1998. The operation of the recharge basin at the beginning of the simulation was performed to allow time for the recharged water to infiltrate into the ground, to reach the water table, and hence to increase the water table elevation during the simulation period of 6 months. Thus, the simulations of the recharge basins were started in October 1998. It is logical to assume that the

timing of the recharge would affect model results. To test this hypothesis, a simulation corresponding to 50% exceedence probability was repeated by filling the recharge basins in February 1999. The model results corresponding to this scenario show that the change in storage increased from 5510 cubic meters to 5830 cubic meters. Consequently, filling of the recharge basins in February or October resulted in some differences in groundwater storage but the change was not significant for the purpose of this study.

At the start of simulation period, the recharge basins were assumed to be filled with water at a depth as computed for the flood frequency analysis. The remaining ground surface was subjected to the recharge boundary condition to represent natural recharge from precipitation. Constant head boundary conditions were assigned at the bottom of the recharge basins, the values of which were computed for various exceedence probabilities as shown in Table 6.1. The constant head boundary was removed, when the computed volume of water infiltrated into the ground. To control the amount of the infiltrated water, a flux section was assigned just below the recharge basins, which computes the rate and volume of water passing through the section. Once the constant head boundary was removed, the recharge basin boundary was replaced with a unit flux boundary condition, the values of which represent natural groundwater recharge from precipitation.

As mentioned before, a single recharge basin is sufficient to collect the flood waters for the exceedence probabilities of 90, 80 and 70 percent. In these cases, the depth of water in the recharge basin ranges from 1.5 m to 6 m. The overall effect of artificial recharge of groundwater is reflected as an average increase in water table elevations of 0.3 m to 2.7 m. The increase in groundwater level is also resulted in increase in groundwater storage, which is approximately equal to the volume of artificially recharged water, i.e. approximately ranging from 530 m^3 to 2200 m^3.
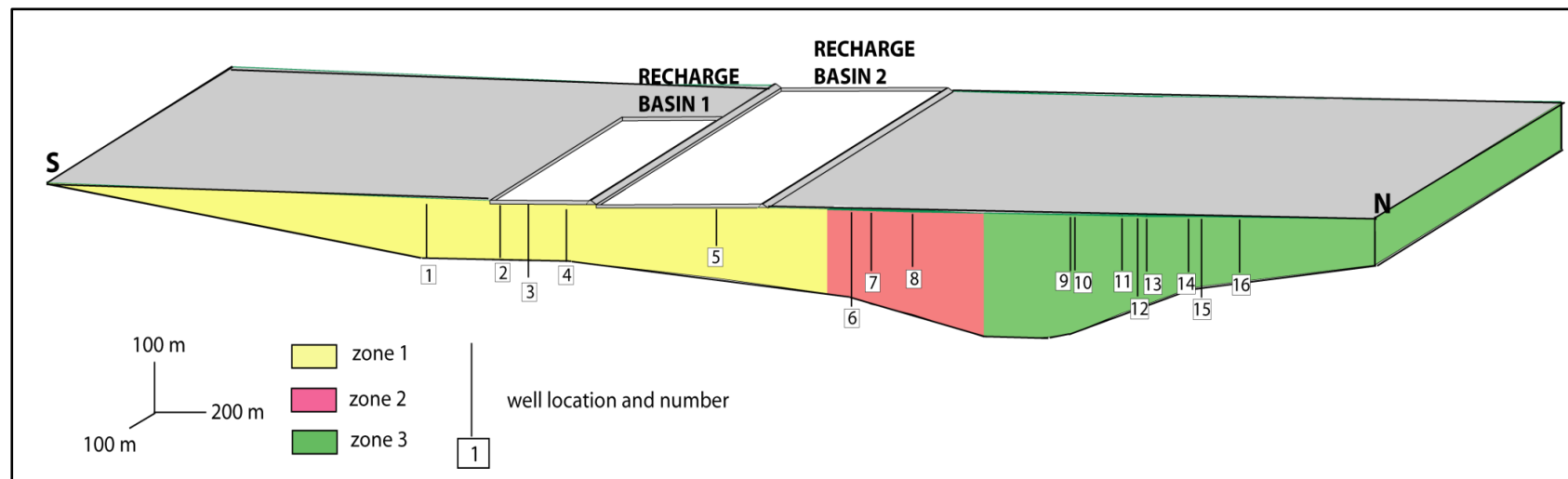
Figure 6.2. Schematic view of recharge basins in the model domain.

Table 6.1. Depth of recharged water and corresponding hydraulic head in recharge basins for different exceedence probabilities.

EXCEEDENCE PROBABILITY (%)	RUNOFF VOLUME (determined from flood frequency analysis) (10^6 m^3)	CORRESPONDING VOLUME OF WATER IN THE MODEL (m^3)	RECHARGE BASIN 1		RECHARGE BASIN 2	
			DEPTH OF RECHARGE WATER (m)	TOTAL HYDRAULIC HEAD (m)	DEPTH OF RECHARGE WATER (m)	TOTAL HYDRAULIC HEAD (m)
90	0.30	531	1.5	110.5	-	-
80	0.74	1378	3.75	112.75	-	-
70	1.18	2205	6	115	-	-
60	1.62	2824	6	115	1	103
50	2.06	3443	6	115	2	104
40	2.51	4062	6	115	3	105
30	2.95	4682	6	115	4	106
20	3.40	5300	6	115	5	107
10	3.83	5920	6	115	6	108

For the simulation of 70% exceedence probability, the computed volume of flood waters completely fills the recharge basin 1. Thus, additional flow of flood waters requires construction of a second recharge basin. Exceedence probabilities from 60% to 10% were modeled by operation of two recharge basins. In the case of two recharge basins, at the start of simulation, flood waters start filling the first basin, which is simulated by assigning a constant head boundary at the bottom of the recharge basin. The remaining ground surface is subjected to natural recharge, i.e. recharge from precipitation. When the first basin is completely filled, i.e. depth of water equals to 6 m in the basin; the flux section drawn below the basin indicates the amount of infiltrating water that corresponds to 70% exceedence probability. Then, two basins start operating simultaneously. This condition is simulated by assigning a constant head boundary at the bottom of the second basin that corresponds to flood-stage for a given probability of exceedence, in addition to constant head boundary of the first basin. As the volume of waters stored in the recharge basins enters into the ground, constant head boundaries are replaced by unit flux boundaries that represent natural recharge rate till the end of the simulation period.

Simulations of the exceedence probabilities ranging from 60% to 10% produce a water depth of 1 m to 6m in the recharge basin 2. The resultant increase in the groundwater levels is about 5.1 m to 7 m. Depending upon probability of exceedence, the groundwater storage is computed as 4920 m^3 to about 7900 m^3.

The Figure 6.3 shows the change in water table elevations with respect to the initial (October 1998) and calibrated groundwater level with no artificial recharge (i.e., April 1999) for various exceedence probabilities. Besides, water budget computations corresponding to each probability analysis are illustrated in Figure 6.4. Figure 6.5 shows the proportions of natural and artificial recharge amounts for each probability level.
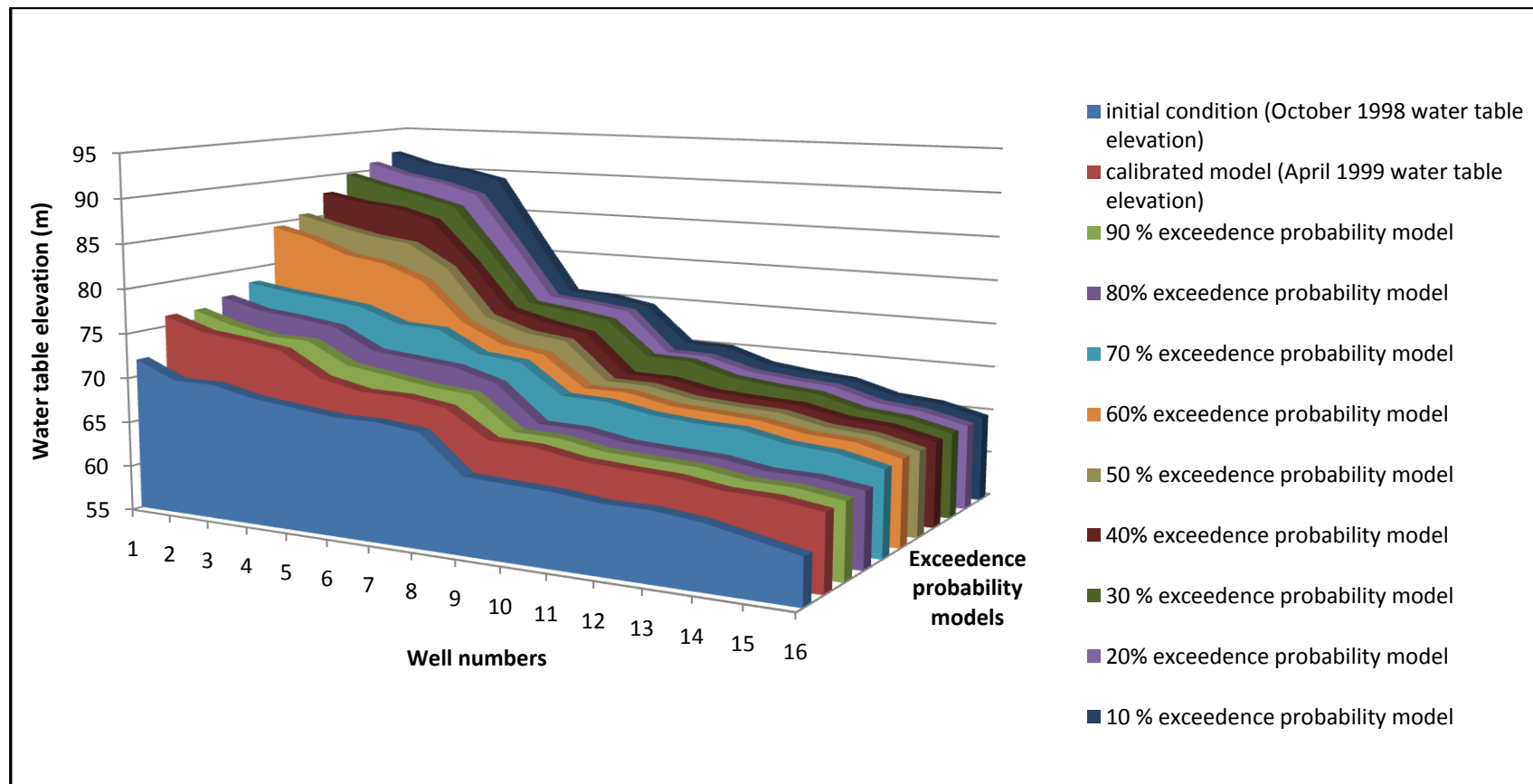
Figure 6.3. Water table elevations obtained from recharge basin applications for various exceedence probabilities, showing initial and calibrated model results.

	calibrated model	90% exceedence probability model	80% exceedence probability model	70% exceedence probability model	60% exceedence probability model	50% exceedence probability model	40% exceedence probability model	30% exceedence probability model	20% exceedence probability model	10% exceedence probability model
outflow	919.7	923.3	930.1	945.1	984.2	1011.9	1018.1	1025.7	1038.7	1054.9
storage	2158.6	2694.3	3527.5	4350.1	4919.6	5510.6	6165.0	6731.4	7334.9	7872.9
inflow	3078.3	3617.6	4457.6	5295.2	5903.8	6522.5	7183.1	7757.1	8373.7	8927.7

Figure 6.4. Water budget calculations computed for the calibrated model and each exceedence probability.

Figure 6.5. Distribution of the artificial and natural recharge amounts for each exceedence probability

6.3.   Underground Dam

Underground dams can enhance the storage of recharged water in the system by reducing or eliminating outflow from the system. Consequently, they can be considered together with the surface spreading methods. In this study, an underground dam was simulated with recharge originating from artificial recharge basins to determine the contribution of dam construction on groundwater levels and storage. In th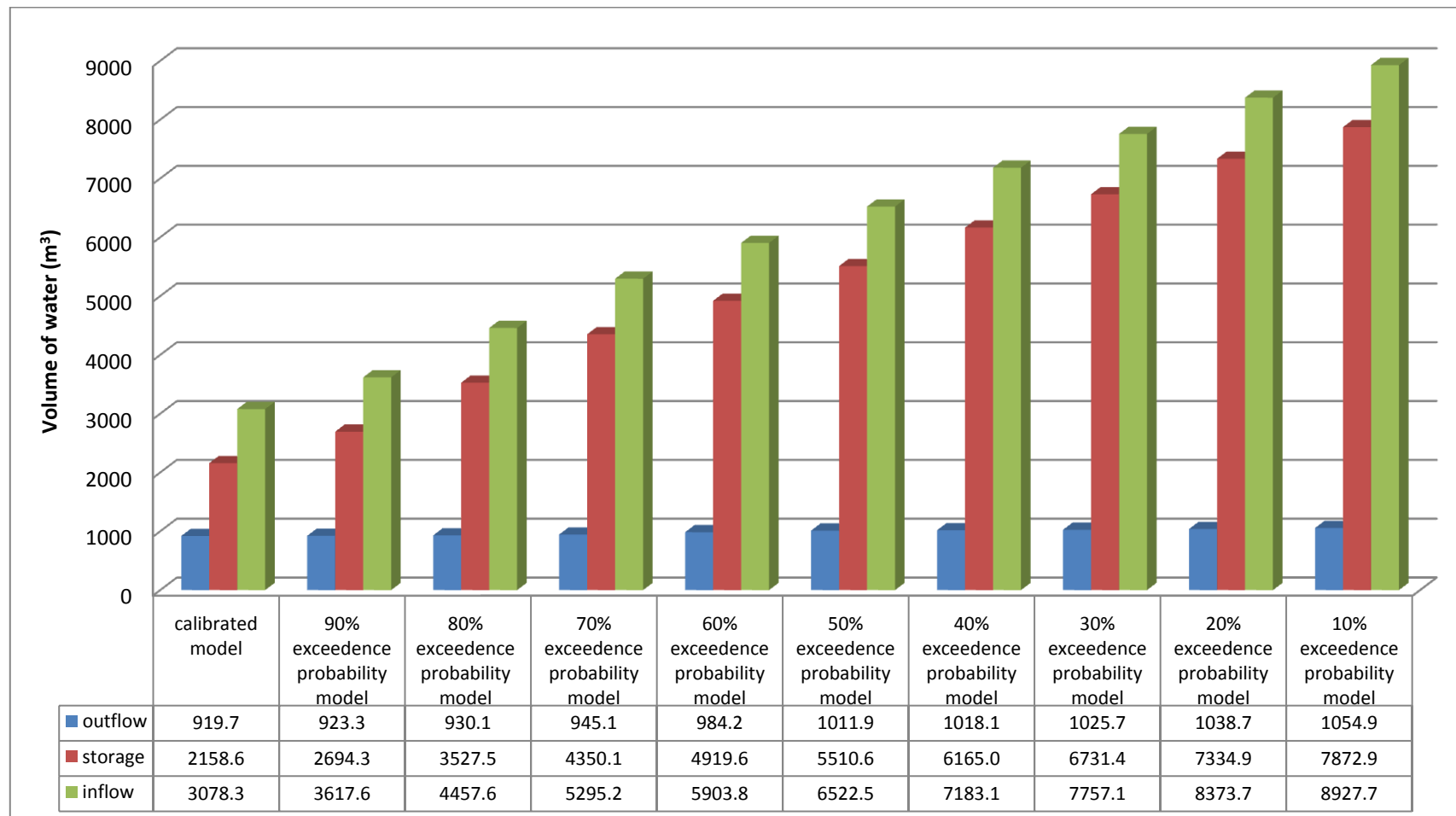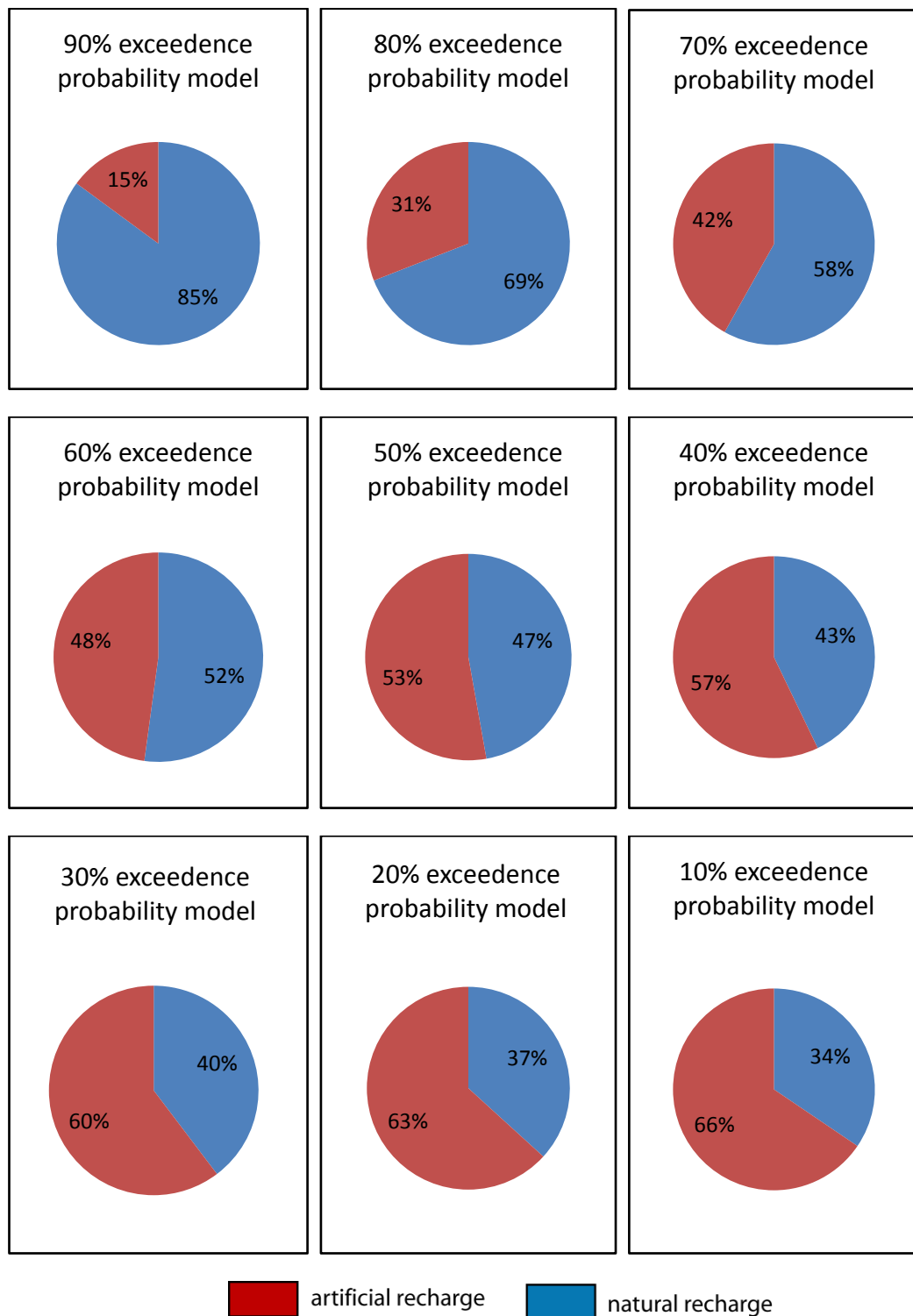e model, the dam construction was simulated at the downstream edge (i.e. along the northern boundary), where flow of water out of the system is prohibited, and therefore groundwater storage in the system is increased further.

The dam construction was represented by assigning a no flow boundary at the downstream edge. Since the main interest in the model is the flow of water in subsurface and the impervious layers are not included in the domain, the actual dimensions of underground dam were not considered and modeled.

6.3.1. Alternative Scenarios with Underground Dam

Simulation period begins on October 1998 and ends on April 1999. As transient analysis was conducted, the initial conditions were determined from the water table elevation drawn for October 1998. The simulations were repeated for the conditions with or without the presence of recharge basins. In the presence of recharge basins, boundary conditions for each exceedence probability and no flow boundary for the underground dam were assigned in addition to natural recharge boundary condition applied to the ground surface. In the case of absence of recharge basins, the recharge from precipitation value was assigned as a boundary condition at the ground surface in addition to no flow boundary condition assigned on the northern part of the model domain. In this case, contribution of the underground dam on the groundwater levels with the absence of surface artificial recharge structures was determined.

When the underground dam is modeled alone, the groundwater levels are mainly increased in the downstream part of the domain, because the dam prevents subsurface outflow and groundwater accumulates in that region. The change in the

water table elevation is shown in Figure 6.6. The increase in groundwater storage basically equals to the amount of subsurface flow calculated for the condition with no dam construction. Figure 6.7 shows the calculated water budgets for conditions with and without underground dam construction.

Simulations were also repeated with the addition of the underground dam to each scenario of artificial recharge basins corresponding to various exceedence probabilities. Figures 6.8-6.16 represent the change in water table elevations for each exceedence probability with the simulation of the underground dam. These figures enable to make a comparison between the water table elevations of the calibrated model (April 1999) and the artificial recharge basins with and without the underground dam for various exceedence probabilities. As expected, the increase in groundwater levels is significant at the downstream edge of the model in addition to the increase in groundwater levels below the recharge basins. Because the dam was represented by a no flow boundary condition, the change in groundwater storage was equal to the sum of artificially recharged water and subsurface outflow volumes.
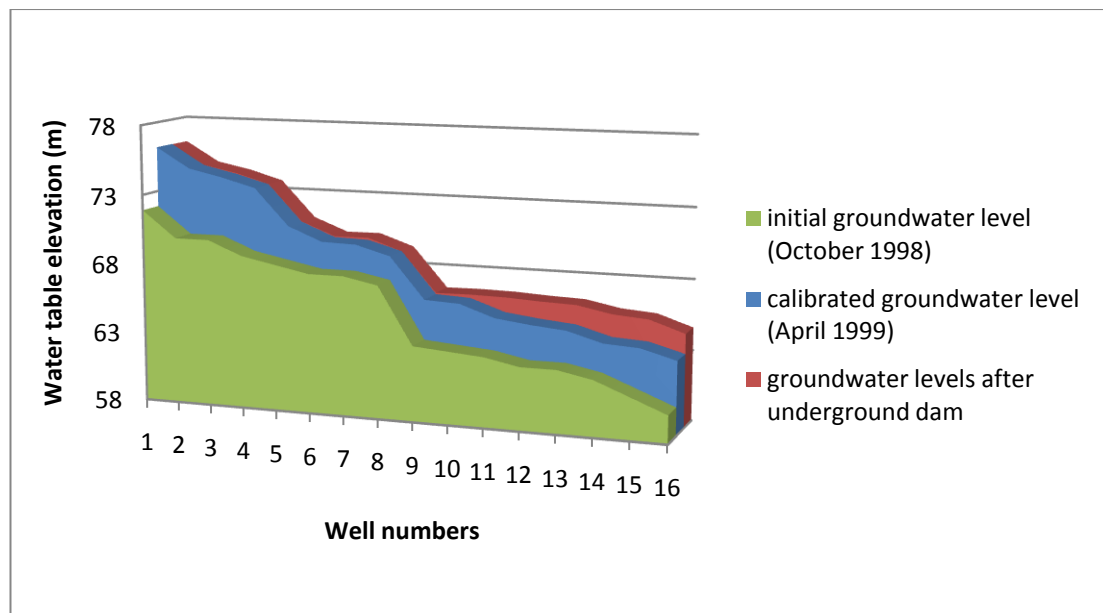
Figure 6.6. Water table elevations corresponding to April 1999 and underground dam simulation.

	calibrated model (April 1999)	underground dam model
■ outflow	919.7	0.0
■ storage	2158.6	3103.1
■ inflow	3078.3	3103.1
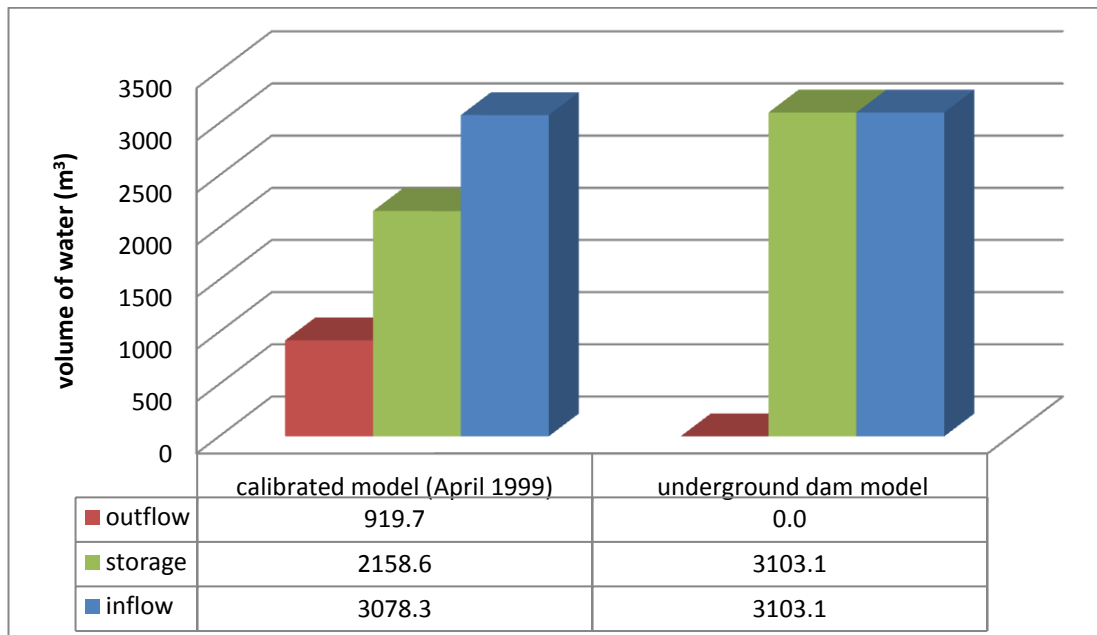
Figure 6.7. Calculated water budget of calibrated model and underground dam simulation.

Figure 6.8. Water table elevations of April 1999 and 90 % exceedence probability corresponding to recharge basin and recharge basin with underground dam.

Figure 6.9. Water table elevations of April 1999 and 80 % exceedence probability corresponding to recharge basin and recharge basin with underground dam.

Figure 6.10. Water table elevations of April 1999 and 70 % exceedence probability corresponding to recharge basin and recharge basin with underground dam.

Figure 6.11. Water table elevations of April 1999 and 60 % exceedence probability corresponding to recharge basin and recharge basin with underground dam.

Figure 6.12. Water table elevations of April 1999 and 50 % exceedence probability corresponding to recharge basin and recharge basin with underground dam.

Figure 6.13. Water table elevations of April 1999 and 40 % exceedence probability corresponding to recharge basin and recharge basin with underground dam.
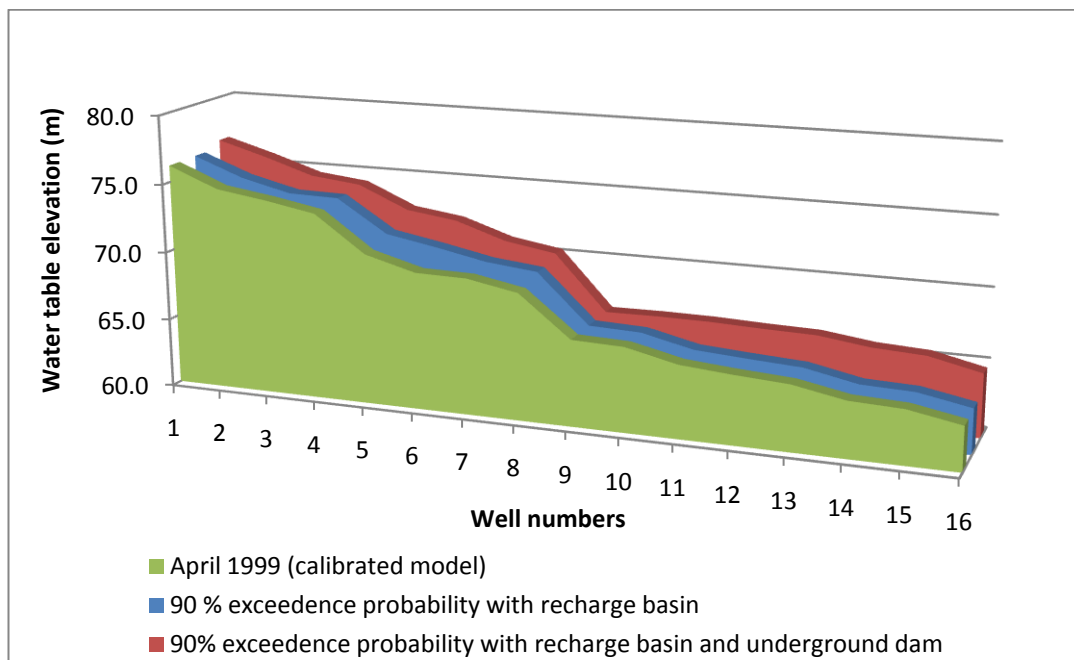

Figure 6.14. Water table elevations of April 1999 and 30 % exceedence probability corresponding to recharge basin and recharge basin with underground dam.

Figure 6.15. Water table elevations of April 1999 and 20 % exceedence probability corresponding to recharge basin and recharge basin with underground dam.
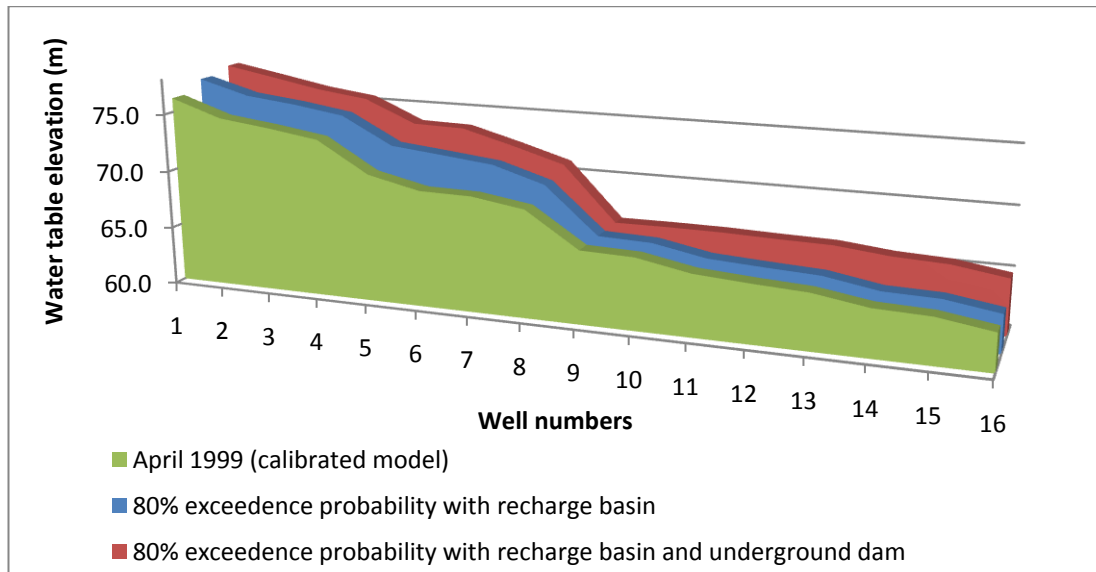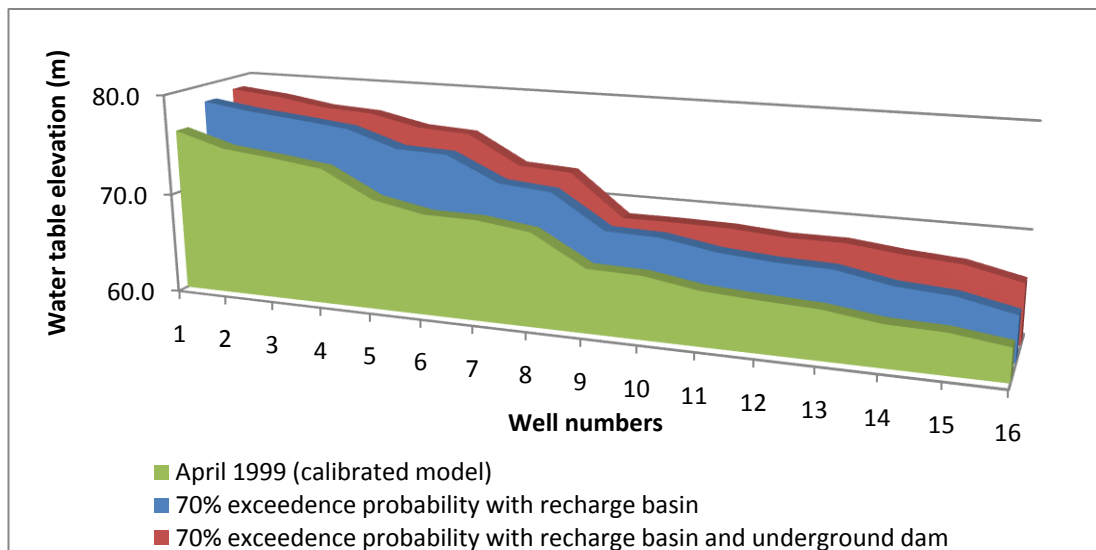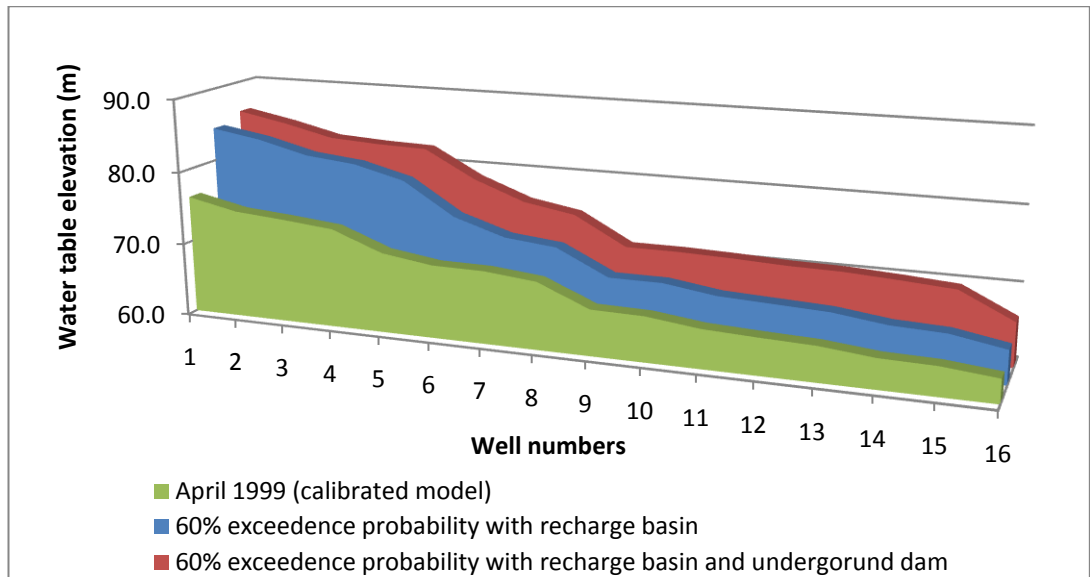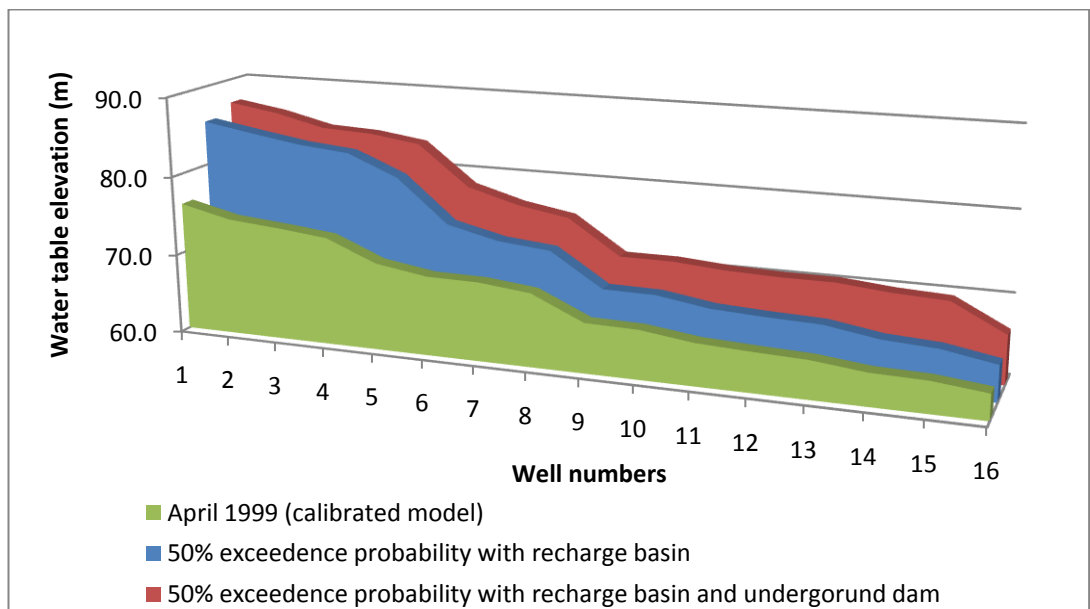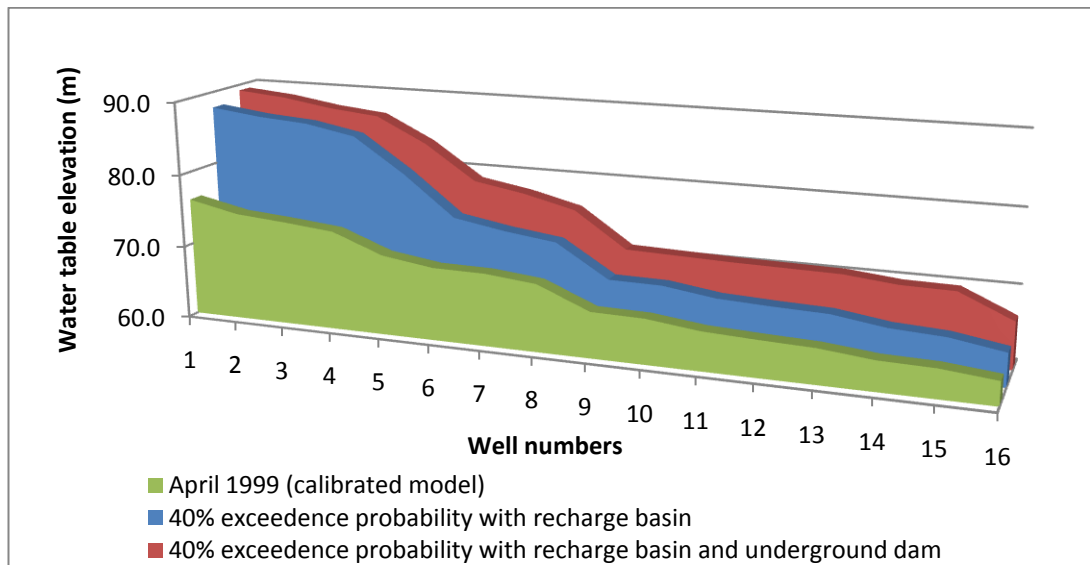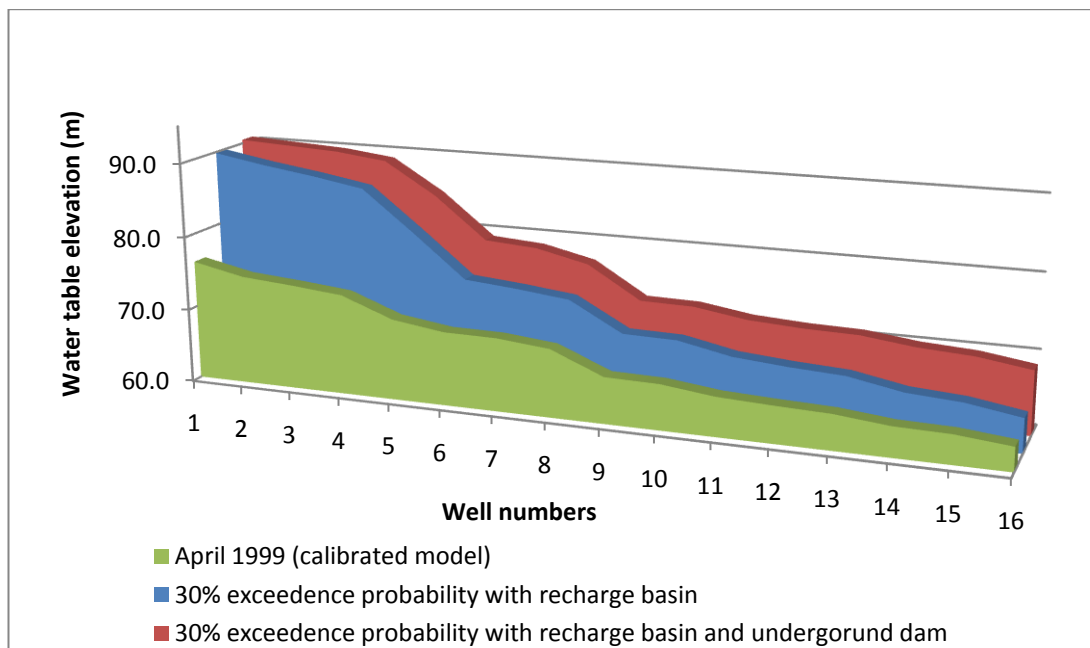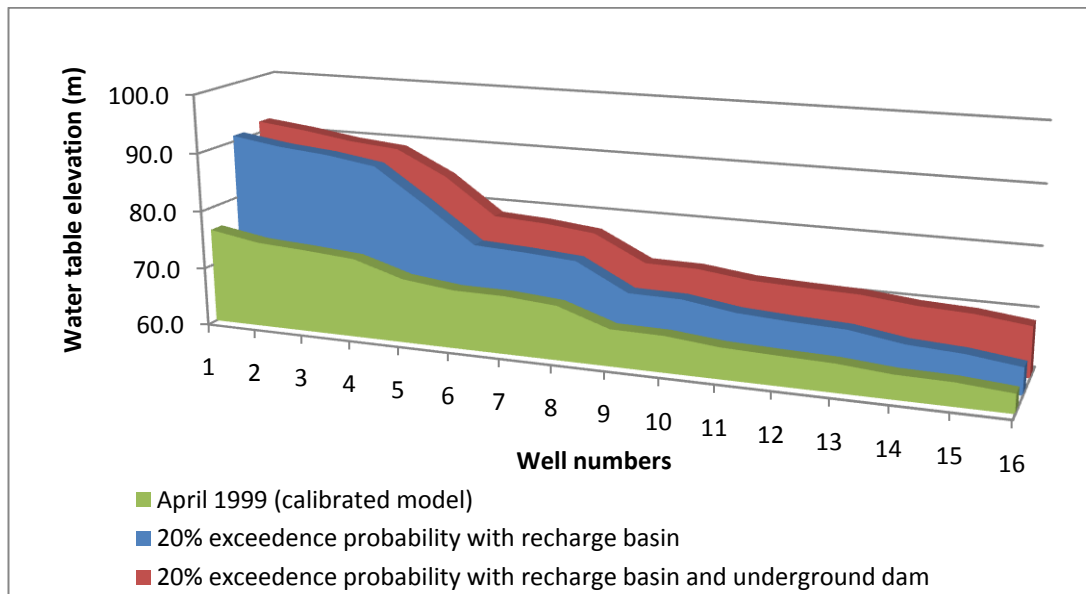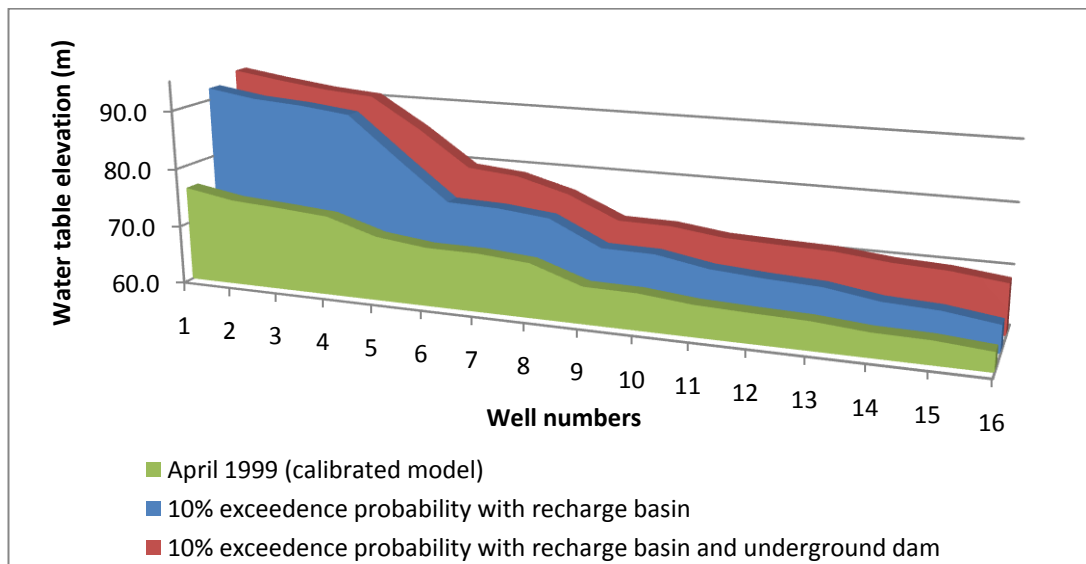

Figure 6.16. Water table elevations of April 1999 and10 % exceedence probability corresponding to recharge basin and recharge basin with underground dam.

CHAPTER 7

DISCUSSION, SUMMARY AND CONCLUSIONS

7.1.   Discussion of the Results

The aim of the study is to investigate the potential for artificial recharge of groundwater in the K. Menderes River basin, specifically in the Eğri Creek subbasin. The most suitable artificial recharge areas include highly porous media with thick unsaturated zone and absence of any impeding layers. In the study, the modeling is achieved in a representative area characterized by these conditions (i.e. the Eğri Creek Basin).

Due to the absence of site specific data, the material properties used in this study were estimated from similar areas with similar lithologies in the literature. The horizontal heterogeneity based on material properties was represented by division of model domain into three zones. However, in the area, vertical heterogeneity cannot be properly evaluated due to the absence of data. During calibration studies, by altering shape and slope of the volumetric water content function, vertical heterogeneity was, to a lesser extent, eliminated.

In order to calibrate the model, measured water table elevations of October 1998 (as an initial condition) and April 1999 were used. The assigned material properties and boundary conditions were modified to obtain a good match between measured and simulated water table elevations of April 1999. However, the validity of the model cannot be checked, since measured water table elevations corresponding to another time period were not available.

Recharge basins and underground dam were selected as artificial recharge methods. The artificial recharge scenarios were tested by conducting simulations for several

exceedence probabilities obtained from the flood frequency analysis of the Eğri Creek. In order to assess the resultant effect of artificial recharge on groundwater levels and groundwater storage, simulations were repeated for a number of exceedence probabilities with the application of recharge basins with and without underground dam conditions. The simulation was performed over a time period between October 1998 and April 1999, for a period of 171 days. Alternative recharge scenarios were compared with water table elevations of the calibrated model, which best represents April 1999 groundwater level, and was referred to as a reference model. Simulation results corresponding to calibrated model, initial water table elevation, and water table elevations obtained for 70%, 50% and 10% exceedence probability models are shown in the Appendix.

The simulation results show that groundwater table elevations rise in different amounts depending upon the probability of exceedence of the recharged flood waters. As exceedence probability decreases, the volume of water collected in the recharge basins increases, thereby providing a significant amount of rise in water table elevations and groundwater storage. The greatest rise in water table elevation is observed below the recharge basins (mainly observed in the wells from 2 to 5 in Appendix), where groundwater mounds are developed. In the study area, the formation of groundwater mounds will not limit recharge, since the thickness of unsaturated zone below the basins are about 35 m, whereas height of groundwater mounds are less than 20 m. In the case of underground dam simulations, the rise in water table elevation is also observed to be significant in the immediate upstream of the underground dam (i.e. along the downstream portion of the domain) which prevents the subsurface outflow from the groundwater system.

The increase in groundwater storage corresponding to various exceedence probabilities for the application of recharge basins with and without underground dam is summarized in Figure 7.1. The results in Figure 7.1 show that by using the recharge basins only, the groundwater storage in the Eğri Creek subbasin can be increased from base conditions of 2150 cubic meters to 2700 cubic meters (for unit thickness) for a 90% exceedence probability, to 7900 cubic meters for a 10%

exceedence probability. The expected average groundwater storage that corresponds to 50% exceedence probability is 5500 cubic meters. These results indicate that the application of artificial recharge basins in the study area is a viable approach and has a great potential to increase groundwater storage. Underground dam construction in the model domain results in approximately 1000 m^3 increase in groundwater storage, however this increase in groundwater levels and storage are not significant to warrant the construction of underground dam. Furthermore, the depth to the impervious bedrock at the outlet of the basin where dam construction is considered is more than 90 meters, thus making its construction economically unfeasible.

The main problem in artificial recharge applications is the decline of infiltration rate as a result of clogging. In order to prevent clogging, recharge basins in the model were operated in a wet-dry cycle, where clogged layer can be removed by draining and rinsing the infiltration basins during dry period.

The quality of water is another important factor in artificial recharge projects. In water spreading methods, such as recharge basin applications, the quality of water is improved through physical, geochemical and bacteriological processes that take place in unsaturated zone during infiltration. Thus, additional treatment of water is not necessary. Besides, in the study area, the source of water considered for recharge is direct runoff from rainfall and is expected to be free of contaminants. Moreover, alternation of coarse and fine particles in the domain results in higher sorption capacity, leading to an increase in water quality.

7.2.   Summary and Conclusions

Artificial recharge of groundwater is designed to accelerate natural recharge into subsurface via engineering systems. It is widely used throughout the world to increase groundwater storage in times of excess water for utilization in times of water deficiency. Design of artificial recharge systems depends on the type of aquifer, permeability of geologic formations, characteristics of unsaturated zone, and heterogeneity of subsurface.
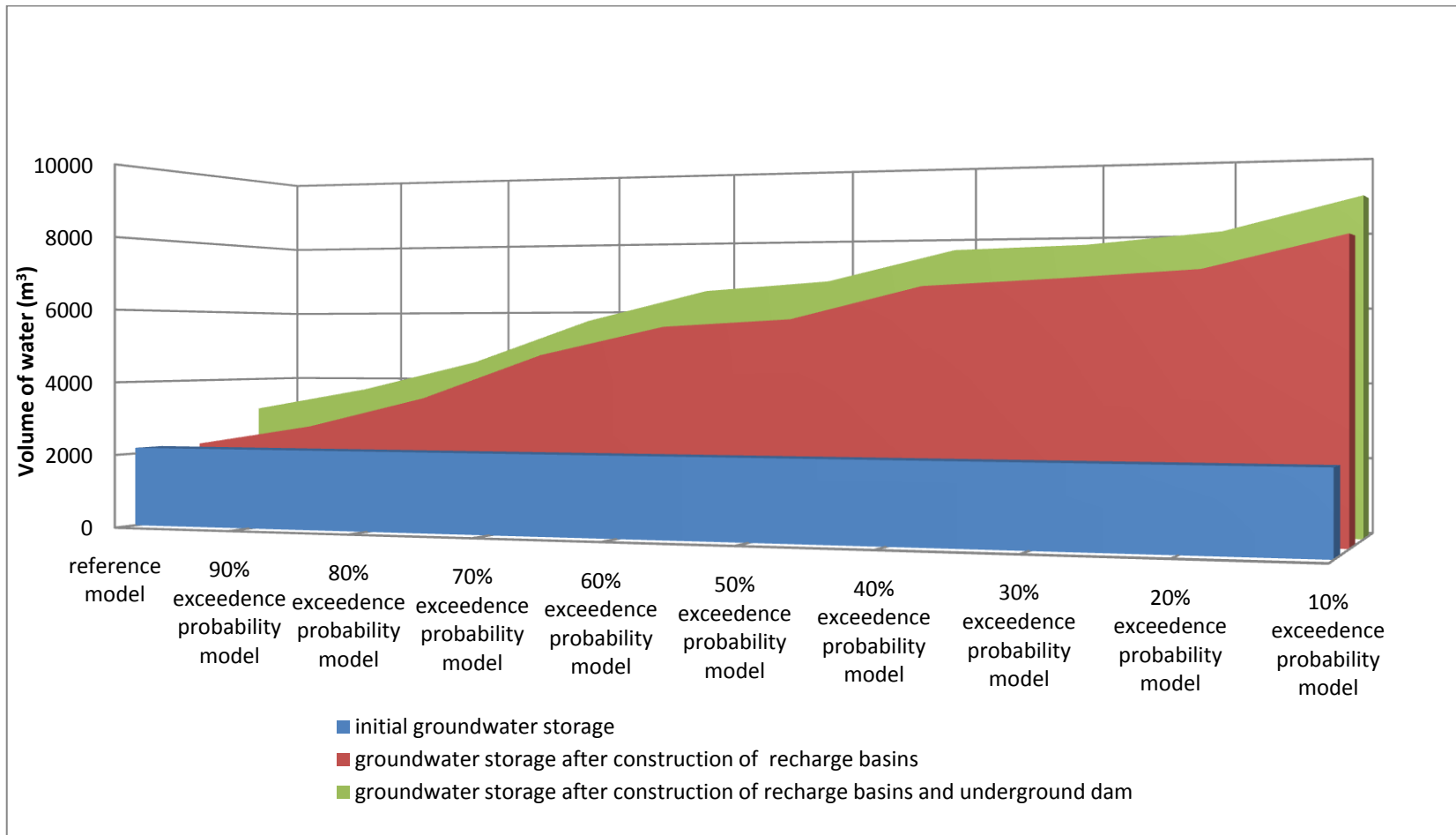
Figure 7.1. Comparison of change in groundwater storage after artificial recharge applications.

The purpose of this study is to assess the potential for artificial recharge of groundwater in the K. Menderes River basin as an alternative management scenario to enhance storage of groundwater in wet seasons to be utilized in dry periods when the demand for irrigation water needs peak out. The Eğri Creek subbasin was selected for the investigation area. Among various artificial recharge methods, surface recharge basins and underground dam were considered. The scope of the study includes characterization of the subsurface conditions, assessment of flood (i.e., recharge) waters in the Eğri Creek for various exceedence probabilities, construction and calibration of a subsurface flow model and prediction of water table and groundwater storage for alternative artificial recharge scenarios.

The characterization involved collection and evaluation of all available data regarding to physiography, climate, geology, hydrology and hydrogeology of the system to develop a conceptual model. The missing data was completed via correlation analysis and literature survey. A flood frequency analysis of the Eğri Creek was conducted to assess the volume of flood waters that can be used as recharge water. Following development of a conceptual model, a mathematical subsurface flow model was developed to represent the subsurface conditions. Data gathered from characterization of the system was converted into the model as initial and boundary conditions, material properties, etc. The model domain was determined from lithologic units in the subsurface based on their hydrogeological properties. The model was subsequently calibrated under transient conditions for a period of 171 days using the measured water table in October 1998 as initial conditions to match the measured water table in April 1999. Model was successfully calibrated with a root mean square error of 1.36 m via trial and error approach by modifying the volumetric water content and unsaturated hydraulic conductivity functions of the subsurface materials.

The calibrated model was subsequently used to assess the potential for the artificial recharge of groundwater in the area. For a number of exceedence probabilities, the calculated amount of flood waters that can be collected in the recharge basins was used to determine the dimensions of the recharge basins. The volume of water

corresponding to various exceedence probabilities was converted into flood stages and was represented by a constant head boundary in the model. When the computed volume of water infiltrated into the subsurface, the recharge basin boundary was replaced by a flux boundary representing recharge from precipitation only. The underground dam was simulated by an impervious boundary located in the downstream of the domain. The underground dam was operated with and without recharge basins to compare the effect of increase in groundwater levels in the model domain.

It is obvious that as the exceedence probability becomes lower, the volume of water that is collected in the basins increases, which results in more increase in water table elevations.

The simulation results with the recharge basin application as an artificial groundwater recharge method show substantial improvement in raising the water table elevation as compared to the natural recharge conditions. The average rise in water table elevation ranges from 0.3 m to 7 m on the basis of the exceedence probability that has been simulated. The increase in groundwater level appears to be more significant at the bottom of the basins where groundwater mounds were developed. The volume of water that was stored artificially varies from 530 cubic meters to 5920 cubic meters, which is reflected in the model as an increase in groundwater storage from base conditions of 2150 cubic meters to 2700 cubic meters for a 90% exceedence probability, to 7900 cubic meters for a 10% exceedence probability per-unit thickness.

The underground dam construction results in more increase in groundwater elevations, as expected, since the dam prevents subsurface outflow of water, and thus further increase in storage occurs. The increase in storage is basically equal to the amount of subsurface flow prior to the dam construction. Simulations of the underground dam with recharge basins produce an average increase of 0.5 to 10 m in groundwater elevations. The greatest increase in water table elevations are produced below the recharge ponds and in the immediate upstream of the dam. The increase in groundwater storage ranges from base conditions of 2150 cubic meters to 3700 cubic

meter and to 8900 cubic meters as exceedence probability decreases from 90% to 10%. The model results indicate that groundwater storage increases about 1000 cubic meter with the addition of underground dam.

To sum up, the assessment of potential for artificial recharge of groundwater in the K. Menderes River Basin was performed in this study. The model results show that both recharge basin and underground dam construction can enhance groundwater storage and produce significant increase in water table elevations. However, the contribution of underground dam on groundwater level is not as significant as recharge basin applications. When the construction and operation of the systems are considered, underground dam method is determined as infeasible.

It should be noted that due to the absence of site specific data, the subsurface materials and their properties were estimated from the studies conducted in similar soil types. The aim of the study is to show the applicability of artificial recharge of groundwater, not to show exact replication of the subsurface. In the future, prior to construction of any artificial recharge systems, a detailed investigation of the unsaturated zone with in-situ and laboratory tests is necessary. Tension infiltrometer or disc permeameter tests can be conducted in-situ to determine hydraulic conductivity of the unsaturated medium and volumetric water content function from measurements of infiltration rate under various suctions. Outflow measurements which consist of subjecting the soil specimen to small increments in matric suction and recording the rate of outflow and total outflow during each step, or centrifuge methods, where a centrifuge is used to drive fluid flow can be used as laboratory tests to measure unsaturated hydraulic conductivity values. When it is not possible to carry out these in-situ or laboratory tests, grain size analyses can also be used in order to estimate necessary functions. It is also recommended to construct a pilot scale recharge pond in order to observe the effects of artificial recharge prior to construction of any large-scale artificial recharge structures.

REFERENCES

Al-Muttair, F.F., and Al-Turbak, A.S., 1991. Modeling of infiltration from an artificial recharge basin with decreasing ponded depth. J. King Saud Univ. Eng. Sci., vol. 3, 89-100.

Al-Yahyai, R., Schaffer, B., Davies, F.S. and Munoz- Carpena, R., 2006. Characterization of soil-water retention of a very gravelly loam soil varied with determination method. Soil Science, vol. 171, 85-93.

Apaydın, A., 2009. Malibogazi groundwater dam: an alternative model for semi-arid regions of Turkey to store and save groundwater. Environ. Earth Sci., vol. 59, 339-345.

Apaydın, A., Aktaş, S.D., and Ekinci, O., 2005. Su kaynaklarının değerlendirilmesinde farklı bir yaklaşım: yeraltı barajları. II. Ulusal Su Mühendisliği Sempozyumu, 153-165.

Aubertin, M., Mbonimpa, M., Bussière, B. and Chapuis, R.P., 2003. A model to predict the water retention curve from basic geotechnical properties. Canadian Geotechnical Journal, vol. 40, no. 6. 1104-1122

Banks, H. O., Richter, R. C., Coe, J. J., McPartland, J. W., and Kretsinger, R., 1954. Artificial recharge in California. California Div. Water Resources, 41 p.

Berend, J.E., 1967. An analytical approach to the clogging effect of suspended matter. Internat. Assoc. Sci. Hydrology Bull., vol. 12, no. 2, 42-55.

Blaney, H.F., 1936. General review- symposium on contribution to ground-water supplies. Am. Geophys. Union Trans., vol. 17, no. 2, 456-458.

Boochs, P. W., and Billib, M., 1994. Management of a small ground water reservoir by recharge water from a surface reservoir. In: Johnson, A.I. and Pyne, D.G., (eds.), Proceedings of the second international symposium on artificial recharge of ground water, 661-668.

Bouwer, H., 1994. Artificial recharge- issues and future. In: Johnson, A.I. and Pyne, D.G., (eds.), Proceedings of the second international symposium on artificial recharge of ground water, 2-10.

Bouwer, H., 2002. Artificial recharge of groundwater: hydrogeology and engineering. Hydrogeology Journal, vol. 10, 121-142.

Brashears, M.L., Jr., 1946. Artificial recharge of ground water on Long Island, New York. Econ. Geology, vol. 41, no. 5, 503-516.

Brashears, M.L., Jr., 1953. Recharging ground-water reservoirs with wells and basins. Minin Eng., vol. 5, 1029- 1932.

Brothers, K., Bernholtz, A., and Katzer, T., 1994. Artificial ground-water recharge in Las Vegas Valley, Clark County, Nevada: Model prediction-"No cone of depression here!". In: Johnson, A.I. and Pyne, D.G., (eds.), Proceedings of the second international symposium on artificial recharge of ground water, 669- 678.

Chapuis, R.P., Chenaf, D., Bussiere, B., Aubertin, M. and Crespo, R., 2001. A user's approach to assess numerical codes for saturated and unsaturated seepage conditions. Can. Geotech. J., vol. 38, 1113-1126

Connorton, B.J. and McIntosh, P., 1994. EUREAU survey on artificial recharge. In: Johnson, A.I. and Pyne, D.G., (eds.), Proceedings of the second international symposium on artificial recharge of ground water, 11-19.

Dewey, H., 1933. The falling water level of the chalk under London. Water and Water Eng., vol. 35, no. 121. 440-447.

Engler, K., Thompson, D.G., and Kazmann, R.G., 1945. Ground water supplies for rice irrigation in the Grand Prairie Region, Arkansas. Arkansas Uni. Bull. 457, 56 p.

Flanigan, J.B., Sorensen, P.A., and Tucker, M.A., 1994. Use of hydrogeologic data in recharge pond design. In: Johnson, A.I. and Pyne, D.G., (eds.), Proceedings of the second international symposium on artificial recharge of ground water, 139-148.

Foster, S., and Tuinhof, A., 2004. Brazil, Kenya: Subsurface dams to augment groundwater storage in basement terrain for human subsistence. Sustainable Groundwater Management Lessons from Practice, Case profile collection no. 5, 1-8.

Fredlund, D.G., and Anqing Xing., 1994. Equations for the soil-water characteristic curve. Canadian Geotechnical Journal., vol. 31, 521- 532.

Geo-slope International, 2007. Seepage modeling with SEEP/W: an engineering methodology, Canada, 2nd edition, 290 p.

Green, R.E., and Corey, J.C., 1971. Calculation of hydraulic conductivity: a further evaluation of some predictive methods. Soil Science Society of America Proceedings, vol. 35, 3- 8.

Harrell, M.A., 1935. Artificial ground-water recharge- a review of investigations and experience. U. S. Geol. Survey open-file report, 34 p.

Hillel, D., 2008. Soil in the environment: crucible of terrestrial life. Elsevier/Academic Press, Amsterdam Boston, 289 p.

Houk, I.E., 1951. Irrigation engineering, vol. 1. New York: John Wiley and Sons, 545 p.

Imbertson, N.M., 1959. Replenishment of ground water with desilted storm water. In: Schiff, L. (ed.), Bienn. Conf. on ground-water recharge, 2d, Berkeley, Calif., Proc: Collins, Colo., Western Soil and Water Management Research Br., 66-70.

Ishaq, A.M., Al-Suwaiyan, M.S., and Al-Sinan, A.A., 1994. Suitability of wastewater effluents to recharge groundwater aquifers in Saudi Arabia. In: Johnson, A.I. and Pyne, D.G., (eds.), Proceedings of the second international symposium on artificial recharge of ground water, 376- 385.

Irwin, J.L., 1931. Report on water sinking experiment in the City of Arcadia well no. 2 Santa Anita Basin, open file report, Los Angeles County Flood Control Dist., 6 p.

Izbicki, J.A., Flint, A.L., and Stamos, C.L., 2007. Artificial recharge through a thick, heterogeneous unsaturated zone. Ground Water, vol. 46, no. 3, 475-488.

Jacobs, K.L. and Holway, J.M., 2004. Managing for sustainability in an arid climate: lessons learned from 20 years of groundwater management in Arizona, USA. Hydrogeology Journal, vol. 12, 52-65.

Jans, M., 1959. North Kern Water Storage District spreading activities. In: Schiff, L. (ed.), Bienn. Conf. on ground-water recharge, 2d, Berkeley, Calif., Proc: Collins, Colo., Western Soil and Water Management Research Br., 54-57.

Jansa, O.V.E., 1952. Artificial replenishment of underground water: Internat. Water Supply Assoc., 2d Cong., Paris, 105 p.

Kim, C.P., Stricker, J.N.M., and Torfs, P.J.J.F., 1996. An analytical framework for the water budget of the unsaturated zone. Water Resources Research, vol. 32, no. 12, 3475-3484.

Kimrey, J.O., 1989. Artificial recharge of groundwater and its role in water management. Desalination, 72, 135-147.

Lal, R., and Shukla, M.K., 2004. Principles of soil physics. Marcel Dekker, New York, 699 p.

Lane, D.A., 1934. Increasing storage by water spreading. Am. Water Works Assoc. Jour., vol. 26, no. 4, 421-429.

Laverty, F.B., 1952. Ground water recharge. Am. Water Works Assoc. Jour., vol. 44, no. 8, 677-681.

Laverty, F.B., Jordan, L.W., and van der Goot, H.A., 1951. Report on tests for the creation of fresh water barriers to prevent salinity intrusion performed in West Coastal Basin, Los Angeles County, California. Los Angeles, Los Angeles County Flood Control District, 70 p.

Lehr, J.H., 1982. Artificial ground-water recharge: a solution to many U.S. water-supply problems. Ground Water, vol. 20, no. 3, 262-266.

Light, M.E., 1994. Design, construction, and operation of a surface recharge facility for the purpose of reusing secondary effluent in an arid climate, Tucson, Arizona, USA. In: Johnson, A.I. and Pyne, D.G., (eds.), Proceedings of the second international symposium on artificial recharge of ground water, 342-351.

Lytle, B.A., 1994. Deep bedrock well injection near Denver, Colorado. In: Johnson, A.I. and Pyne, D.G., (eds.), Proceedings of the second international symposium on artificial recharge of ground water, 81-90.

Markus, M.R., Thompson, C.A., and Ulukaya, M., 1994. Enhanced artificial recharge utilizing inflatable rubber dams. In: Johnson, A.I. and Pyne, D.G., (eds.), Proceedings of the second international symposium on artificial recharge of ground water, 120-128.

Mallants, D., Volckaert, G., and Marivoet, J., 1999. Sensitivity of protective barrier performance to changes in rainfall rate. Waste Management, vol. 19, 467-475.

Muckel, D.C., 1945. Replenishing ground-water supplies by sinking water through wells or shafts. U. S. Soil Conserv. Service, 8 p.

Munévar, A., and Marino, M.A., 1999. Modeling analysis of ground water recharge potential on alluvial fans using limited data. Ground Water, vol. 37, no. 5, 649-659.

Mushtaq, H., and Mays, L.W., 1994. Operation of recharge basin systems: an optimal control approach. In: Johnson, A.I. and Pyne, D.G., (eds.), Proceedings of the second international symposium on artificial recharge of ground water, 352- 361.

Nielsen, D.R., van Genuchten, M.Th., and Biggar, J.W., 1986. Water flow and solute transport proceses in the unsaturated zone. Water resources research, vol. 22, no. 9, 89-108.

Nilsson, A., 1988. Groundwater dams for small-scale water supply. Intermediate Technology Publications, London, UK, 69 p.

Osman, Y.Z., and Bruen, M.P., 2002. Modelling stream-aquifer seepage in an alluvial aquifer: an improved loosing stream package for MODFLOW. Journal of Hydrology, vol. 264, 69-86.

Phillips, S.P., 2003. Aquifers, artificial recharge of. Encyclopedia of Water Science, vol. 1, no. 1, 33-36.

Peters, J.H., 1994. Artificial recharge and water supply in the Netherlands, state of art and future trends. In: Johnson, A.I. and Pyne, D.G., (eds.), Proceedings of the second international symposium on artificial recharge of ground water, 28-39.

Pyne, R.D.G., 1994. Seasonal storage of reclaimed waste water and surface water in brackish aquifers using aquifer storage and recovery (ASR) wells. In: Johnson, A.I. and Pyne, D.G., (eds.), Proceedings of the second international symposium on artificial recharge of ground water, 282- 298.

Reddy, K.R., 2008. Enhanced aquifer recharge. In: Darnault, C.J.G. (ed.), Overexploitation and Contamination of Shared Groundwater Resources, 275-287.

Richter, R.C., and Chun, R.Y.D., 1959. Geologic and hydrologic factors affecting infiltration rates at artificial recharge sites in California. In: Schiff, L. (ed.), Bienn. Conf. on ground-water recharge, 2d, Berkeley, Calif., Proc: Collins, Colo., Western Soil and Water Management Research Br., 48-52.

Schiff, L., and Dyer, K.L., 1964. Some physical and chemical considerations in artificial ground-water recharge. International Assoc. Sci. Hydrology Pub., vol. 64, 347-358.

Signor, D.C., Growitz D.J., and Kam, W., 1970. Annotated bibliography on artificial recharge of ground water, 1955-67. Geological Survey Water-Supply Paper 1990, 141p.

Simpson, T.R., 1948. Recharge by percolation wells, Excerpts from report on percolation, Feather River and tributaries, counties of Sutter and Yuba, California. California Div. Water Resources, 4 p.

Soyer, R., 1947. Recharge of aquifers. Technique Sanitaire et Municipal, vol. 42, 58-69.

Stakelbeek, A., Roosma, E., and Holzhaus, P.M., 1994. Deep well infiltration in the North-Holland dune area. In: Johnson, A.I. and Pyne, D.G., (eds.), Proceedings of the second international symposium on artificial recharge of ground water, 258- 269.

Thiem, G., 1923. Effect and purpose of recharge wells. Gesundheits- Ingenieur, vol. 46, no. 34, 331-333.

Todd, D.K., 1959. Annotated bibliography on artificial recharge of ground water through 1954. Geological Survey Water-Supply Paper 1477, 115 p.

Van Genuchten, M.Th., 1980. A closed form equation for predicting the hydraulic conductivity of unsaturated soils. Soil sci. soc. Am. J., vol. 44, 892-898.

Wang, H.F., and Anderson, M.P., 1982. Introduction to groundwater modeling: finite difference and finite element methods. W. H. Freeman and Company, USA, 237 p.

Wiese, B., and Nutzmann, G., 2007. Infiltration of surface water into ground-water under transient pressure gradients. IGB, 55-64.

Winslow, C.E.A., and Phelps, E.B., 1906. Investigations on the purification of Boston sewage. U. S. Geol. Survey Water-Supply Paper 185, 163 p.

Yazıcıgil, H., Doyuran, V., Karahanoğlu, N.,Yanmaz, M., Çamur, Z., Toprak, V., Rojay, B., Yılmaz K.K., Şakıyan, J., Süzen, L., Yeşilnacar, E., Gündoğdu, A., Pusatlı, T., and Tuzcu, B., 2000. "Investigation and Management of Groundwater Resources in Küçük Menderes River Basin under the scope of Revised Hydrogeological Studies", Final Report: Vol. I: Main Report, Vol. II: Meteorology and Hydrology, Vol. III: Geology, Vol. IV: Groundwater Database, Vol. V: Hydrogeology, Vol. VI: Groundwater Chemistry, Quality and Contamination, Vol. VII: Groundwater Flow Model Project, Project no: 98-03-09-01-01. Middle East Technical University, Ankara.

APPENDIX

MODEL OUTPUTS

In this study, SEEP/W software is used to model recharge basins and underground dam as artificial recharge of groundwater methods. The model domain is 5.098 km long and 300 m wide with a thickness of 1 m. The model outputs corresponding to (1) calibrated model; (2) recharge basin applications representing 70 % exceedence probability model (2.1), 50 % exceedence probability model (2.2), and 10% exceedence probability model (2.3); (3) underground dam applications representing underground dam alone (3.1), 70% exceedence probability model with underground dam (3.2), 50% exceedence probability model with underground dam (3.3), and 10% exceedence probability model with underground dam (3.4) are illustrated in this part.

1. CALIBRATED MODEL (reference model)
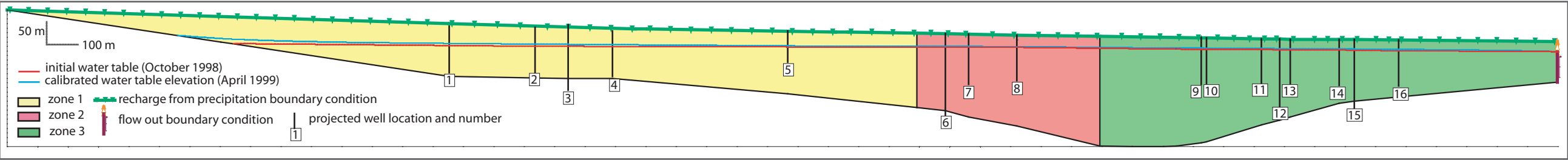
Figure A.1. Calibrated model

2. RECHARGE BASIN APPLICATIONS
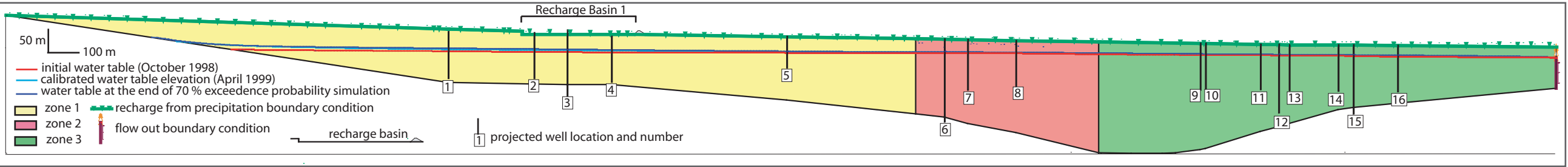
2.1. 70 % EXCEEDENCE PROBABILITY MODEL

Figure A.2. 70% exceedence probability model with recharge basin

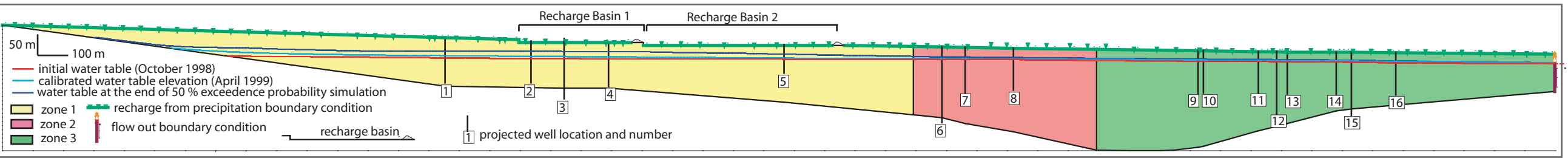### 2.2. 50 % EXCEEDENCE PROBABILITY MODEL

Figure A.3. 50% exceedence probability model with recharge basin
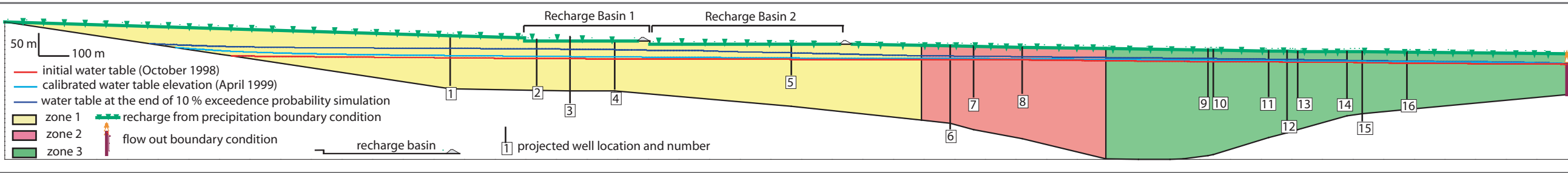
2.3. 10 % EXCEEDENCE PROBABILITY MODEL

Figure A.4. 10% exceedence probability model with recharge basin

112

3. UNDERGROUND DAM APPLICATIONS
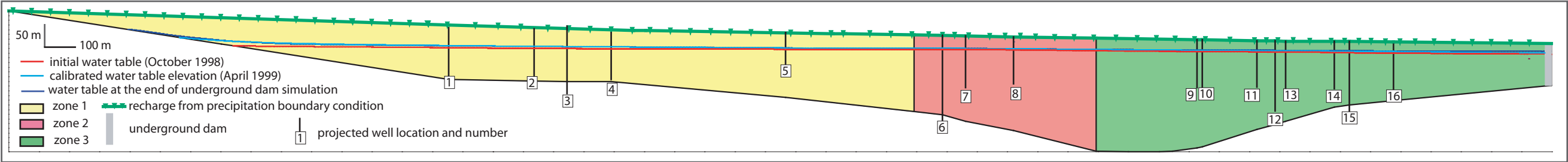
3.1. UNDERGROUND DAM

Figure A.5. Underground dam model

3.2. 70 % EXCEEDENCE PROBABILITY MODEL WITH RECHARGE BASIN AND UNDERGROUN DAM
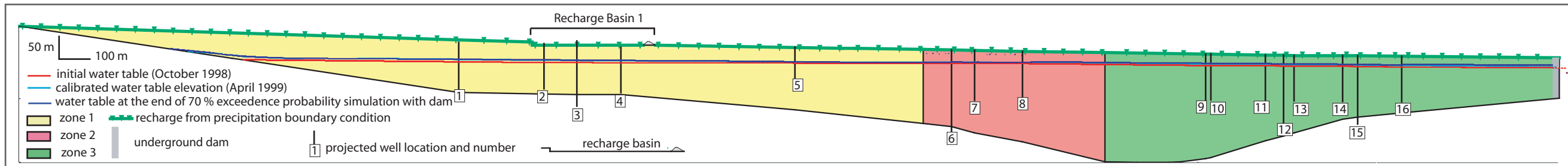

Figure A.6. 70% exceedence probability model with recharge basin and underground dam model

3.3. 50 % EXCEEDENCE PROBABILITY MODEL WITH RECHARGE BASINS AND UNDERGROUND DAM
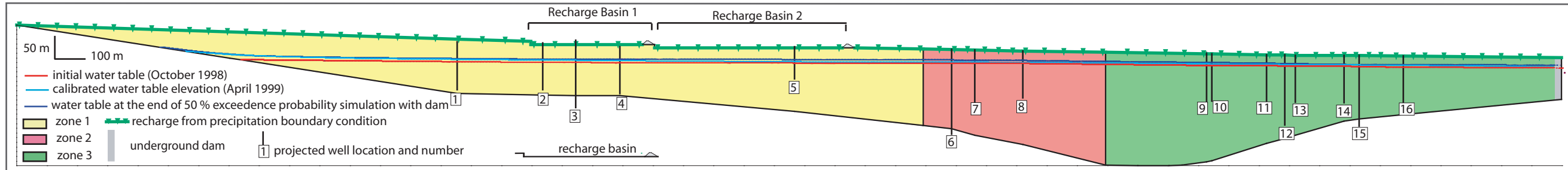

Figure A.7. 50% exceedence probability model with recharge basin and underground dam model

3.4. 10 % EXCEEDENCE PROBABILITY MODEL WITH RECHARGE BASINS AND UNDERGROUND DAM
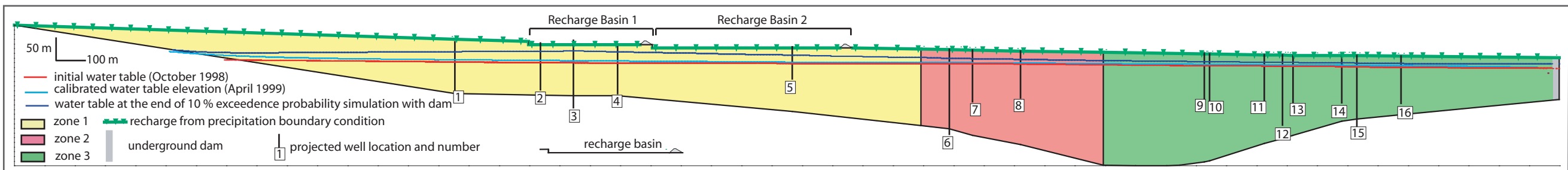

Figure A.8. 10% exceedence probability model with recharge basin and underground dam model

113